

JOINT TRANSPORTATION RESEARCH PROGRAM

INDIANA DEPARTMENT OF TRANSPORTATION
AND PURDUE UNIVERSITY



Documentation of the INDOT Experience and Construction of the Bridge Decks Containing Internal Curing in 2013



Timothy J. Barrett, Albert E. Miller, W. Jason Weiss

RECOMMENDED CITATION

Barrett, T. J., Miller, A. E., & Weiss, W. J. (2015). *Documentation of the INDOT experience and construction of the bridge decks containing internal curing in 2013* (Joint Transportation Research Program Publication No. FHWA/IN/JTRP-2015/10). West Lafayette, IN: Purdue University. <http://dx.doi.org/10.5703/1288284315532>

AUTHORS

Timothy J. Barrett

Graduate Research Assistant
Lyles School of Civil Engineering
Purdue University

Albert E. Miller

Graduate Research Assistant
Lyles School of Civil Engineering
Purdue University

W. Jason Weiss, PhD

Jack and Kay Hockema Professor and Director of Pankow Materials Laboratory
Lyles School of Civil Engineering
Purdue University
(541) 737-1885
jasonweiss99@gmail.com
Corresponding Author

ACKNOWLEDGMENTS

The research performed in this study was conducted in the Charles Pankow Materials Laboratory at Purdue University. The authors would like to express their deepest gratitude and acknowledge those who have made the laboratory and its operation possible. This work was supported in part by the Joint Transportation Research Program administered by the Indiana Department of Transportation and Purdue University under SPR-3752.

JOINT TRANSPORTATION RESEARCH PROGRAM

The Joint Transportation Research Program serves as a vehicle for INDOT collaboration with higher education institutions and industry in Indiana to facilitate innovation that results in continuous improvement in the planning, design, construction, operation, management and economic efficiency of the Indiana transportation infrastructure. https://engineering.purdue.edu/JTRP/index_html

Published reports of the Joint Transportation Research Program are available at: <http://docs.lib.purdue.edu/jtrp/>

NOTICE

The contents of this report reflect the views of the authors, who are responsible for the facts and the accuracy of the data presented herein. The contents do not necessarily reflect the official views and policies of the Indiana Department of Transportation or the Federal Highway Administration. The report does not constitute a standard, specification, or regulation.

COPYRIGHT

Copyright 2015 by Purdue University. All rights reserved.
Print ISBN: 978-1-62260-352-7
ePUB ISBN: 978-1-62260-353-4

1. Report No. FHWA/IN/JTRP-2015/10	2. Government Accession No.	3. Recipient's Catalog No.	
4. Title and Subtitle Documentation of the INDOT Experience and Construction of the Bridge Decks Containing Internal Curing in 2013		5. Report Date March 2015	6. Performing Organization Code
6. Author(s) Timothy J. Barrett, Albert E. Miller, W. Jason Weiss		8. Performing Organization Report No. FHWA/IN/JTRP-2015/10	
9. Performing Organization Name and Address Joint Transportation Research Program Purdue University 550 Stadium Mall Drive West Lafayette, IN 47907-2051		10. Work Unit No.	11. Contract or Grant No. SPR-3752
12. Sponsoring Agency Name and Address Indiana Department of Transportation State Office Building 100 North Senate Avenue Indianapolis, IN 46204		13. Type of Report and Period Covered Final Report	
12. Sponsoring Agency Name and Address (continued)		14. Sponsoring Agency Code	
15. Supplementary Notes Prepared in cooperation with the Indiana Department of Transportation and Federal Highway Administration.			
16. Abstract <p>The Indiana Department of Transportation (INDOT) constructed four bridge decks utilizing internally cured, high performance concrete (IC HPC) during the summer of 2013. These decks implement research findings from the research presented in the FHWA/IN/JTRP-2010/10 report where internal curing was proposed as one method to reduce the potential for shrinkage cracking, leading to improved durability. The objective of this research was to document the construction of the four IC HPC bridge decks that were constructed in Indiana during 2013 and quantify the properties and performance of these decks. This report contains documentation of the production and construction of IC HPC concrete for the four bridge decks in this study. In addition, samples of the IC HPC used in construction were compared with a reference high performance concrete (HPC) which did not utilize internal curing. These samples were transported to the laboratory where the mechanical properties, resistance to chloride migration, and potential for shrinkage and cracking was assessed. Using experimental results and mixture proportions, the diffusion based service life of the bridge decks was able to be estimated. Collectively, the results indicate that the IC HPC mixtures that were produced as a part of this study exhibit the potential to more than triple the service life of the typical bridge deck in Indiana while reducing the early age autogenous shrinkage by more than 80% compared to non-internally cured concretes.</p>			
17. Key Words internal curing, internally cured concrete, lightweight aggregate, shrinkage, cracking, bridge deck, service life		18. Distribution Statement No restrictions. This document is available to the public through the National Technical Information Service, Springfield, VA 22161.	
19. Security Classif. (of this report) Unclassified	20. Security Classif. (of this page) Unclassified	21. No. of Pages 104	22. Price

EXECUTIVE SUMMARY

DOCUMENTATION OF THE INDOT EXPERIENCE AND CONSTRUCTION OF THE BRIDGE DECKS CONTAINING INTERNAL CURING IN 2013

Introduction

The Indiana Department of Transportation (INDOT) constructed four bridge decks utilizing internally cured, high-performance concrete (IC HPC) during the summer of 2013. These decks implement findings from the research presented in the FHWA/IN/JTRP-2010/10 (<http://dx.doi.org/10.5703/1288284314262>) report in which internal curing was proposed as one method to reduce the potential for shrinkage cracking, leading to improved durability. The objective of this research was to document the construction of the four IC HPC bridge decks that were constructed in Indiana during 2013 and quantify the properties and performance of these decks. This report contains documentation of the production and construction of IC HPC concrete for these bridges. Samples of the IC HPC used in construction were compared to a reference high performance concrete (HPC) which did not utilize internal curing. The samples collected in the field were transported to the laboratory, where the mechanical performance, resistance to chloride migration, and potential for shrinkage and cracking were assessed. Using experimental results and mixture proportions, the diffusion based service life of the bridge decks was able to be estimated. The intent of this report is to provide data that can be used to quantify the performance of internally cured concrete, with the goal of developing a strategy to determine if and where internal curing should be used by INDOT.

Findings

The construction process was documented for four bridge decks made using IC HPC. These concretes were able to be designed, batched, and placed and are now in service. While avoidable issues were observed during batching related to corrections of water, batching tolerances, and fluctuations in air content (which apply to any concrete), the IC HPC was able to be batched and placed using slight modifications to conventional methods. The production of the IC HPC mixtures was implemented using a mixed specification with prescriptive and performance-based measures representing an improvement on previous specifications, which did not specifically have provisions that consider durability. To aid in the implementation of internal curing in the field, a new quality control technique for lightweight aggregate utilizing a centrifuge has been developed and is now standardized in Indiana

Testing Method 222. Additionally, a series of spreadsheets that automate calculations necessary for quality control for lightweight aggregates, mixture proportioning, and moisture adjustments have been made available as a part of this report (see Appendix G and Appendix H).

The results of laboratory testing indicate that the compressive strength, modulus of elasticity, and tensile strength of the IC HPC mixtures were not substantially different than those of the HPC mixtures, and as such current codified equations can be used to predict the modulus of elasticity and tensile strength if the compressive strength is known. The chloride migration of these concretes was assessed, and it was shown that each of the mixtures tested had a charge passed in the rapid chloride permeability test of less than 1500 C at 91 days. Additional testing provided equivalent results when performing the Nordtest, Stadium migration test, or electrical resistivity test. Using experimental results to determine the chloride diffusion and permeability of each mixture in conjunction with the mixture proportions and chemical compositions of the cementitious materials, the initiation time of the diffusion-based service life of the IC HPC bridge decks was estimated to be between approximately 60 to 90 years, compared to approximately 18 years for conventional Class C bridge deck concrete used in Indiana. The susceptibility to early age shrinkage and cracking was evaluated where it was shown that IC HPC concretes exhibited a reduction in early age shrinkage of 70 to 90%, resulting in a reduction in residual stresses of 80% or more while reducing thermally induced stress by up to 55% when compared to HPC mixtures. Collectively, these results indicate that the IC HPC mixtures produced as a part of this study exhibit the potential for substantially increased service life while markedly reducing the potential for early age cracking.

Implementation

It should be emphasized that the implementation of such technologies as presented within this report alone does not guarantee higher performance, as the production of such concrete requires a degree of technical competence in design, production, and construction of concrete materials. As is the case with the production of any concrete, internally cured or not, performance will be directly tied to the careful accounting of water, be it on the surface of aggregates, in the mixing drum after washing, or elsewhere. Special attention should be paid to the proper operation of batching systems due to complexities with entering "jog rates" and moisture contents, while placement techniques should be reviewed to minimize unwanted effects, and proper finishing and curing techniques must always be practiced. Only after performing the basics of concrete production properly will the full benefits of internal curing be actualized.

CONTENTS

1. SCOPE OF RESEARCH	1
1.1 Problem Statement and Objectives	1
1.2 Overview of Mixture Specifications	1
1.3 Project Information	2
1.4 Research Approach	3
2. BACKGROUND AND INTRODUCTION.	4
2.1 Introduction and Background	4
2.2 Design Approach for Field Applications	7
2.3 Quality Control and Production with Internal Curing.	8
2.4 Summary and Conclusions	12
3. MIXTURE PROPORTIONING FOR INTERALLY CURED CONCRETE	12
3.1 Introduction	12
3.2 Obtaining Fine Lightweight Aggregate Properties for Mixture Design	13
3.3 Using Fine Lightweight Aggregate Properties to Design and Internally Cure a Concrete Mixture	19
3.4 Summary and Conclusions	21
4. BRIDGE DECK PRODUCTION AND CONSTRUCTION DOCUMENTATION	22
4.1 Introduction	22
4.2 Bridge #1	23
4.3 Bridge #2	27
4.4 Bridge #3	29
4.5 Bridge #4	32
4.6 Summary	34
4.7 Conclusions.	34
5. LABORATORY TESTING OF FIELD PRODUCED SAMPLES: MECHANICAL AND TRANSPORT BEHAVIOR EVALUATION	35
5.1 Introduction	35
5.2 Objectives	35
5.3 Testing Methods	35
5.4 Results	38
5.5 Conclusions.	47
6. SERVICE LIFE ESTIMATION	47
6.1 Introduction	47
6.2 Objectives	48
6.3 Experimental Investigation	48
6.4 Results and Discussion.	49
6.5 Summary and Conclusions	51
7. LABORATORY MEASUREMENTS OF SHRINKAGE BEHAVIOR	52
7.1 Introduction	52
7.2 Objectives	52
7.3 Mixture Proportions and Mixing Procedure	52
7.4 Testing Methods	53
7.5 Results	53
7.6 Conclusions.	57
8. SUMMARY AND CONCLUSIONS.	59
8.1 Introduction	59
8.2 Summary of Conclusions	59
8.3 Final Recommendations.	61
REFERENCES	62

APPENDICES.....	66
Appendix A.....	66
Appendix B.....	79
Appendix C.....	82
Appendix D.....	83
Appendix E.....	84
Appendix F.....	86
Appendix G.....	96
Appendix H.....	96

LIST OF TABLES

Table	Page
Table 2.1 Mixture proportions of internally cured high-performance concrete observed in moisture correction study	10
Table 4.1 Concrete mixture design and as-batched proportions for bridge #1 [lb/yd ³]. Admixtures are provided in [oz/cwt]	24
Table 4.2 Aggregate moisture properties on the day of bridge #1 construction	24
Table 4.3 Concrete mixture design and as-batched proportions for bridge #2 [lb/yd ³]. Admixtures are provided in [oz/cwt]	27
Table 4.4 Aggregate moisture properties on the day of bridge deck #2 construction	28
Table 4.5 Surface moisture variability throughout production	28
Table 4.6 Concrete mixture design and as-batched proportions for bridge #3 [lb/yd ³]. Admixtures are provided in [oz/cwt]	31
Table 4.7 Aggregate moisture properties on the day of bridge deck #3 construction	31
Table 4.8 Concrete mixture design and as-batched proportions for bridge #4 [lb/yd ³]. Admixtures are provided in [oz/cwt]	33
Table 4.9 Aggregate moisture properties on the day of bridge deck #4 construction	34
Table 4.10 Price (\$/yd ³) for each mixture in this study	35
Table 5.1 Results of chloride migration tests and resistivity test for the samples procured on the day of construction of the first bridge deck railing. The results of each test are presented in the corresponding units used in the calculation of results of each test	41
Table 5.2 Results of chloride migration tests and resistivity test for the samples procured on the day of construction of the second bridge deck. The results of each test are presented in the corresponding units used in the calculation of results of each test	43
Table 5.3 Results of chloride migration tests and resistivity test for the samples procured on the day of construction of the third bridge deck. The results of each test are presented in the corresponding units used in the calculation of results of each test	45
Table 5.4 Results of chloride migration tests and resistivity test for the samples procured on the day of construction of the fourth bridge deck. The results of each test are presented in the corresponding units used in the calculation of results of each test	47
Table 6.1 Concrete mixture proportions as batched	48
Table 6.2 Results from moisture desorption testing for water vapor permeability	49
Table 6.3 Calculated chloride diffusion coefficients and associated tortuosity from migration cell testing	50
Table 7.1 Mixture proportions of samples created to study the shrinkage of IC HPC and HPC concretes	52
Table 8.1 Price [\$ /yd ³] for each mixture in this study	60
Table C.1 Results of single operator single laboratory absorption testing using the centrifuge method	80
Table C.2 Results from multiple operator single laboratory variability testing for absorption using both the paper towel test (top) and the centrifuge method (bottom)	81
Table D.1 As-batched concrete mixture proportions for each truck during construction of bridge deck #3 [lb/yd ³]. Admixtures are provided in [oz/cwt]	81

Table E.1 As-batched concrete mixture proportions for each truck during construction of bridge deck #4 [lb/yd ³]. Admixtures are provided in [oz/cwt]	82
Table E.2 As-batched concrete mixture proportions for each truck during construction of bridge deck #4 [lb/yd ³]. Admixtures are provided in [oz/cwt]	82
Table E.3 As-batched concrete mixture proportions for each truck during construction of bridge deck #4 [lb/yd ³]. Admixtures are provided in [oz/cwt]	83

LIST OF FIGURES

Figure	Page
Figure 1.1 INDOT district map showing approximate location of the four bridge decks constructed in Indiana in 2013	3
Figure 2.1 (a) Schematic representation of void space creation due to chemical shrinkage and (b) schematic representation of approximately equal void space creation in high- and low-porosity systems	5
Figure 2.2 Example of (a) the paper towel method and (b) centrifuge methods for achieving pre-wetted surface dry conditions in LWA	8
Figure 2.3 Aggregate moisture states represented schematically with definitions listed below each state pictured	9
Figure 2.4 Comparison of proper (Surface Moisture) and improper (Total Moisture Approach) definitions for surface moisture of LWA. The solid horizontal line indicates the upper threshold of allowable variation in w/cm during production as stated in the INDOT specifications	10
Figure 2.5 Effect on w/cm due to underestimation of surface moisture of (a) normal weight coarse aggregate (CA) and (b) fine aggregate (FA). The solid horizontal line indicates the upper threshold of allowable variation in w/cm during production as stated in the INDOT specifications	11
Figure 2.6 Effect on w/cm due to underestimation of surface moisture on LWA. Dashed lines indicate plus or minus one standard deviation when the surface moisture is determined by the paper towel and centrifuge methods. The solid horizontal line indicates the upper threshold of allowable variation in w/cm during production as stated in the INDOT specifications	11
Figure 2.7 LWA piles being soaked prior to batching of internally cured concrete. Note that the height of pile (a) was less than 5 feet tall while the height of pile (b) was in excess of 9 feet tall	11
Figure 2.8 Varying surface moistures of a single LWA sample after a period of soaking in water. Values were obtained using the centrifuge method	12
Figure 3.1 Worksheet used for laboratory and field determination of absorption, surface moisture, and total moisture	14
Figure 3.2 Worksheet used for laboratory and field determination of relative density (specific gravity)	15
Figure 3.3 Examples of pycnometers that can be used for determining the specific gravity of pre-wetted lightweight aggregate (mason jar style shown at left and volumetric flask shown at right)	15
Figure 3.4 Graph showing the relationship of absorption to relative density	16
Figure 3.5 Worksheet used for laboratory desorption testing of pre-wetted lightweight fine aggregate	17
Figure 3.6 Example of a 94% relative humidity chamber used for desorption testing	18
Figure 3.7 Summary of properties to be used in designing an internally cured concrete mixture	19
Figure 3.8 Mixture design spreadsheet used to internally cure a concrete mixture	20
Figure 3.9 Mixture design spreadsheet used to calculate batch weights on the day of batching	22
Figure 4.1 Photograph of bridge deck #1 taken approximately 2 months after casting	25
Figure 4.2 Photograph of the underside of bridge deck #1 approximately 2 months after casting. The voids seen are primarily due to consolidation issues and were later patched with an INDOT approved filler material	26
Figure 4.3 Compressive strength of samples produced from the first bridge deck mixtures compared to a reference mixture. The dashed line indicates the minimum acceptable limit as per the specifications	26
Figure 4.4 Sealed resistivity measurements of samples produced from the first bridge deck mixtures compared to a reference mixture	26
Figure 4.5 Internally cured bridge deck being placed in 2013 on US 150 over Lost River in Orange County, Indiana	29
Figure 4.6 Digital composite of two images taken depicting the pump type and technique at the second bridge deck cast	29
Figure 4.7 Compressive strength of samples produced from the second bridge deck mixtures compared to a reference mixture. The dashed line indicates the minimum acceptable limit as per the specifications	30
Figure 4.8 Sealed resistivity measurements of samples produced from the second bridge deck mixtures compared to a reference mixture	30
Figure 4.9 Internally cured bridge deck being cast in 2013 on US 31 over Hutto Creek in Indiana	32
Figure 4.10 Compressive strength of samples produced from the third bridge deck mixtures compared to a reference mixture. The dashed line indicates the minimum acceptable limit as per the specifications	32
Figure 4.11 Sealed resistivity measurements of samples produced from the third bridge deck mixtures compared to a reference mixture	32

Figure 4.12	Internally cured bridge deck being cast in 2013 on SR 933 over Baugo Creek in Indiana	34
Figure 4.13	Finishing of an internally cured bridge deck with an excess of paste visible at the surface	34
Figure 4.14	Compressive strength of samples produced from the fourth bridge deck mixtures compared to a reference mixture. The dashed line indicates the minimum acceptable limit as per the specifications	35
Figure 4.15	Sealed resistivity measurements of samples produced from the fourth bridge deck mixtures compared to a reference mixture	35
Figure 5.1	A picture schematic of the uniaxial resistivity testing setup	37
Figure 5.2	A picture of the RCPT test during operation	37
Figure 5.3	A picture of the Nordtest during operation	38
Figure 5.4	A picture of the Stadium migration test during operation	38
Figure 5.5	Compressive strength evolution of samples procured on the day of construction of the first bridge deck. The dashed line indicates the minimum required strength at 28 days as outlined in the special provisions (INDOT, 2014a)	39
Figure 5.6	Evolution of Young's elastic modulus of samples procured on the day of construction of the first bridge deck railing	39
Figure 5.7	Young's elastic modulus of samples procured on the day of construction of the first bridge deck railing plotted as a function of the square root of the corresponding measured compressive strength. The dashed line indicates the result from AASHTO, Section C5.4.2.4 for normal weight concrete while the solid line indicates $\pm 20\%$	39
Figure 5.8	Evolution of splitting tensile strength of samples procured on the day of construction of the first bridge deck railing	39
Figure 5.9	Splitting tensile strength of samples procured on the day of construction of the first bridge deck plotted as a function of the square root of the corresponding measured compressive strength. The dashed line indicates the result from AASHTO, Section 5.8.2.2 while the solid line indicates $\pm 20\%$	40
Figure 5.10	Evolution of the sealed uniaxial resistivity of samples procured on the day of construction of the first bridge deck railing	40
Figure 5.11	Compressive strength evolution of samples procured on the day of construction of the second bridge deck. The dashed line indicates the minimum required strength at 28 days as outlined in the special provisions	41
Figure 5.12	Evolution of Young's elastic modulus of samples procured on the day of construction of the second bridge deck railing	41
Figure 5.13	Young's elastic modulus of samples procured on the day of construction of the second bridge deck plotted as a function of the square root of the corresponding measured compressive strength. The dashed line indicates the result from AASHTO, Section C5.4.2.4 for normal weight concrete while the solid line indicates $\pm 20\%$	42
Figure 5.14	Evolution of splitting tensile strength of samples procured on the day of construction of the first bridge deck railing	42
Figure 5.15	Splitting tensile strength of samples procured on the day of construction of the first bridge deck plotted as a function of the square root of the corresponding measured compressive strength. The dashed line indicates the result from AASHTO, Section 5.8.2.2 while the solid line indicates $\pm 20\%$	42
Figure 5.16	Evolution of the sealed uniaxial resistivity of samples procured on the day of construction of the first bridge deck railing	43
Figure 5.17	Compressive strength evolution of samples procured on the day of construction of the third bridge deck. The dashed line indicates the minimum required strength at 28 days as outlined in the special provisions	43
Figure 5.18	Evolution of Young's elastic modulus of samples procured on the day of construction of the third bridge deck railing	44
Figure 5.19	Young's elastic modulus of samples procured on the day of construction of the third bridge deck plotted as a function of the square root of the corresponding measured compressive strength. The dashed line indicates the result from AASHTO, Section C5.4.2.4 for normal weight concrete while the solid line indicates $\pm 20\%$	44
Figure 5.20	Evolution of splitting tensile strength of samples procured on the day of construction of the third bridge deck	44
Figure 5.21	Splitting tensile strength of samples procured on the day of construction of the third bridge deck plotted as a function of the square root of the corresponding measured compressive strength. The dashed line indicates the result from AASHTO, Section 5.8.2.2 while the solid line indicates $\pm 20\%$	44
Figure 5.22	Evolution of the sealed uniaxial resistivity of samples procured on the day of construction of the third bridge deck	45
Figure 5.23	Compressive strength evolution of samples procured on the day of construction of the fourth bridge deck. The dashed line indicates the minimum required strength at 28 days as outlined in the special provisions	45

Figure 5.24	Evolution of Young’s elastic modulus of samples procured on the day of construction of the fourth bridge deck railing	46
Figure 5.25	Young’s elastic modulus of samples procured on the day of construction of the fourth bridge deck plotted as a function of the square root of the corresponding measured compressive strength. The dashed line indicates the result from AASHTO, Section C5.4.2.4 for normal weight concrete while the solid line indicates $\pm 20\%$	46
Figure 5.26	Evolution of splitting tensile strength of samples procured on the day of construction of the fourth bridge deck	46
Figure 5.27	Splitting tensile strength of samples procured on the day of construction of the fourth bridge deck plotted as a function of the square root of the corresponding measured compressive strength. The dashed line indicates the result from AASHTO, Section 5.8.2.2 while the solid line indicates $\pm 20\%$	46
Figure 5.28	Evolution of the sealed uniaxial resistivity of samples procured on the day of construction of the fourth bridge deck	47
Figure 6.1	Estimated desorption isotherm for IC HPC 4 and HPC 4	50
Figure 6.2	Total chloride content versus time for each mixture. (Corrosion initiation threshold for reinforcing steel indicated by dashed line at 0.5%)	51
Figure 6.3	Field inspection of IC HPC bridge deck on State Road 933 over Baugo Creek, Indiana, USA	51
Figure 7.1	Picture of the linear autogenous “tube” shrinkage test during operation	53
Figure 7.2	Picture of the concrete dual ring test upon completion of the test	53
Figure 7.3	(a) Total strain due to drying and autogenous deformations and (b) total mass loss of IC HPC 1 and HPC 1 mixtures	54
Figure 7.4	Linear autogenous shrinkage of IC HPC 1 and HPC 1 mixtures	54
Figure 7.5	Residual stress developed in the dual ring test for IC HPC 1 and HPC 1 mixtures	55
Figure 7.6	(a) Total strain due to drying and autogenous deformations and (b) total mass loss of IC HPC 2 and HPC 2 mixtures	55
Figure 7.7	Linear autogenous shrinkage of IC HPC 2 and HPC 2 mixtures.	56
Figure 7.8	Residual stress developed in the dual ring test for IC HPC 2 and HPC 2 mixtures.	56
Figure 7.9	(a) Total strain due to drying and autogenous deformations and (b) total mass loss of IC HPC 3 and HPC 3 mixtures	57
Figure 7.10	Linear autogenous shrinkage of IC HPC 3 and HPC 3 mixtures	57
Figure 7.11	Residual stress developed in the dual ring test for IC HPC 3 and HPC 3 mixtures	58
Figure 7.12	(a) Total strain due to drying and autogenous deformations and (b) total mass loss of IC HPC 4 and HPC 4 mixtures	58
Figure 7.13	Linear autogenous shrinkage of IC HPC 4 and HPC 4 mixtures	58
Figure 7.14	Residual stress developed in the dual ring test for IC HPC 4 and HPC 4 mixtures	59

1. SCOPE OF RESEARCH

1.1 Problem Statement and Objectives

The Indiana Department of Transportation (INDOT) constructed four bridge decks utilizing internally cured high-performance concrete (IC HPC) during the summer of 2013. These decks are being considered as one method to reduce cracking and to improve durability based on research findings presented in the FHWA/IN/JTRP-2010/10 report (<http://dx.doi.org/10.5703/1288284314262>) (Schlitter, Henkensiefken, et al., 2010). While many laboratory studies on internally cured concrete have been conducted and have shown promise for the use of internally cured concrete, the documentation of the field implementation of this technology is limited and the quantification of the performance of these materials is still needed (Di Bella, 2012). The objective of this research is to document the construction of the four IC HPC bridge decks that were constructed in Indiana during 2013 and to collect samples at each site that can be used to quantify the properties and performance of these decks. The purpose of this documentation is to provide data that can be used in the experimental features program to quantify the performance of internally cured concrete with the goal of developing a strategy to determine if and where internal curing should be used by INDOT.

The documentation provided by this project will focus on three main areas:

1. Documentation of construction and measurement of the constituent materials, variability, and fresh concrete properties.
2. Documentation of the properties that influence long-term service life, including chloride diffusion and other transport properties.
3. Documentation of the shrinkage cracking resistance with a comparison of IC HPC and reference (non-internally cured) mixtures.

It should be noted that in addition to measuring the performance of the IC HPC used in the bridge deck construction, it is essential to bench-mark a similar reference concrete. This report will present data for an equivalent high-performance concrete (HPC) that contained no internal curing. In addition to the three objectives of documentation highlighted previously, a series of training tools have been developed to aid in the field implementation of internally cured concrete.

1.2 Overview of Mixture Specifications

The mixture specifications for the IC HPC implemented in this study is outlined in “Special Provisions” provided in contract documents; a sample of this specification from one of the contracts in this study has been provided in Appendix A. It is stated that the IC HPC shall contain portland cement with two pozzolanic materials (fly ash or slag and silica fume) in addition to pre-wetted lightweight fine aggregate for the purpose of internal curing. The stated objective of this mixture is to

produce a bridge deck concrete of high durability, low permeability, and low cracking potential.

1.2.1 High Performance

The higher performance inherent to the IC HPC comes from three key specification measures. The first is through the use of two supplementary cementitious materials in combination with the portland cement which will result in a refinement of the pore network, leaving an overall denser microstructure (Mindess et al., 2003). The specification requires a minimum of 390 lb/yd³, a content of 20 to 25% of Class F or C fly ash (by mass), and content of 3 to 7% of silica fume (by mass). It is permitted to substitute ground granulated blast furnace slag (ggbfs) in an amount of 15 to 20% (by mass) in lieu of fly ash. An additional benefit of the use of supplementary cementitious materials is the net reduction in cement consumption for the production of concrete bridge decks. IC-HPC conforming to this specification can result in net reduction in cement usage of 23 to 32% (18 to 27% using ggbfs).

The second aspect of the specification that improves the performance of the mixture is a desire by INDOT to limit the design total paste volume to 25.0%. This limitation was intended to limit the shrinkage potential of high-performance mixtures, based on research presented in the FHWA/IN/JTRP-2008/29-2 report (<http://dx.doi.org/10.5703/1288284314307>) (Radlinski & Olek, 2010). It should be noted however that this mixture includes internal curing to mitigate significant early age shrinkage and making this limitation less necessary for the intent of shrinkage reduction (revisions to the specification in 2014 have relaxed the limit on total paste volume to 26.0% and it may be further possible to reduce this limitation with higher paste volumes). A secondary effect of this limitation is the inherent maximum cementitious materials content of the concrete mixture. In current specifications for Class C bridge deck concretes (Indiana’s current bridge deck class concrete), this limitation does not exist. During the production of this concrete, producers target minimum strength values which can be easily achieved through the addition of cement to the mixture. A recent study concluded that Class C bridge deck concretes frequently have cement contents in excess of 650 lbs/cu yd which may lead to increased susceptibility to the formation of transverse cracking in bridge decks (Frosch, Gutierrez, & Hoffman, 2010).

The final specification measure which promotes higher performance is the limitation on water-to-cementitious-materials ratio (w/cm) of 0.36 to 0.43, with a stated allowable tolerance of ± 0.025 of the design target w/cm. This limitation on w/cm leads to the production of concrete that, when a high degree of hydration is reached, will have minimized the capillary porosity (Powers & Brownard, 1946). The minimization of capillary porosity will result in concrete that has a lower permeability and diffusivity (Mindess, Young, & Darwin, 2003). A secondary consequence of

specifying the low paste volume and w/cm is the inherent necessity for producers to perform aggregate moisture tests and account for excess water in the mixture at all times during the production of IC HPC. This topic will be discussed in greater detail in subsequent chapters.

1.2.2 Internal Curing

The internal curing in the IC HPC is specified to be achieved using a pre-wetted lightweight aggregate (LWA). The amount of LWA necessary for internal curing is specified to supply 7 lb of water per 100 lb of cementitious materials. This quantity was multiplied by 1.025 to account for an additional margin of safety which was a choice intended by the INDOT to account for allowable errors that may occur when batching lightweight aggregate (i.e., the design is set to supply a total of 7.17 lb of water per 100 lb of cement). The approved mixture design is to ensure a fixed volume of LWA is supplied (not less than 20% of the total volume of fine aggregate volume) based upon laboratory measured values for the LWA absorption and specific gravity at 24 hours. It is the understanding of the authors of this report that revisions to the 2014 special provisions increase this minimum volume of LWA to 30% and that the author of the special provisions intends to carry this value forward in future versions of the document. According to the specification, at the time of production the LWA absorption and specific gravity is to be measured. The target batch weight of LWA is then specified to be determined by multiplying the weight of dry LWA necessary to supply 7.17 lb of water per 100 lb of cement (as determined by the 24-hour laboratory moisture properties of the LWA) by the total moisture of the LWA measured on the day of production.

In preparation for the production of IC HPC, the contractor is to soak the lightweight aggregate with a suitable sprinkler system for a minimum of 48 hours or until the absorption of the LWA is consistently maintained above the design absorption value. The stockpile of LWA is to be drained for 12 to 15 hours immediately prior to its use in IC HPC construction. Manipulation of the stockpile is to be done as necessary to achieve a uniform moisture state while wetting and draining. To determine the LWA moisture state on the day of production, the specification cites the provisions in Appendix B of ACI 211.2 which utilizes a centrifuge spinning at 500 rpm for 20 minutes in order to achieve a pre-wetted surface dry condition for absorption testing. It should be noted that based on research provided in this report (Miller, Barrett, Zander, & Weiss, 2014), the 2014 specification has been updated to specify the use of a centrifuge spinning at 2000 rpm for 3 minutes to achieve a pre-wetted surface dry condition of the LWA. Additionally, this research has resulted in the publication of Indiana Testing Method 222 which details the centrifuge method for determining the moisture states of LWA for the purposes of internal curing for use in not only the laboratory, but also of the properties of the material in the field for the pre-wetted (soaked) and drained stockpiles.

1.2.3 Performance Measures

In order to ensure that the IC HPC mixtures achieve the stated goals of improved durability and reduced permeability, certain performance measures based on standardized tests were specified. At the point of placement, the concrete mixture is to have a measured slump between 2.5 to 5.5 inches, an air content of $6.5 \pm 1.5\%$, and the measured relative yield should not vary more than 0.010 of the target. The specified compressive strength at 28 days shall be a minimum of 5000 psi. Finally, the IC HPC shall achieve a target resistance to chloride ion permeability of no greater than 1500 coulombs as measured by the rapid chloride penetration tests (ASTM C 1202/ AASHTO T277) at 56 days of age (AASHTO, 2007). It should be noted that the specification for Class C concrete does not include any limitations on measures of resistance to chloride penetration, only specifying a maximum w/cm of 0.443 and a minimum 28-day compressive strength of 4000 psi.

1.3 Project Information

Four bridge decks were chosen throughout the state of Indiana to be cast with IC HPC. Figure 1.1 shows the approximate location of the four bridges being numbered 1 through 4 in chronological order of placement. The intent of showing the locations of the bridges is to highlight the specific selection of these projects which resulted in the introduction to internal curing to four different INDOT districts. General information about each of the bridge decks is listed below.

Bridge #1: Contract B-33379, NB I-69 over Little Black Creek, Grant County, Indiana

Concrete Producer: Erie Haven, Inc.
Bridge Design Type: Continuous Reinforced Concrete Slab
3 Spans: 21', 28', 21'
Deck thickness: 15.5"
AADT (2007): 27,450 with 40% being trucks

Bridge #2: Contract B-34199, US 150 over Lost River, Orange County, Indiana

Concrete Producer: Irving Materials, Inc.
Bridge Design Type: Continuous Composite Steel Beam Bridge
3 Spans: 69'-9", 84'-6", 69'-9"
Deck thickness: 8"
AADT (2011): 1,900 with 16% being trucks

Bridge #3: Contract B-35326, US 31 over Hutto Creek, Scott County, Indiana

Concrete Producer: Shelby Materials
Bridge Design Type: Composite Steel Beam Bridge
Single Span: 55'
Deck thickness: 8"
AADT (2012): 12,500 with 6% being trucks

Bridge #4: Contract B-30498, SR 933 over Baugo Creek, St. Joseph County, Indiana

Concrete Producer: Transit-Mix, Inc.
Bridge Design Type: Continuous Composite Prestressed Concrete Bulb-T Beam Bridge
2 Spans: 84'-6", 84'-6"
Deck thickness: 8"
AADT (2011): 15,000 with 4% being trucks

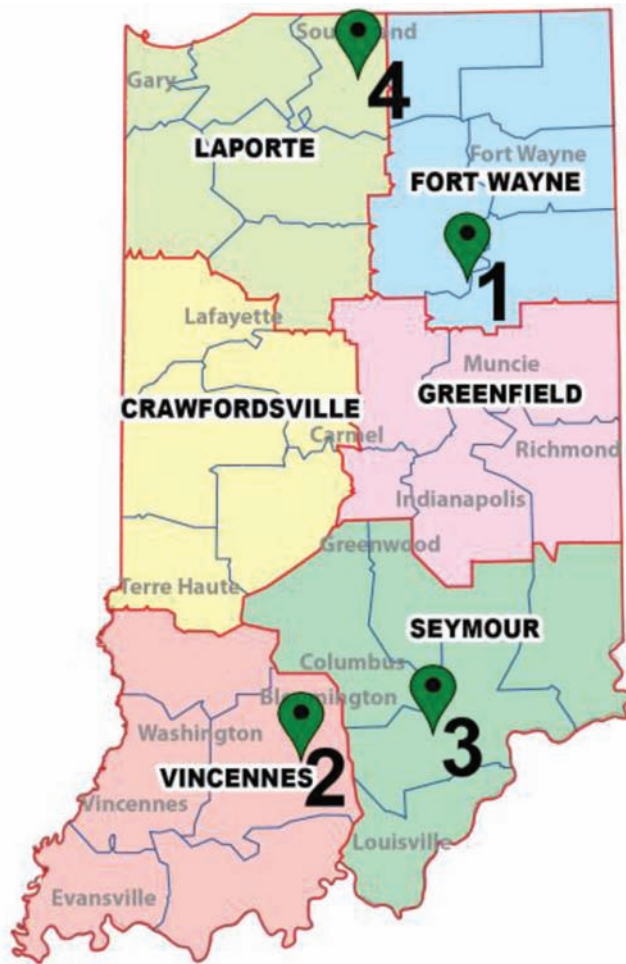


Figure 1.1 INDOT district map showing approximate location of the four bridge decks constructed in Indiana in 2013.

1.4 Research Approach

The goal of this project was to provide INDOT with documentation of the construction and performance of the four IC HPC bridge decks cast in 2013. Specific tasks considered in this project to accomplish these objectives are outlined as follows.

1.4.1 Chapter 2: Literature Review

A literature review was conducted in order to provide a succinct background on internal curing while highlighting laboratory research that has previously been performed on internally cured concrete. The information provided has been presented in a manner directed at the field implementation of internal curing with an emphasis on suitable simplifications for the field as well as highlighting quality control aspects that should be considered when dealing with lightweight aggregates during concrete production.

1.4.2 Chapter 3: Mixture Proportioning for Internally Cured Concrete

As a part of the training tools developed for this report, a spreadsheet was created and made available (see Appendix H) which enables for the calculations for internal curing using pre-wetted lightweight aggregate presented in Chapter 2 to be automated for any field produced concrete. This chapter details how the spreadsheet works and provides batch weights that account for the different moisture corrections commonly found in commercial batching software. It is intended that this tool will enable transportation departments, concrete producers, and lightweight aggregate manufacturers to easily develop new internally cured concrete mixtures or to internally cure an existing mixture design.

1.4.3 Chapter 4: Bridge Deck Production and Construction Documentation

This chapter presents the documentation of the mixture approval procedure and the bridge deck construction. This includes the documentation of both the trial batch (which must take place a minimum of 28 days prior to the construction of the bridge deck itself) and the day of production of the bridge deck. The documentation includes a background on the design of the bridge deck and the IC HPC mixture, the constituent materials used, the weather at the time of construction, variations during production/construction, the fresh properties of the concrete, truck haul times, and general production/construction processes. Specimens for laboratory testing were collected at the trial batch as well as the day of construction and a comparison of this production data will be presented in an effort to understand the potential variability between mixture qualification at the trial batch and the day of construction.

1.4.4 Chapter 5: Laboratory Testing of Field Produced Samples: Mechanical and Transport Behavior Evaluation

A series of samples were made using the IC HPC mixture from each bridge deck construction with an additional set of samples being obtained from a reference mixture of HPC without internal curing. These samples were evaluated under standard testing conditions in a laboratory to evaluate the development of mechanical properties as well as to evaluate the transport behavior of the field produced specimens. This chapter presents the data with a focus on impact on design and performance specifications. The mechanical performance of the mixtures is presented in the context of current structural design equations, providing a necessary reference for design engineers. The transport behavior was characterized by a series of standardized tests which are commonly used and/or referenced in performance specifications. These

tests include the rapid chloride permeability test, the Nord Migration Test, the Stadium Migration Tests, and the electrical resistivity test. The purpose of performing these tests is to enable the development of acceptance criterion for use in performance specifications.

1.4.5 Chapter 6: Service Life Estimation

In order to quantify the effects of steps taken by INDOT to create a higher durability, lower permeability concrete for use in bridge decks, a service life model was utilized to estimate the time for chloride to reach a critical level which is assumed to be synonymous with the initiation of corrosion for each of the bridge deck materials tested. This chapter presents the results of a simulation which utilizes measured material properties to estimate the diffusion-based service life of the bridge decks under regional environmental exposure conditions, however it should be noted that the presence of cracking is not considered in this estimate. The results of this service life estimation coupled with the evaluation of the shrinkage behavior is intended to motivate the value of utilizing internally cured high-performance concrete in bridge deck construction and may be utilized in the future by INDOT to make decisions on when to use IC HPC based on estimated service life that may be achieved.

1.4.6 Chapter 7: Laboratory Measurements of Shrinkage Behavior

The field mixtures presented in Chapters 4–6 were recreated under controlled laboratory settings in order to assess the shrinkage behavior of each mixture. To evaluate the shrinkage of each mixture, linear autogenous shrinkage tubes were cast, the dual ring test was performed, and linear drying shrinkage prisms were made. The intent of this chapter motivate and quantify the effects of internal curing on the shrinkage of high-performance concretes.

1.4.7 Chapter 8: Summary and Conclusions

Chapter 8 provides a summary of the results presented in this study, offers concluding remarks on the field implementation of IC HPC by the Indiana Department of Transportation, and recommends future steps for continued success in the production of higher performance, internally cured concrete.

2. BACKGROUND AND INTRODUCTION

2.1 Introduction and Background

When concrete is restrained from shrinking freely, the potential for cracking can increase. There is increasing pressure to design bridges and pavements that are longer lasting, more economic and easier to maintain while embracing sustainable construction

materials. The concrete industry has worked to make concrete more sustainable by: (1) reducing the cement clinker necessary for the production of cement (i.e., blended cement and portland limestone cement), (2) reducing cement content necessary for the production of one cubic meter of concrete (i.e., lower cement contents), and (3) through the improvement of the service life of the concrete. The solutions posed through this sustainability initiative have led to increased usage of supplementary cementitious materials, inert fillers, and reduced water-to-cementitious-materials ratios (w/cm) for improved performance. It should be recognized however that as the use of lower water to cement ratios with refined pore networks becomes prevalent, so does the potential for shrinkage and shrinkage cracking (Weiss, Yang, & Shah, 1998).

The increased shrinkage and increased cracking potential for high-strength concrete has been well documented and is a major factor contributing to the practical implementation and limitations of these materials (Bentz et al., 1998; Igarashi, Bentur, & Kovler, 2000; Jensen & Hansen, 1996, 2001a; Persson, 1997; Weiss, 1999; Wiegrink, Marikunte, & Shah, 1996). By intentionally designing a lower water to binder ratio concrete with a refined pore network, the ingress of potentially deleterious species such as water, chlorides, and sulfates can be delayed and service life can be enhanced. Unfortunately, cracking due to shrinkage results in a path for the ingress of ionic species which can accelerate deterioration (Mehta & Monteiro, 1993; Raoufi & Weiss, 2012; Shah, Wang, & Weiss, 2000; Weiss, Yang, & Shah, 2000). In response to the increased potential for cracking in high-strength concrete several mitigation strategies have been proposed (Bentz & Jensen, 2006, Radlinska et al., 2008; Shah, Weiss, & Yang, 1998).

This paper will review the origins of the shrinkage of high-performance concrete, provide a background on the concept of internal curing (IC) to mitigate this shrinkage, and review the benefits of using internal curing. A series of recommendations for field implementation will be offered and a new quality control technique for understanding aggregate moisture properties will be discussed.

2.1.1 The Case for Internal Curing

This chapter begins by discussing the factors that lead to the increased shrinkage of low w/c concrete at early ages. In 1900, Le Chatelier identified that chemical shrinkage occurs when cement reacts with water (Le Chatelier, 1900). Simply stated, chemical shrinkage can be explained to occur as a result of the chemical reaction between cement and water, where the volume of the reactants is larger than the volume of the hydrated products that are produced. The chemical shrinkage is dependent on the chemistry of a particular cementitious system and can be calculated or measured; however, in general the chemical

shrinkage results in a 9% volume reduction in the hydrated product (Geiker, 1983, Tazawa, Miyazawa, & Kasai, 1995). In cementitious systems chemical shrinkage can result in problems after setting, where the hydrated products form a rigid structure and begin resisting volumetric change. Figure 2.1a shows a schematic representation showing the measured chemical shrinkage over time contrasted with the measured bulk shrinkage of a sealed material (termed autogenous shrinkage). For the volume of the system to be conserved as it undergoes elastic deformation (i.e., shrinkage), the difference between the volume of chemical shrinkage and autogenous shrinkage must result in and be equal to the formation of expansive vapor filled space in the pore structure (a process also referred to as self-desiccation), which results in the development of stress (Hammer, 1999; Sant, Lura, & Weiss, 2006). The level of stress that develops depends on the size of the pores that empty when the vapor filled space forms. While the chemical shrinkage is dependent on the cement chemistry and the degree of hydration; it is not dependent on the water to cement ratio. Rather, the autogenous shrinkage is dependent on the size of the pores that are emptied and the curvature of the meniscus that develops which is heavily influenced by the water to cement ratio.

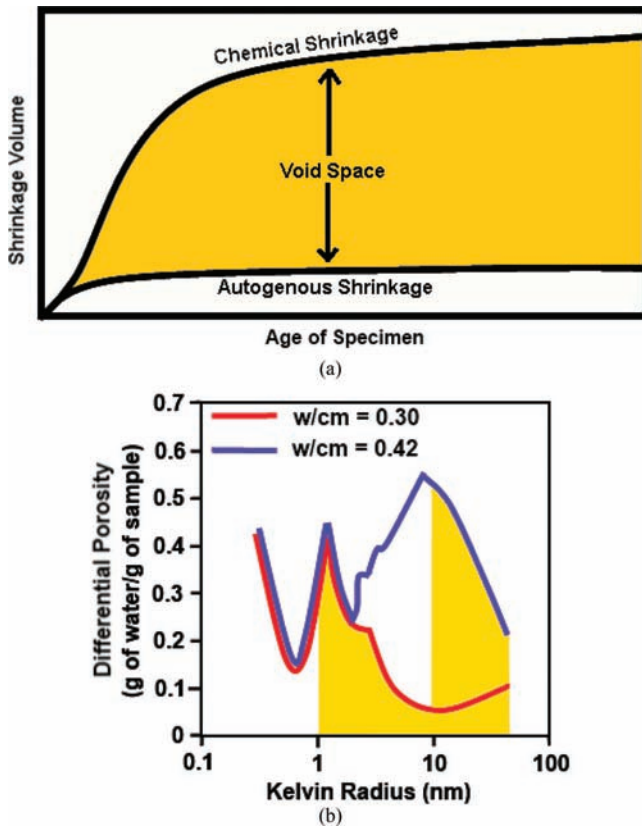


Figure 2.1 (a) Schematic representation of void space creation due to chemical shrinkage and (b) schematic representation of approximately equal void space creation in high- and low-porosity systems.

The Kelvin equation (Equation 2.1) can be used to relate the change in RH due to self-desiccation (defined as the partial pore vapor pressure) due to the formation of a meniscus in a vapor filled cylindrical pore of radius, r . Equation 2.1 presents the Kelvin equation solved for the radius of the partially filled pore (i.e., void space created) that must accompany the reduction in RH and is consistent with the phenomenological observation of void space creation due to chemical shrinkage. It is important to acknowledge that while self-desiccation occurs for all systems, it is particularly problematic for low w/cm materials and materials with finer (i.e., smaller radius) pores, as indicated by the inverse relationship described by the Kelvin equation (Castro, 2011). Figure 2.1b further depicts this using a graphic recreation of data by (De La Varga, Castro, Weiss, and Brameshuber 2010), where the differential porosity of low (w/cm = 0.30) and high (w/cm = 0.42) porosity mortars were measured. The yellow shaded area under each curve represents an approximately equal volume of water lost due to self-desiccation in each system (with the largest pores emptying first), from which it can readily be seen that equal amounts of self-desiccation result in much smaller pores being emptied in lower w/cm materials.

$$r = \frac{2\gamma}{\ln(RH)} \left(\frac{V_m}{RT} \right) \quad (2.1)$$

where γ is the surface tension of the pore fluid (N/m), V_m is its molar volume (m^3/mol), R is the universal gas constant ($8.314 \text{ J}/(\text{mol}\cdot\text{K})$), and T is the temperature (K). This demonstrates that due to the continued hydration, the formation of partially filled pores will occur and the largest pores will empty first. The consequence of these partially filled pores within a sealed, rigid medium is the development of a pore underpressure, which results in a measurable volume change on the bulk of the material, or autogenous shrinkage. The pore pressure developed, σ_{cap} , can be approximated by the Young-Laplace equation for capillary pressure of a spherical pore of radius, r , as shown in Equation 2.2. While the previous section discusses the change in RH due to pore size effects, it should also be noted that the RH of the hydrating cementitious systems will also be influenced by the dissolved salts in the pore solution according to Raoult's Law (Lura, 2003). This equation demonstrates that the pressure developed is inversely related to the size of the pore being emptied, generating larger stresses when smaller pores desiccate.

$$\sigma_{cap} = \frac{2\gamma}{r} \quad (2.2)$$

where γ is the surface tension of the pore fluid (dyne/cm). The shrinkage developed in the partially saturated system, ϵ_{sh} , due to the capillary pressure can be estimated using the approach by Bentz et al., shown in Equation 2.3 (Bentz et al., 1998):

$$\varepsilon_{sh} = -\frac{S_w \sigma_{cap}}{3} \left(\frac{1}{K_b} - \frac{1}{K_s} \right) \quad (2.3)$$

where S_w is the degree of water saturation (0-1), σ_{cap} is defined by Equation 2.2 (Pa), K_b is the drained bulk modulus of the porous material (Pa), and K_s is the bulk modulus of the hydrated solid (Pa). It should be noted that this equation has been revisited by Vlahinic et al. to account for the changing bulk modulus as a function of degree of saturation, and has been addressed in detail elsewhere (Vlahinić, Jennings, & Thomas, 2009). Equation 2.3 has been shown to be yield general agreement for the estimation of shrinkage strain generated above RH of approximately 60% (Bentz et al., 1998).

2.1.2 Internal Curing

In 1946, Powers and Brownyard published their studies of the hydrated cement paste, which Powers later modified to provide a succinct method to model the volumetric composition of cement paste as a function of degree of hydration (Powers & Brownyard, 1946). Jensen and Hansen revisited this work and proposed a series of equations to describe the volumetric proportions of the phases of a hydrating cement paste and showed that for sealed systems (where water is not absorbed or lost from the system) below a w/cm of approximately 0.42, complete hydration cannot be achieved (Jensen & Hansen, 2001b). This implies that at a specific degree of hydration (DOH) the capillary water will be completely consumed without hydrating all the cement in the system. When the suggested definition for pore sizes laid forth by Powers (i.e., gel pores and capillary pores) is used in conjunction with Equation 2.1, it becomes apparent that the capillary pores will empty at a RH of approximately 80%. Measurements of the internal RH of low w/cm systems have indicated that the self-desiccation of the capillary water can occur in the first few weeks of hydration (Castro, 2011). Bentz and Snyder identified that to reduce the potential for shrinkage, water could be supplied in a volume that was equal to the chemical shrinkage (i.e., approximately the amount of void space created, as shown in Figure 2.1). They developed an equation for supplying the appropriate volume of water to replace this void space using pre-wetted lightweight fine aggregates (LWA) (Bentz & Snyder, 1999). The use of internal reservoirs such as LWA to supply water necessary to replace the volume of chemical shrinkage of a hydrating cementitious system is referred to as the process of internal curing. Bentz later updated this supply and demand relationship to Equation 2.4, which tailors to field design methodologies (Bentz, Lura, & Roberts, 2005):

$$M_{LWA} = \frac{C_f \cdot CS \cdot \alpha_{max}}{S \cdot \phi_{LWA}} \quad (2.4)$$

where M_{LWA} is the mass of dry lightweight aggregate (kg/m^3) necessary to fill the voids created by chemical shrinkage with water, C_f is the cement content (kg/m^3), CS is the chemical shrinkage (approximately 6.4 mL of

water/100 g of cement reacted), α_{max} is the maximum degree of hydration (0-1), S is the degree of saturation of the LWA, and ϕ_{LWA} is the design absorption of the lightweight aggregate (kg of water/kg of dry LWA) taken as the 24 h absorption value. In this approach, the amount of water supplied is approximated to be equal to the volume of chemical shrinkage for convenience, a value that is dependent on the maximum degree of hydration for a given w/c. In recent years, more work was done to understand the sorption kinetics of lightweight aggregate and subsequently Bentz's equation been refined by the work of Castro to account for the time dependence of the absorption of the LWA and the desorption behavior in a desiccating environment (Castro, 2011):

$$M_{LWA} = \frac{C_f \cdot CS \cdot \alpha_{max}}{t^A \cdot \phi_{LWA,24h} \cdot \psi} \quad (2.5)$$

where the degree of saturation can be described replaced by t^A , the absorption of the LWA as a function of time and ψ refers to the aggregates ability to desorb (release water) and is the fraction of water released at a high (93%) relative humidity. Researchers have been able to successfully implement both approaches to internal curing presented here in laboratory studies to show improved resistance to the potential for shrinkage and cracking (Schlitter, Henkensiefken, et al., 2010).

2.1.3 Experimental Studies for Evaluation of Shrinkage and Shrinkage Cracking of IC Systems

As discussed in previous sections, the reduction in RH due to self-desiccation generates pore pressures in the paste. For the typical expanded LWA that is used in North America, the pores of the LWA are generally larger than the pores in the paste. The water will be drawn from the larger pores of the LWA through capillary suction and refill the pores in the cement paste as they empty. The result is that during the early stages of hydration, the LWA will maintain an elevated RH in the paste. The effectiveness of using the LWA for the purposes of IC has been measured through studies of the internal RH of cementitious systems (Lura, Jensen, & Igarashi, 2007). More recently, the migration of water from the LWA to the surrounding paste has been observed directly using x-ray and neutron imaging, where it was shown that during the early stages of hydration, the water in the LWA migrates to the surrounding paste to refill the void space being created (Henkensiefken, Nantung, & Weiss, 2011; Lura et al., 2006; Trtik et al., 2011).

Before exploring the findings of experimental shrinkage studies, it should be noted that with the advent of internal curing, the measurement of shrinkage in cementitious materials has also been reassessed and new testing methods have been developed to fully measure the shrinkage that develops at early ages. In general, the shrinkage of hardened concrete can be divided into five main subsets: chemical, drying,

autogenous, thermal, and carbonation shrinkage. Each of these have a natural set of requisite boundary conditions governing the time periods and environmental conditions in which they should be measured, and it has been shown that it can become non-trivial to separate some of these interactions (Jensen & Hansen, 2001a). Specifically, the autogenous shrinkage is driven by the hydration reaction and is thus occurring from the time of set throughout the full extent of hydration. This makes tests such as the classical “drying shrinkage” test, ASTM C 157 (2008), more complicated in interpretation than perhaps first meets the eye since it measures many types of shrinkage (Radlinska et al., 2008). In addition one must acknowledge the occurrence of autogenous shrinkage that occurs during the first 24 hours after casting and prior to the start of drying. To address this, the so-called “tube test” has been developed to measure the autogenous shrinkage directly, and has recently been standardized under ASTM C 1698 (ASTM, 2009; Jensen & Hansen, 2001a). This method employs a closed corrugated tube with high radial stiffness in an isothermal environment, resulting in a linearization of the autogenous shrinkage occurring. This method has been used widely to demonstrate the mitigation potential for internal curing with LWA (Bentur, Igarashi, & Kovler, 2001; Geiker, Bentz, & Jensen, 2004; Radlinska, 2008).

While it is important to measure the free autogenous shrinkage, when the autogenous shrinkage is restrained from moving freely, tensile stresses can develop in the concrete and may result in damage development and an increase in potential for cracking. For some time, the potential for cracking due to restrained shrinkage has been quantified using the so-called “single ring” test, ASTM C 1581 (ASTM, 2004b; Hossain & Weiss, 2004; Moon & Weiss, 2006). This test method has been used to show the reduction in potential for shrinkage cracking when IC is provided at varying levels of LWA replacement of normal fine aggregate (Henkensiefken, Bentz, Nantung, & Weiss, 2009). It should be noted however that, similar to the problems with the drying shrinkage test, it can become difficult to utilize the single ring test to accurately quantify the autogenous shrinkage strain directly in systems that may experience expansion due to swelling during the release of IC water (Lura, 2003). To overcome some of the drawbacks associated with this test, a new test has been developed which utilizes two concentric rings of invar housed in a semi-adiabatic chamber with a temperature regulation coil (Schlitter, Senter, Bentz, Nantung, & Weiss, 2010). This test has been utilized to show that nearly all of the autogenous shrinkage can be successfully mitigated through internal curing and greatly reduce the early age cracking potential (Schlitter, Bentz, & Weiss, 2013). The dual ring test has also been used to show the benefits of using internal curing with high-volume fly ash systems to reduce the potential for autogenous and thermal shrinkage cracking (Barrett, De La Varga, Schlitter, & Weiss, 2011; Barrett, De La Varga, & Weiss, 2012).

Additional tests on pastes shrinking around a metal rod were performed by Lura to show the reduction in potential for cracking through the use of LWA for IC (Lura, Jensen, & Weiss, 2009). An alternative to the ring tests which utilizes a linear cracking frame was used by Cusson and Hoogeveen to also demonstrate the reduction in cracking potential when IC is used (Cusson & Hoogeveen, 2008). Using a similar apparatus with temperature control, Byard, Schindler, and Barnes (2014) showed that internal curing significantly delayed the time to cracking when compared to reference mixtures. A recent study by House et al. (2014) showed the potential use of an expanded slag aggregate for the purpose of IC and showed that on large restrained beams the time to cracking due to combined autogenous and drying shrinkage could be delayed substantially.

The improvement to the durability of internally cured concretes has also been explored, where the chloride migration of field produced concretes was studied and service life predictions indicate improvements due to the extended degree of hydration from internal curing (Di Bella, 2012). Another study compared the time to initiate corrosion of a plain and internally cured concrete undergoing restrained shrinkage and concluded that substantial improvement to service life can be realized when autogenous shrinkage cracking is mitigated through internal curing (Raoufi & Weiss, 2012). It has also been shown that properly air entrained concretes that adhere to the recommendations for supplying LWA for the purpose of IC summarized herein do not experience freezing and thawing issues when compared to mixtures without IC (Jones, House, & Weiss 2014).

While many studies have been conducted in the laboratory documenting the benefits of internal curing, relatively few studies have documented the quality control aspects of internally cured concrete or the actual use of internal curing in practice. The following section discusses field implementation and discusses some considerations for producing high-quality internally cured concrete.

2.2 Design Approach for Field Applications

Several approximations can be made to simplify Equation 2.4 or Equation 2.5 to streamline the implementation of internal curing mixture design in the field (Bentz et al., 2005). In ASTM C1761-13b (ASTM, 2013b) a conservative minimum desorption value of 85% is recommended and as such has been used as the minimum amount of desorption that would allow a lightweight aggregate to be used in the design of internally cured concrete with the simplified approach presented in Equation 2.6. The authors would like to note that, while a minimum desorption of 85% may be a convenient value for specification, an aggregate with a lower desorption may be successfully used for the purposes of internal curing if the desorption is measured and accounted for in the mixture design. In practice it can be assumed that the mixture will reach

a degree of hydration of 100% and for design purposes the absorption of the LWA at 24 hours can be used. The total volume of chemical shrinkage for a given cementitious system can be either measured or approximated as a summation of the chemical shrinkage of each cementitious component times their respective mass fractions as outlined in a recent state of the art review (ASTM, 2012c; Bentz & Weiss, 2011). These approaches can be involved and as such several approximations have been suggested. For mixtures only containing cement as binder, it is appropriate to use a chemical shrinkage value of 0.065 ml/g, and for mixtures containing supplementary cementitious materials, 0.082 ml/g is a reasonable estimate for chemical shrinkage (Bentz, 1997; Haecker, Bentz, Feng, & Stutzman, 2003; Jensen & Hansen, 1996, 2001b; Lura, 2003). Using these assumptions, concrete with only cement can be internally cured with 7 kg of internal curing water per 100 kg of cement, as shown in Equation 2.6a. To be conservative, systems containing cement and supplementary cementitious materials should contain 8 kg of internal curing water per 100 kg of binder, as described by Equation 2.6b.

$$M_{LWA} = \frac{7 \cdot C_f}{\Phi_{LWA,24h}} \quad (2.6a)$$

$$M_{LWA} = \frac{8 \cdot C_f}{\Phi_{LWA,24h}} \quad (2.6b)$$

2.3 Quality Control and Production with Internal Curing

When moving from small-scale tests in the laboratory to full-scale field tests, there are several important quality control considerations that need to be considered. As internal curing is commonly used with concrete mixtures that can be classified as high performance (with $w/c < 0.42$), it is especially important that the moisture state of the lightweight fine aggregate is well defined. At the beginning of each day of production, quality control methods need to be performed to accurately account for free moisture from the aggregate.

ASTM 1761-13b describes one method that can be used to determine the moisture state, often called the “paper towel method,” pictured in Figure 2.2a (ASTM, 2013b). In this procedure, pre-wetted lightweight aggregate is dried and tested by dabbing a paper towel on the surface of the aggregate until the paper towel no longer picks up moisture, signifying that a pre-wetted surface-dry condition has been reached. Another method has been proposed, called the “centrifuge method,” is an alternative method to the paper towel method for determining the pre-wetted surface dry condition for lightweight fine aggregate (Miller, Barrett, et al., 2014). In the centrifuge method (seen in Figure 2.2b), the pre-wetted lightweight aggregate is placed in a centrifuge, and the surface moisture is extracted by the mechanical action of the centrifuge; a detailed outline of this procedure has been provided in

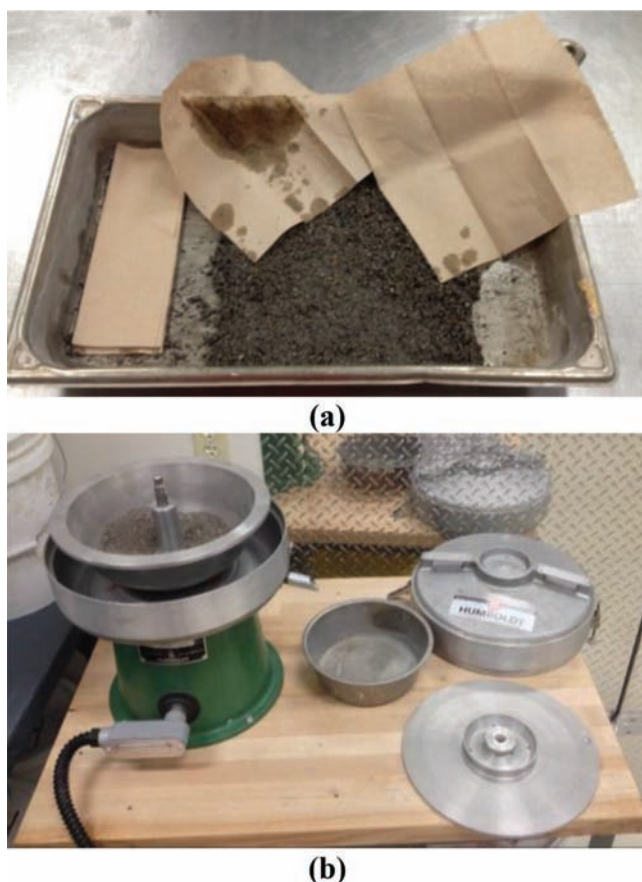


Figure 2.2 Example of (a) the paper towel method and (b) centrifuge methods for achieving pre-wetted surface dry conditions in LWA.

Appendix B. The centrifuge method has been shown to yield results comparable to the paper towel method with a higher level of precision (Miller, Spragg, et al., 2014). Using the paper towel method or the centrifuge method will give useful information for both the design and batching of internally cured concrete, including the absorption and the surface moisture of the pre-wetted fine lightweight aggregate.

The absorption of the pre-wetted lightweight aggregate is used in the design of internally cured concrete using Equation 2.6 and is used to determine the mass replacement of normal weight fine aggregate with lightweight fine aggregate. Typically, this design absorption value is determined in a laboratory after 24 hours of submersion in water. The absorption of the aggregate also needs to be verified at the time of batching in the field. It is likely that the in situ absorption after pre-wetting in the field will not be identical to the 24-hour laboratory absorption, and it is frequently higher. This can be addressed in one of two ways. The first option is that the concrete mixture can be redesigned to account for the additional in situ absorption. While this method could be technically correct, it is time intensive and can result in a smaller volume of protected paste, decreasing the efficacy of internal curing (Bentz & Snyder, 1999). The second

option, which the authors recommend, is to confirm that the design absorption has been met or exceeded and to batch the designed volume of lightweight aggregate (accounting for the increased mass of water in absorbed in the LWA due to batching).

The surface moisture of the pre-wetted fine lightweight aggregate must be accurately determined to properly account for free moisture in the overall system. As the lightweight aggregate must be pre-wetted to achieve the design absorption, aggregate stockpiles often contain a high level of surface moisture (free water). If surface moisture is underestimated, the aggregate will contain more free water and the w/cm will be higher than the designed value. This may result in decreased strength and increased permeability (Castro, 2011; Popovics, 1990). Likewise, if the surface moisture is overestimated, the aggregate will contain less free water adjusted for and the mixture will have a lower w/cm than designed, which can lead to decreased workability and problems with consolidation (Kennedy, 1940).

For conventional normal-weight aggregates, it is common practice for surface moisture to be calculated by subtracting absorbed moisture from total moisture, where total moisture, absorbed moisture, and surface moisture are defined as shown in Figure 2.3, where W_{wet} is the mass of wet aggregate or pre-wetted LWA (g), W_{ssd} is the mass of saturated surface-dry aggregate or mass of pre-wetted surface-dry LWA (g), and W_{od} is the mass of oven-dry aggregate or LWA (g). While this approach is acceptable for conventional aggregates, it is less precise for high-absorption lightweight aggregates used for internal curing. This discrepancy can be seen by calculating surface moisture as the difference of total moisture and absorbed moisture as:

$$\left(\frac{W_{wet} - W_{ssd}}{W_{ssd}} \right) \neq \left(\frac{W_{wet} - W_{od}}{W_{od}} \right) - \left(\frac{W_{ssd} - W_{od}}{W_{od}} \right) \quad (2.7)$$

As Equation 2.7 shows, the resulting surface moisture value is, by definition, incorrect by a factor of (W_{ssd}/W_{od}). The reason for the difference between conventional and lightweight aggregates is two-fold. Lightweight aggregate typically has a much higher

absorption capacity than conventional normal weight aggregate. Also, the pre-wetting period intended to make the LWA reach an appropriate absorption for internal curing leaves the lightweight aggregate stockpile with more surface moisture than a conventional aggregate stockpile.

The potential implications of improperly accounting for surface moisture can be easily seen with data from the field. The production of a high-performance internally cured bridge deck concrete was observed. The fine lightweight aggregate stockpile was pre-wetted using a sprinkler system for 72 hours, after which the sprinklers were turned off and the stockpile was allowed to drain for 16 hours. Before batching the internally cured high-performance concrete, the moisture state (absorbed moisture, surface moisture, and total moisture) was determined for all aggregates, including the pre-wetted lightweight aggregate. The total moisture of the lightweight aggregate was determined by drying using ASTM C566-13, and was found to be 30.0% (ASTM, 2013a). Absorption was then determined using the centrifuge method, and was found to be 20.0% (Miller, Barrett, et al., 2014). Using common practice, surface moisture could be incorrectly determined to be the difference between the total moisture and the absorption (30.0% - 20.0%), or 10.0%. However, using the correct formula, the proper surface moisture value would be 12.0%. This discrepancy is shown in Figure 2.4, where the “surface moisture” line shows the proper definition being used, and the “total moisture approach” shows the improper method for the determining surface moisture.

The example shows that by using standard practice with lightweight aggregate, surface moisture can easily be underestimated. This underestimation can vary as surface moisture and absorption vary, but will always be an underestimation; however, the example represents experimentally determined results from the field. The misrepresentation of surface moisture will affect the free water within the concrete mixture, increasing the w/cm. Table 2.1 shows a mixture design for the high-performance internally cured concrete that was placed

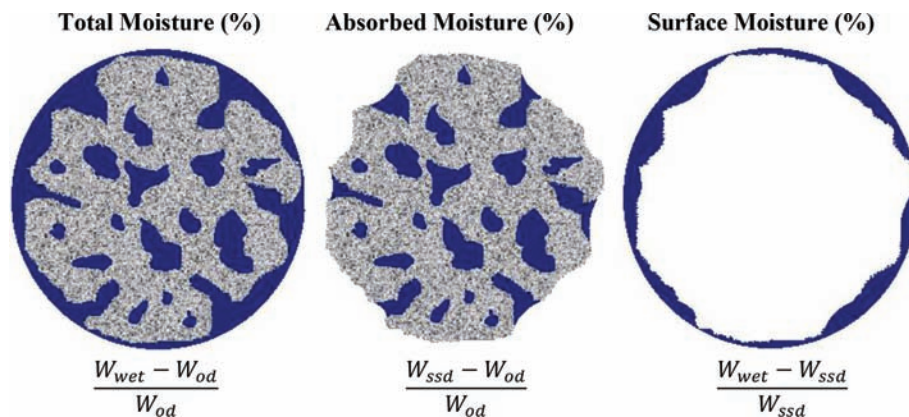


Figure 2.3 Aggregate moisture states represented schematically with definitions listed below each state pictured.

TABLE 2.1
Mixture proportions of internally cured high-performance concrete observed in moisture correction study.

Material	SSD Design Weights (kg/m ³)
Type I Cement	264
Ground Granulated Blast Furnace Slag	68
Silica Fume	9
Water	136
Natural Sand (Indiana #23)	1032
Crushed Limestone (Indiana #9)	1421
Lightweight Fine Aggregate	226

in bridge deck using the aggregate described in the example above.

The mixture design shown in Table 2.1 had a design water-to-cementitious-materials ratio of 0.40. If the surface moisture of the LWA is underestimated by 2%, an additional 4.4 kilograms of water per cubic meter would be added to the mixture. This results in the actual batched water-to-cement ratio being 0.413. In addition to increasing the water-to-cement ratio, the concrete mixture would also contain less lightweight aggregate, and therefore less internal curing, than designed. As the materials are batched, the scales will measure the weight of aggregate for the mixture, but will not be accounting for the proper moisture state.

While properly determining the surface moisture of the LWA is significant in the production of IC concrete, it is also always important to properly account for the moisture state of normal-weight aggregate. The volume percentage of normal-weight coarse and fine aggregate makes up a much larger portion of the total aggregate content than the LWA in IC concrete. The surface moisture of both fine and coarse aggregate must be measured at the beginning of production every day to properly estimate the free moisture in the concrete

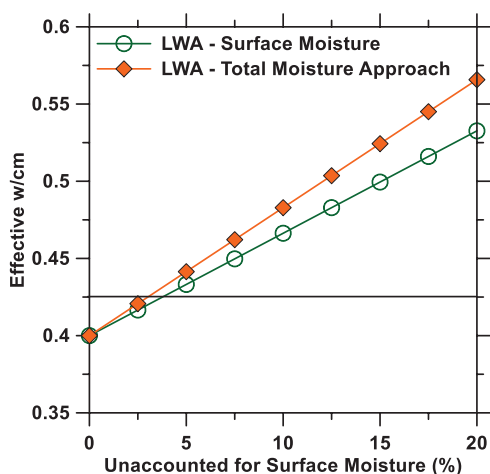


Figure 2.4 Comparison of proper (Surface Moisture) and improper (Total Moisture Approach) definitions for surface moisture of LWA. The solid horizontal line indicates the upper threshold of allowable variation in w/cm during production as stated in the INDOT specifications.

mixture. Knowing the moisture state of fine aggregate, coarse aggregate, and LWA will enable the w/cm to be tightly controlled. Figure 2.5 shows how underestimating surface moisture of normal-weight coarse and fine aggregate (CA and FA respectively) will impact the final w/cm of the concrete mixture.

If the surface moisture of the LWA is underestimated as previously described and the surface moisture of both coarse and fine aggregate is underestimated by 1%, the resulting concrete mixture will have an additional 32 kg of water per cubic meter. This increases the w/cm of the example mixture shown in Table 2.1 from 0.40 to 0.46.

It should be highlighted that in the standard specification for the production of internally cured, high-performance concrete in the state of Indiana, the maximum allowable variation in w/cm on the day of production is $\pm 0.025\%$ (INDOT, 2014a). For the example problem discussed herein, this upper limit is a w/cm of 0.425 and is indicated on Figure 2.4, Figure 2.5, and Figure 2.6 by a solid horizontal line. By inspection of Figure 2.5, it becomes readily apparent that a properly run total moisture test for the coarse and fine aggregates on the day of production should limit the fluctuation in w/cm to a value that is below the upper threshold set by the DOT. Figure 2.6 shows the effect of unaccounted for surface moisture on the LWA with the red (large) dashed lines indicating the variability in the paper towel method and the blue (small) dashed lines indicating the variability in the centrifuge method (Miller, Barrett, et al., 2014). This data indicates that a properly run test using paper towel method can inherently be out of specification due to the variability in the test. In contrast, a properly run test using the centrifuge method reduces the variability in results by an order of magnitude and can adequately be utilized to make field moisture adjustments when using pre-wetted lightweight aggregates. The key takeaway from this information is that properly conducted aggregate moisture tests for the coarse and fine aggregate using traditional techniques and for lightweight aggregate using the centrifuge method should result in the production of concrete that has an effective w/cm of ± 0.015 , where by using the paper towel test this variation increases to ± 0.042 . It should be noted that this range of variation in effective w/cm is only applicable if other sources of water addition are controlled; some examples of this may include wash water and water added en route or at the jobsite.

As previously discussed, the centrifuge method reduces the variation in results in tests requiring the LWA to be in a pre-wetted surface dry condition by an order of magnitude when compared to the paper towel method. A second strength of the centrifuge method is the consistency of the method when the amount of surface water on the LWA may vary while the absorption is approximately constant. This scenario may be representative of field stockpiles of LWA that has been soaked for a period of time then allowed to drain. It can be anticipated that the LWA should

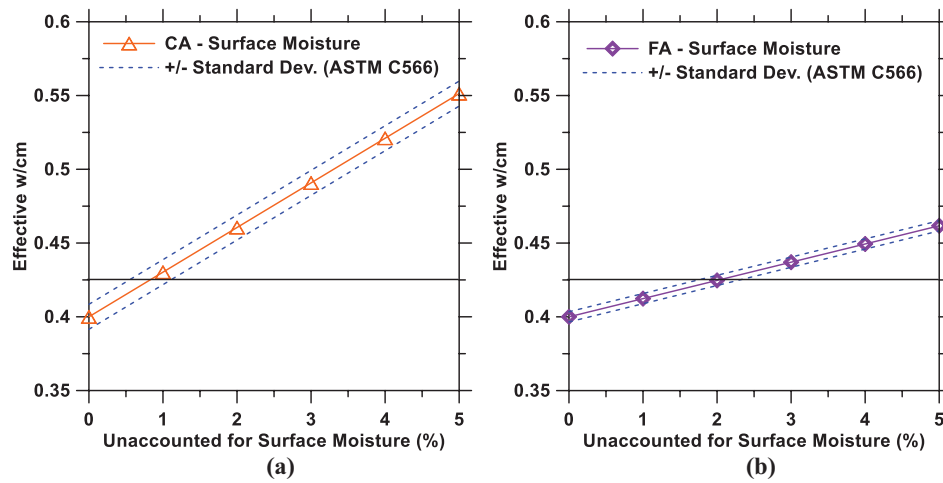


Figure 2.5 Effect on w/cm due to underestimation of surface moisture of (a) normal weight coarse aggregate (CA) and (b) fine aggregate (FA). The solid horizontal line indicates the upper threshold of allowable variation in w/cm during production as stated in the INDOT specifications.

have approximately uniformly absorbed moisture throughout the pile, while the surface moisture at any location will be a function of the shape of the pile and the duration of time the pile has been allowed to drain. For example, Figure 2.7 shows two LWA stockpiles of varying heights, in which it should be expected that the shorter stockpile shown in (a) would have more uniformity in surface moisture when compared to (b) assuming they have drained for the same period of time. Figure 2.8 shows data from Miller and colleagues that simulates this variation in surface moisture throughout a LWA

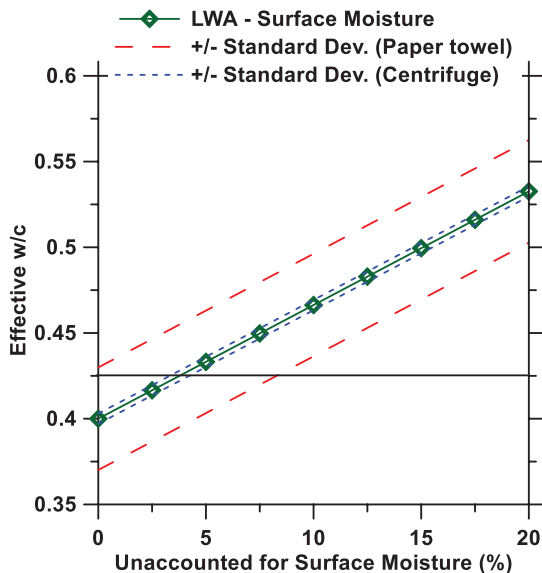


Figure 2.6 Effect on w/cm due to underestimation of surface moisture on LWA. Dashed lines indicate plus or minus one standard deviation when the surface moisture is determined by the paper towel and centrifuge methods. The solid horizontal line indicates the upper threshold of allowable variation in w/cm during production as stated in the INDOT specifications.



Figure 2.7 LWA piles being soaked prior to batching of internally cured concrete. Note that the height of pile (a) was less than 5 feet tall while the height of pile (b) was in excess of 9 feet tall.

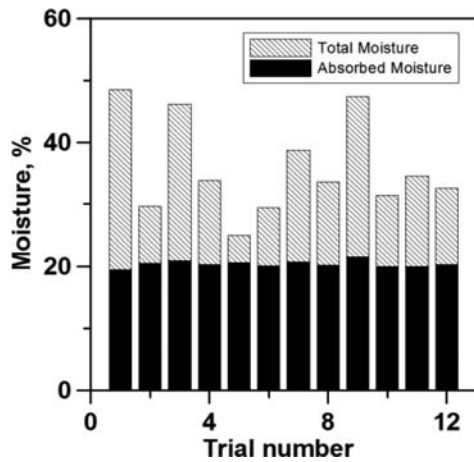


Figure 2.8 Varying surface moistures of a single LWA sample after a period of soaking in water. Values were obtained using the centrifuge method (Miller, Barrett, et al., 2014).

stockpile, demonstrating that the centrifuge method is able to recover the same absorption regardless of the surface moisture on the aggregate (Miller, Barrett, et al., 2014). The authors would like to note that while the centrifuge method may be usable for any lightweight aggregate in the pile, during production care should be exercised with efforts being given to work the pile in order to uniformly distribute the surface moisture. To this point, it is generally recommended that the LWA stockpile be limited in height and have as many free directions of drainage flow as possible available in an effort to minimize non-uniformity in surface moisture throughout the pile. Additionally, the stockpile of LWA should also be worked on a regular basis to prevent any irregularities in moisture states.

2.4 Summary and Conclusions

This chapter presented a literature review on internal curing, providing the necessary background for understanding the science of this approach toward mitigating autogenous shrinkage and putting the technique in the context of field application. Comments were made on the use of a new testing technique which utilizes a centrifuge to determine the moisture state of the lightweight aggregate. An example was then provided to instill the importance for determining the moisture states of all the aggregates if a higher performance concrete truly is desired. Finally, a few comments on field preparation of LWA stockpiles were offered.

3. MIXTURE PROPORTIONING FOR INTERNALLY CURED CONCRETE

3.1 Introduction

This chapter describes a step-by-step procedure to accompany a series of worksheets that have been prepared and made available for the use of producing internally cured concrete in the laboratory or in the field using pre-wetted fine lightweight aggregate (see Appendix G and Appendix H). This chapter

outlines how to obtain and use the pre-wetted lightweight aggregate properties to adjust the mixture design during batching and production. The basis of obtaining the LWA moisture properties will be through the use of the centrifuge method, as it has been shown to consistently and accurately enable the lightweight aggregate to be conditioned to the pre-wetted surface-dry state (Miller, Barrett, et al., 2014; Miller, Spragg, et al., 2014). Aggregate can be soaked (for 24-hour design values) or taken from the pre-wetted aggregate stockpile (for batching values) and tested in the centrifuge (a standalone test method has been outlined in Appendix B) to attain information about the properties of the aggregate including absorption, desorption, and specific gravity. These properties are all important when designing an internally cured concrete mixture (Barrett, Miller, & Weiss, 2014; Bentz et al., 2005; Bentz & Weiss, 2011). While knowing how to perform these tests properly is significant, it is equally important that they are implemented into the concrete mixture design properly. It should be mentioned here that the INDOT Office of Materials Management (OMM) has developed a Concrete Mix Design Sheet (CMDS) for use with the new class of internally cured, high-performance structural concretes which was used for the case study presented later within this report. Readers are encouraged to contact Tony Zander with the INDOT OMM to obtain a copy and detailed instructions on the use of the CMDS if desired.

This chapter begins by describing a series of steps that can be followed to easily implement internal curing in the field. First, a lightweight aggregate should be selected as an internal curing agent. This lightweight aggregate must then be characterized for absorption, desorption, and specific gravity.

Laboratory testing of the LWA shall be performed following a period of pre-wetting for a given amount of time. Currently, ASTM C1761-13b specifies that this testing is done after 72 hours of soaking in water (ASTM C1761-13b) (ASTM, 2013b), however, there can be complications when using a 72-hour design properties. Firstly, many field trials do not provide sufficient time for 72-hour conditioning. In addition, there are multiple factors that may result in the 72-hour design parameters not being reached in the field, whereby a concrete mixture designed and produced under these conditions may be left with insufficient internal curing or result in improper yielding. For this reason, research at Purdue has focused on the use of design values determined after 24 hours of pre-wetting. Using 24-hour properties instead of 72-hour properties will serve to prevent potential problems, as the 24-hour absorption and specific gravity will be smaller than those at 72 hours (and hence more easily exceeded in the field). The use of the 24-hour parameters will then result in a larger volume of lightweight aggregate being used for internal curing and is therefore more conservative. On the day of casting, the field-conditioned aggregate should contain an amount of absorbed water that exceeds the 24-hour lab absorption used in the mixture design. Rather than re-proportioning

the mixture, the volume of lightweight aggregate will remain fixed and the specific gravity will be used to adjust batch weights for additional absorbed water. In this case, the mixture will have the complete internal curing benefits without the need to redesign the mixture. Worksheets have been created to simplify this testing process and to make it easily implementable. The proper use of these sheets will be explained in further detail in the following section.

Secondly, this chapter describes how a plain concrete mixture (non-internally cured) can be modified to provide internal curing. This may be a mixture designed following ACI 211 or a mixture that a ready-mix producer has produced before and feels comfortable and confident in producing consistently (the second is recommended when available). A spreadsheet has been developed to input the plain mixture and proportions and properties of the lightweight aggregate material. The worksheet will provide a series of calculations to calculate the amount of internal curing water needed to completely account the volume reduction from chemical shrinkage. A calculation will then be performed to determine the amount of lightweight aggregate needed to supply this internal curing water.

Thirdly, this chapter discusses the spreadsheet provided as an approach to perform mixture adjustments at the time of production. Once the internally cured mixture has been designed, it is probable that it will have to be adjusted on the day of batching in the field for varying absorption and specific gravity (due to pre-wetting durations that differ from 24 hours soaking under water). The design spreadsheet incorporates these inputs for the properties determined on the day of production, and this chapter will show how to use this to assure that the mixture retains its internal curing capabilities while achieving proper yield.

While batching systems may vary, it is common for the system inputs to be in terms of saturated surface-dry design weight, absorption, total moisture, and specific gravity. The system then calculates free moisture (surface moisture) by subtracting absorption from total moisture. Many of these batching systems have built in limits for these values. It is common for the lightweight aggregate to exceed both the absorption and total moisture limits due to its high absorption capacity and the pre-wetting duration leaving the stockpile with large amounts of free moisture. If this is the case, it is often necessary to “trick” the computer system into batching the right amount of lightweight aggregate. This can be accomplished by setting the absorption input to 0% and setting the total moisture to the value of free moisture. The batching system will then account for the free moisture correctly. In the event that this method is not an option, it should be noted that several other solutions exist however they depend on the specific batching system being used. It is strongly recommended that these batching software issues be addressed prior to the day of production and be assessed on a case-by-case basis.

3.2 Obtaining Fine Lightweight Aggregate Properties for Mixture Design

As previously stated, the first step in designing an internally cured mixture is to obtain the properties of the lightweight aggregate to be used in the mixture. This testing can be performed in the laboratory to obtain an absorption value at any time. It is recommended that this value be determined after 24 hours of soaking. The authors note that these procedures may vary slightly from those listed within ITM 222, as this research represents work which preceded the publishing of said standard. For questions and needs for clarifications on the procedures listed within ITM 222 readers are encouraged to contact Tony Zander with the INDOT OMM for further information.

3.2.1 Laboratory Testing of Lightweight Aggregate Absorption

To begin the 24-hour laboratory absorption testing, the lightweight aggregate should be oven dried. This is done by placing the aggregate in an oven at $110 \pm 5^\circ\text{C}$ ($230 \pm 10^\circ\text{F}$) until constant mass is attained (usually, this is achieved after 24 hours in the oven). If an oven is not available, it is acceptable to use a hot plate or equivalent device to dry the aggregate to a constant mass. The aggregate is then removed from the oven and allowed to cool. At this time, the aggregate can be submerged in a container of water and allowed to soak for 24 hours. This is typically done in a 5 gallon bucket. After a period of 24 hours, the excess water can be decanted (drained from the aggregate). Care must be taken to avoid loss of fine material when decanting the excess water. The pre-wetted lightweight aggregate should then be stirred to eliminate segregation that may have occurred while soaking.

At this point, the 24-hour absorption of the pre-wetted lightweight aggregate can be determined. To do this, the worksheet shown in Figure 3.1 has been created to aid in calculations.

The following section describes a series of steps to use Figure 3.1 to obtain the absorption, surface moisture, and total moisture of the pre-wetted lightweight aggregate.

1. The mass of the empty centrifuge bowl must be measured and recorded as M_1 .
2. Tare the scale with the centrifuge bowl on top. Add approximately 600 grams of pre-wetted lightweight aggregate to the centrifuge bowl. Record the mass of pre-wetted aggregate added to the centrifuge bowl as M_{WET} .
3. Remove the centrifuge bowl from the scale. In order to avoid excessive vibration during centrifugation, the material should be evenly distributed in the centrifuge bowl. This can be easily done by holding the bowl level and shaking it with a circular motion.
4. Place the centrifuge bowl in the centrifuge. On top of the centrifuge bowl, place a filter paper ring and lid and secure the assembly with the nut. Place the outer housing over the assembly and fasten it with clamps. At this point, the sample is ready for centrifugation.

Absorption, Surface Moisture, and Total Moisture

Procedure	Measurement	Value
Measure mass of empty centrifuge bowl	M_1	
Measure mass of pre-wetted lightweight aggregate added to tared centrifuge bowl (600 ± 5 g)	M_{WET}	
Measure mass of centrifuge bowl and pre-wetted surface-dry aggregate after centrifugation	M_2	
Calculate mass of pre-wetted surface dry aggregate, M_{PSD}	$M_{PSD} = M_2 - M_1$	
Measure mass of empty pan used for oven-drying aggregate	M_3	
Measure mass of pan and oven dry aggregate	M_4	
Calculate mass of oven-dry aggregate, M_{OD}	$M_{OD} = M_4 - M_3$	

Results

Calculate desired properties	Result	Value
Absorption (%) = $\frac{M_{PSD} - M_{OD}}{M_{OD}} \times 100$	Absorption	
Surface Moisture (%) = $\frac{M_{WET} - M_{PSD}}{M_{PSD}} \times 100$	Surface Moisture	
Total Moisture (%) = $\frac{M_{WET} - M_{OD}}{M_{OD}} \times 100$	Total Moisture	

Sample Information: _____ Sample Date: _____

Sampled By: _____ Sample Time: _____

notes:

Figure 3.1 Worksheet used for laboratory and field determination of absorption, surface moisture, and total moisture.

- Turn the centrifuge on, and select 2000 rpm as the testing speed. Allow the sample to spin for three minutes at this speed. After three minutes, turn the centrifuge off. Once the bowl has stopped spinning, remove the outer housing, lid nut, lid, and centrifuge filter paper.
- Remove the centrifuge bowl. Tare the scale. Place the bowl on the scale, and record the mass of the pre-wetted surface-dry aggregate and the centrifuge bowl as M_2 .
- The mass of the empty centrifuge bowl (M_1) must be subtracted from M_2 to obtain the mass of the pre-wetted surface-dry aggregate (M_{PSD}). The spreadsheet will automatically make this calculation.
- Record the weight of an empty pan to be used for oven-drying the aggregate as M_3 . Transfer the material from the centrifuge bowl to the pan for oven-drying. It may be necessary to use a scraper and a brush to remove aggregate that has been pressed to the side of the centrifuge bowl. Care should be taken to assure that all material from the centrifuge bowl is transferred to the pan.
- Place the pan and aggregate in an oven at 110 ± 5 °C (230 ± 10 °F) until constant mass is reached. If an oven is not available, it is acceptable to use a hot plate or other device to reach an oven dried state.
- Once the aggregate has been oven-dried, remove it from the oven and allow it to cool.
- Measure the mass of the pan and oven-dry aggregate and record it as M_4 .
- The mass of the oven-dry aggregate (M_{OD}) can be calculated by subtracting M_3 from M_4 .
- The 24-hour absorption can be determined following the absorption equation in the Results section of the worksheet. The spreadsheet will calculate the absorption automatically.

3.2.2 Laboratory Testing of Lightweight Aggregate Relative Density (Specific Gravity)

Next, the relative density of the aggregate after 24 hours of soaking should be determined. To begin the 24-hour laboratory relative density testing, the lightweight aggregate should be oven dried. This is done by placing the aggregate in an oven at 110 ± 5 °C

Relative Density

Procedure	Measurement	Value
Measure mass of pycnometer filled to calibration mark	M_{PW}	
Measure mass of pre-wetted surface-dry lightweight aggregate added to tared empty pycnometer (~300 g)	M_{PSD}	
Measure mass of pycnometer with pre-wetted surface-dry lightweight aggregate and water to calibration mark	M_{PS}	
Measure mass of empty pan used for oven-drying aggregate	M_5	
Measure mass of pan and oven dry aggregate	M_6	
Calculate mass of oven-dry aggregate, M_{OD}	$M_{OD} = M_6 - M_5$	

Results

Calculate desired properties	Result	Value
Relative Density (PSD) = $\frac{M_{PSD}}{M_{PW} + M_{PSD} - M_{PS}}$	Pre-Wetted Surface-Dry Relative Density	
Relative Density (OD) = $\frac{M_{OD}}{M_{PW} + M_{PSD} - M_{PS}}$	Oven-Dry Relative Density	

Material: _____ Sample Date: _____

Sampled By: _____ Sample Time: _____

notes:

Figure 3.2 Worksheet used for laboratory and field determination of relative density (specific gravity).

(230 ± 10 °F) until constant mass is attained (usually, this is achieved after 24 hours in the oven). If an oven is not available, it is acceptable to use a hot plate or equivalent device to dry the aggregate to a constant mass. The aggregate is then removed from the oven and allowed to cool. At this time, the aggregate can be placed in a container of water and allowed to soak for 24 hours. This can be done in a 5 gallon bucket. After a period of 24 hours, the excess water can be decanted (drained from the aggregate). Care must be taken to avoid loss of fine material when decanting the excess water. The pre-wetted lightweight aggregate should then be stirred to eliminate segregation that may have occurred while soaking. At this point, the 24-hour relative density of the pre-wetted lightweight aggregate can be determined. To do this, the worksheet shown in Figure 3.2 has been created to aid in calculations.

A pycnometer is required to test the specific gravity. Either a mason jar or volumetric flask style pycnometer (shown in Figure 3.3) may be used.

The following section describes a series of steps to use Figure 3.2 to measure the relative density of the pre-wetted lightweight aggregate.



Figure 3.3 Examples of pycnometers that can be used for determining the specific gravity of pre-wetted lightweight aggregate (mason jar style shown at left Test Mark Industries, 2015 and volumetric flask shown at right Capitol Scientific, 2015).

1. The mass of the pycnometer filled with water to the calibration mark should be measured and recorded as M_{PW} .
2. Remove the water from the pycnometer.
3. Tare the scale with the centrifuge bowl on top. Add approximately 600 grams of pre-wetted lightweight aggregate to the bowl.
4. Remove the centrifuge bowl from the scale. In order to avoid excessive vibration during centrifugation, the material should be evenly distributed in the centrifuge bowl. This can be easily done by holding the bowl level and shaking it with a circular motion.
5. Place the centrifuge bowl in the centrifuge. On top of the centrifuge bowl, place a filter paper ring and lid and secure the assembly with the nut. Place the outer housing over the assembly and fasten it with clamps. At this point, the sample is ready for centrifugation.
6. Turn the centrifuge on, and select 2000 rpm as the testing speed. Allow the sample to spin for three minutes at this speed. After three minutes, turn the centrifuge off. Once the bowl has stopped spinning, remove the outer housing, lid nut, lid, and centrifuge filter paper.
7. Place the empty pycnometer on the scale and then tare the scale.
8. Add approximately 300 g of pre-wetted surface-dry material from the centrifuge bowl to the pycnometer, and record the added mass as M_{PSD} .
9. Add water to the pycnometer to cover the aggregate (fill to about 2/3 of the capacity of the pycnometer). The pycnometer must then be agitated to eliminate all air bubbles. The pycnometer can be rolled, tapped, or shaken to do this. This step can take in excess of 10 minutes to eliminate all entrapped air bubbles.
10. Once air bubbles are no longer visible, fill the pycnometer with water to the calibration mark. Tare the scale. Place the pycnometer with sample and water filled to the calibration mark on the scale and record this mass as M_{PS} .
11. Calculate the 24-hour pre-wetted surface-dry specific gravity as described in the Results section of the worksheet. The spreadsheet will automatically calculate this value.

The pre-wetted surface-dry specific gravity is the specific gravity that should be used in the SSD design of the internally cured mixture; however, it is common for this number to change by the day of production. Specific gravity is dependent on the amount of absorbed water in the aggregate. It beneficial to also calculate the oven-dry specific gravity, as this value can later be used to calculate the specific gravity at any absorption value. The following steps, continued from the procedure above, describe how to do this.

1. Measure the mass of an empty pan that will be used to oven-dry the contents of the pycnometer and record this as M_5 .
2. Empty the water and aggregate from the pycnometer into the pan. The excess water can be drained, but it is very important to not lose any fine material (any excess water in the pan will be boiled off (evaporated) in the oven, so it is acceptable to have free water in the pan).
3. Place the pan with aggregate in an oven at $110 \pm 5 \text{ }^\circ\text{C}$ ($230 \pm 10 \text{ }^\circ\text{F}$) until a constant mass is attained.
4. Remove the pan from the oven, allow it to cool, and record the mass of the pan and oven dried aggregate as M_6 .

5. The oven-dry mass of the aggregate can then be determined by subtracting M_5 from M_6 .
6. Calculate the oven-dry specific gravity of the lightweight aggregate using the equation shown in the Results section of the worksheet. The spreadsheet will automatically calculate this result.

The equation for calculating oven-dry relative density is shown below as Equation 3.1, and the equation for calculating pre-wetted surface-dry relative density is shown below as Equation 3.2.

$$\text{Relative Density (OD)} = \frac{M_{OD}}{M_{PW} + M_{PSD} - M_{PS}} \quad (3.1)$$

$$\text{Relative Density (PSD)} = \frac{M_{PSD}}{M_{PW} + M_{PSD} - M_{PS}} \quad (3.2)$$

It should be noted that, when calculating the relative density in the oven-dry state and when calculating relative density in the pre-wetted surface dry state, the only difference in the equation is the term in the numerator (M_{OD} is changed to M_{PSD}). For a given sample of lightweight aggregate, the relationship between oven-dry mass and pre-wetted surface-dry mass is given using the absorption, as shown in Equation 3.3.

$$M_{PSD} = M_{OD} \times (1 + \text{Absorption}) \quad (3.3)$$

Using this relationship, we can calculate the pre-wetted surface-dry specific gravity of that aggregate at any known absorption using Equation 3.4.

$$\begin{aligned} \text{Relative Density (PSD)} \\ = \text{Relative Density (OD)} \times (1 + \text{Absorption}) \end{aligned} \quad (3.4)$$

To further illustrate this concept, Figure 3.4 shows how relative density increases linearly as absorption increases.

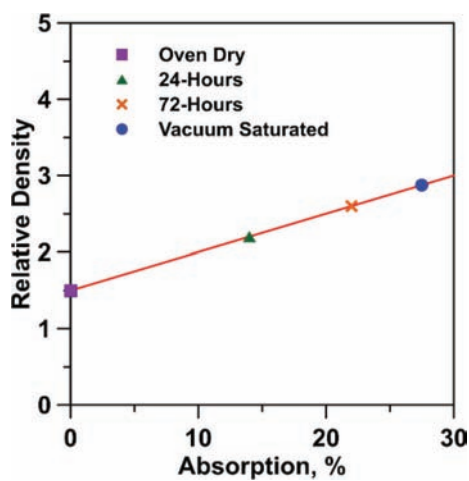


Figure 3.4 Graph showing the relationship of absorption to relative density.

3.2.3 Laboratory Testing of Lightweight Aggregate Desorption

Desorption can be determined for the pre-wetted lightweight aggregate. This property should be checked periodically to confirm that the aggregate still has a desorption that is favorable for internal curing. Figure 3.5 has been created to assist in performing this testing.

This test requires the use of a chamber capable of maintaining a relative humidity of 94% and a scale with accuracy of at least 0.01 g. This is typically done by placing a supersaturated salt solution in an airtight container. To maintain 94% relative humidity, supersaturated Potassium Nitrate (KNO₃) solution is used and the temperature must be kept at 23 ± 1°C

(Greenspan, 1977). An example of one such setup is shown in Figure 3.6.

Figure 3.6 shows a chamber with a shelf at mid-height. Supersaturated KNO₃ solution sits on the bottom shelf, while the specimens being tested sit above the solutions. A relative humidity sensor is included in the chamber so that this can be monitored. This can also be achieved using a mason jar or another type of vessel that can be sealed. The saturated salt solution is then made in the bottom of the jar. Then, wire fabric or some other material is used to hold the sample above the solution.

To begin the desorption test, the test sample must first be conditioned. The lightweight aggregate should be oven dried. This is done by placing the aggregate in an oven at 110 ± 5 °C (230 ± 10 °F) until constant

Desorption

Procedure	Measurement	Value
Measure mass of empty pan for desorption sample	M ₇	
Measure mass of pre-wetted surface-dry lightweight aggregate added to tared empty pan (~5 g)	M _{PSD}	
Measure mass of pan and sample every 24 hours to determine equilibrium mass (M _{EQ} , ± 0.01 g from previous day's mass)	Day 1	
	Day 2	
	Day 3	
	Day 4	
	Day 5	
	Day 6	
	Day 7	
	Day 8	
	Day 9	
	Day 10	
	M _{EQ}	
Calculate mass of aggregate at equilibrium	M ₉₄ = M _{EQ} - M ₇	
Measure mass of pan and oven dry aggregate	M ₈	
Calculate mass of oven-dry aggregate, M _{OD}	M _{OD} = M ₈ - M ₇	
Calculate mass of water in M ₉₄ sample	M _{W94} = M ₉₄ - M _{OD}	
Calculate total mass of water in pre-wetted surface-dry sample	M _{WPSD} = M _{PSD} - M _{OD}	

Results

Calculate desired properties	Result	Value
$W_{LWA} = \frac{M_{PSD} - M_{94}}{M_{OD}}$	Mass of water released at 94% RH	
Percent Desorption = $\frac{M_{WPSD} - M_{W94}}{M_{WPSD}} \times 100$	% Desorption	

Material: _____ Sample Date: _____

Sampled By: _____ Sample Time: _____

notes:

Figure 3.5 Worksheet used for laboratory desorption testing of pre-wetted lightweight fine aggregate.



Figure 3.6 Example of a 94% relative humidity chamber used for desorption testing.

mass is attained (usually, this is achieved after 24 hours in the oven). If an oven is not available, it is acceptable to use a hot plate or equivalent device to dry the aggregate to a constant mass. The aggregate is then removed from the oven and allowed to cool. At this time, the aggregate can be placed in a container of water and allowed to soak for 24 hours. This can be done in a 5 gallon bucket. After a period of 24 hours, the excess water can be decanted (drained from the aggregate). Care must be taken to avoid the loss of fine material when decanting the excess water. The pre-wetted lightweight aggregate should then be stirred to eliminate segregation that may have occurred while soaking. The aggregate is now prepared for testing. The following section describes a series of steps to use Figure 3.5 to measure the desorption of the pre-wetted lightweight aggregate.

1. Measure the mass of an empty pan (a petri dish may also work) that will hold the sample throughout the test and record this mass as M_7 .
2. Tare the scale with the centrifuge bowl on top. Add approximately 600 grams of pre-wetted lightweight aggregate to the bowl.
3. Remove the centrifuge bowl from the scale. In order to avoid excessive vibration during centrifugation, the material should be evenly distributed in the centrifuge bowl. This can be easily done by holding the bowl level and shaking it with a circular motion.
4. Place the centrifuge bowl in the centrifuge. On top of the centrifuge bowl, place a filter paper ring and lid and secure the assembly with the nut. Place the outer housing over the assembly and fasten it with clamps. At this point, the sample is ready for centrifugation.
5. Turn the centrifuge on, and select 2000 rpm as the testing speed. Allow the sample to spin for three minutes at this speed. After three minutes, turn the centrifuge off. Once the bowl has stopped spinning, remove the outer housing, lid nut, lid, and centrifuge filter paper.
6. Stir the sample in the centrifuge bowl to minimize any segregation that may have occurred during centrifugation.
7. Tare the empty pan on the scale. Add approximately 5 grams of the pre-wetted surface-dry material to the pan and record this as M_{PSD} in the worksheet.
8. Place the pan in the 94% relative humidity chamber.

9. Measure the mass of the sample every 24 hours and record these measurements as Day 1, Day 2, etc.
10. Repeat daily measurements until the change in mass between two 24-hour measurements is less than 0.01 g. When this criterion is reached, the final mass measurement is recorded as M_{EQ} .
11. Place the aggregate and pan in an oven at 110 ± 5 °C (230 ± 10 °F) until constant mass is obtained.
12. Remove the pan from the oven, allow it to cool, and record the mass as M_8 .
13. Calculate the mass of water in the aggregate in the pre-wetted surface-dry condition (M_{WPSD}) and the mass of water in the aggregate at equilibrium in the 94% relative humidity chamber (M_{W94}) as described in the worksheet. If the spreadsheet is used, these values will be automatically calculated.
14. Calculate the desorption of the aggregate as described in the worksheet. If the spreadsheet is used, these values will be automatically calculated.

3.2.4 Field Testing of Lightweight Aggregate Absorption and Surface Moisture

Absorption must again be tested in the field on the day of production. It is essential to confirm that the absorption is above the design value so that the system will contain the designed amount of internal curing water. Additionally, the surface moisture (free moisture) is needed so that the batch water can be adjusted. It is common for contracts to require a period of pre-wetting (usually a minimum of 48 hours) followed by a draining period (usually a minimum of 12 hours). On the day of production, begin by obtaining a sample of pre-wetted lightweight aggregate from the stockpile. The stockpile should be turned by the loader operator before this sample is taken to obtain a representative sample.

At this point, the in-situ absorption and surface moisture of the pre-wetted lightweight aggregate can be determined. To do this, the worksheet shown in Figure 3.1 can be used again. The following section describes a series of steps to use Figure 3.1 to get the absorption and surface moisture of the pre-wetted lightweight aggregate.

1. The mass of the empty centrifuge bowl must be measured and recorded as M_1 .
2. Tare the scale with the centrifuge bowl on top. Add about 600 grams of pre-wetted lightweight aggregate to the bowl. Record the mass of pre-wetted aggregate added to the bowl as M_{WET} .
3. Remove the centrifuge bowl from the scale. In order to avoid vibration during centrifugation, the material should be evenly distributed in the centrifuge bowl. This can be easily done by holding the bowl level and shaking it with a circular motion.
4. Place the centrifuge bowl in the centrifuge. On top of the centrifuge bowl, place a filter paper ring and lid and secure the assembly with the nut. Place the outer housing over the assembly and fasten it with clamps. At this point, the sample is ready for centrifugation.
5. Turn the centrifuge on, and select 2000 rpm as the testing speed. Allow the sample to spin for three minutes at this

- speed. After three minutes, turn the centrifuge off. Once the bowl has stopped spinning, remove the outer housing, lid nut, lid, and centrifuge filter paper.
6. Remove the centrifuge bowl. Tare the scale. Place the bowl on the scale, and record the mass of the pre-wetted surface-dry aggregate and the centrifuge bowl as M_2 .
 7. The mass of the empty centrifuge bowl (M_1) must be subtracted from M_2 to obtain the mass of the pre-wetted surface-dry aggregate (M_{PSD}). The spreadsheet will automatically make this calculation.
 8. Record the weight of an empty pan to be used for oven-drying the aggregate as M_3 . Transfer the material from the centrifuge bowl to the pan for oven-drying. It may be necessary to use a scraper and a brush to remove aggregate that has been pressed to the side of the centrifuge bowl. Care should be taken to assure that all material from the centrifuge bowl is transferred to the pan.
 9. Place the pan and aggregate in an oven at $110 \pm 5 \text{ }^\circ\text{C}$ ($230 \pm 10 \text{ }^\circ\text{F}$) until constant mass is reached. If an oven is not available, it is acceptable to use a hot plate or other device to reach an oven dried state.
 10. Once the aggregate has been oven-dried, remove it from the oven and allow it to cool.
 11. Measure the mass of the pan and oven-dry aggregate and record it as M_4 .
 12. The mass of the oven-dry aggregate (M_{OD}) can be calculated by subtracting M_3 from M_4 .
 13. The absorption and surface moisture can be determined following the equations in the Results section of the worksheet. The spreadsheet will calculate the absorption and surface moisture automatically.

3.2.5 Field Testing of Lightweight Aggregate Relative Density (Specific Gravity)

As previously discussed in Section 3.2.2, the specific gravity will change as the absorption changes. The specific gravity will have to be retested in the field on the day of production. On the day of production, begin by obtaining a sample of pre-wetted lightweight aggregate from the stockpile. The stockpile should be turned by the loader operator before this sample is taken to obtain a representative sample. To determine the specific gravity, the worksheet shown in Figure 3.2 can be used again to aid in calculations. The following section describes a series of steps to use Figure 3.2 to get the relative density of the pre-wetted lightweight aggregate.

1. The mass of the pycnometer filled with water to the calibration mark should be measured and recorded as M_{PW} .
2. Remove the water from the pycnometer.
3. Tare the scale with the centrifuge bowl on top. Add approximately 600 grams of pre-wetted lightweight aggregate to the bowl.
4. Remove the centrifuge bowl from the scale. In order to avoid vibration during centrifugation, the material should be evenly distributed in the centrifuge bowl. This can be easily done by holding the bowl level and shaking it with a circular motion.
5. Place the centrifuge bowl in the centrifuge. On top of the centrifuge bowl, place a filter paper ring and lid and secure the assembly with the nut. Place the outer housing

over the assembly and fasten it with clamps. At this point, the sample is ready for centrifugation.

6. Turn the centrifuge on, and select 2000 rpm as the testing speed. Allow the sample to spin for three minutes at this speed. After three minutes, turn the centrifuge off. Once the bowl has stopped spinning, remove the outer housing, lid nut, lid, and centrifuge filter paper.
7. Place the empty pycnometer on the scale and then tare the scale.
8. Add approximately 300 g of pre-wetted surface-dry material from the centrifuge bowl to the pycnometer, and record the added mass as M_{PSD} .
9. Add water to the pycnometer to cover the aggregate (fill to about 2/3 of the capacity of the pycnometer). The pycnometer must then be agitated to eliminate all air bubbles. The pycnometer can be rolled, tapped, or shaken to do this. This step can take in excess of 10 minutes to eliminate all entrapped air bubbles.
10. Once air bubbles are no longer visible, fill the pycnometer with water to the calibration mark. Tare the scale. Place the pycnometer with sample and water filled to the calibration mark on the scale and record this mass as M_{PS} .
11. Calculate the pre-wetted surface-dry specific gravity as described in the Results section of the worksheet. The spreadsheet will automatically calculate this value.

The pre-wetted surface-dry specific gravity is the specific gravity that should be used in the SSD design of the internally cured mixture. It should be noted that this value can be calculated as discussed in Section 3.2.2 using the known value of oven-dry specific gravity and the absorption on the day of production.

Once the absorption, surface moisture, specific gravity, and desorption have been calculated, the fourth tab of the testing spreadsheet (shown in Figure 3.7) will auto-populate and give the properties that are needed for the internally cured concrete mixture design.

The following section will discuss how these values are applied to the internally cured concrete mixture design.

3.3 Using Fine Lightweight Aggregate Properties to Design and Internally Cure a Concrete Mixture

Once the 24-hour absorption, desorption, and relative density have been determined for the lightweight aggregate to be used to internally cure a concrete mixture, it is possible to design the internally cured mixture. A spreadsheet, shown in Figure 3.8, has been

Inputs for Mixture Design

LWA Absorption:	
LWA Desorption:	
LWA PSD Specific Gravity	
Surface Moisture	

Figure 3.7 Summary of properties to be used in designing an internally cured concrete mixture.

created to aid field technicians in internally curing any plain concrete mixture.

In Figure 3.8, inputs shown in orange are typically obtained from the concrete producer, while inputs shown in green are obtained from the lightweight aggregate producer or testing agency. This design method takes a plain (i.e., not internally cured) concrete mixture and converts it to an internally cured mixture based on the assumption that the volume of internal curing water added is equal to the chemical shrinkage of the cementitious materials (Bentz et al., 2005). Once the plain mixture design inputs are added, the lightweight aggregate properties (absorption, desorption, specific gravity) are then placed in cells under “Internal Curing

Properties.” Once these inputs have been added, the sheet will automatically calculate the replacement of normal weight sand with pre-wetted lightweight aggregate. The SSD design concrete mixture (based on lightweight aggregate properties determined after 24-hour laboratory testing) is then shown at the bottom of the spreadsheet in the section titled “IC Mixture Design.”

The mixture design given by this approach assumes that the aggregate on the day of batching will have an absorbed moisture content equal to that of a 24-hour laboratory soak. Many specifications require a pre-wetting time of at least 72 hours. The increased soaking time typically results in stockpiled aggregate with absorption greater than that of the 24-hour design absorption.

Project: _____ Date: _____

Mixture ID: _____

Operator: _____

Plain Mixture Design

Target Air, %	6.5%
w/c	0.421

Legend

Ready Mix Input
LWA Input

Materials	Weight	SG (SSD)	Volume, ft ³
Cement	455	3.15	2.315
GGBFS	130	2.99	0.697
Fly Ash	0	2.64	0.000
Silica Fume	25	2.2	0.182
Sand	1231	2.623	7.521
Coarse Aggregate 1	1795	2.763	10.411
Coarse Aggregate 2	0	2.763	0.000
Water	257	1	4.119
Air	0	0	1.755
Σ	3893	-	26.999

Internal Curing Properties

LWA Absorption:	15.0%
LWA Desorption:	85.0%
LWA PSD Specific Gravity	1.750
Cement Factor	610
Chemical Shrinkage:	0.07
Degree of Hydration	1
PSD LWA Replacement	385
SSD Sand Replaced	577
% Volume Replacement	46.9%

IC Mixture Design

Materials	Weight	SG (SSD)	Volume, ft ³
Cement	455	3.15	2.315
GGBFS	130	2.99	0.697
Fly Ash	0	2.64	0.000
Silica Fume	25	2.2	0.182
Sand	654	2.623	3.994
Lightweight Aggregate	385	1.750	3.527
Coarse Aggregate 1	1795	2.763	10.411
Coarse Aggregate 2	0	2.763	0.000
Water	257	1	4.119
Air	0	0	1.755
Σ	3701	-	26.999

Figure 3.8 Mixture design spreadsheet used to internally cure a concrete mixture.

Because of this, the mixture must be slightly adjusted on the day of batching to achieve proper yield. The entire mixture is not redesigned. Instead, only the specific gravity of the lightweight aggregate is adjusted. As long as the stockpiled aggregate absorption is above that of 24 hour, this allows for the system to retain the full benefit of internal curing. The second sheet of the mixture design spreadsheet (shown in Figure 3.9) makes this adjustment.

The first column of Figure 3.9 lists the materials in the mixture. The second column uses the 24-hour design weights from Figure 3.8. The third column then adjusts the lightweight aggregate batch weight for the specific gravity on the day of batching (an input located at the top of this spreadsheet). The free moisture of each aggregate is then listed in the fourth column. The fifth column adjusts the batch weights to account for the surface moisture. Finally, the last column uses the batch size (an input located at the top of this spreadsheet) to output the target batch weights for the materials going into the concrete truck.

The worksheet to determine absorption, surface moisture, and total moisture (Figure 3.1) can again be used to calculate the absorption (to verify that the 24-hour design absorption has been met or exceeded) and surface moisture. Additionally, the relative density (specific gravity) should be retested in the field using the relative density worksheet (Figure 3.2). These day of batching properties are then input in the spreadsheet shown in Figure 3.9. As was discussed in Chapter 2, the definition of surface moisture commonly used for fine and coarse aggregates is not appropriate for high-absorption aggregates such as lightweight aggregates. The surface moisture for lightweight aggregate input

in this worksheet should instead be calculated using the equation in the provided worksheet (Figure 3.1).

The calculations in this spreadsheet hold the volume of lightweight aggregate in the internally cured concrete mixture constant while adjusting the design weight for the current specific gravity. The spreadsheet also calculates the target batch weights, which allows the batch tickets to be checked to verify that batching tolerances were achieved.

3.4 Summary and Conclusions

This chapter served to discuss how to use developed spreadsheets to calculate properties of lightweight aggregate and how to implement these properties into the mixture design process for internally cured concrete. The properties of the lightweight aggregate that are important for design are absorption, desorption, and relative density. To make an initial design, these properties should be determined after a 24-hour soaking period. Once the properties are obtained, any existing mixture can be internally cured using the mixture proportion design sheet. It is then necessary to repeat testing using the same worksheets the day of batching in the field to make sure that the mixture is produced as designed. The absorption needs to be checked to make sure that it is equal to or higher than the 24-hour absorption used in the original design. The surface moisture (free moisture) must be calculated correctly to achieve the design w/c. Finally, the relative density must be tested again in the field to adjust the additional absorbed moisture. This will allow the volume of lightweight aggregate to remain constant and will prevent the mixture from under-yielding.

Project: _____ Date: _____

Mixture ID: _____

Operator: _____

Batch Size, yd ³	9
LWA Specific Gravity Day of Batching	1.755

Materials	Design SSD Weight based on 24 hour PSD absorption, lbs/yd ³	Design SSD Weight to be Input Day of Batching, lbs/yd ³	Tested Aggregate Surface Moisture, %	Target Batch Weight, lbs/yd ³	Target Batch Weight, lbs
Cement	455	455	-	455	4095
GGBFS	130	130	-	130	1170
Fly Ash	0	0	-	0	0
Silica Fume	25	25	-	25	225
Sand	654	654	2.82%	672	6050
LWA	385	388	6.87%	415	3736
Coarse Aggregate 1	1795	1795	1.90%	1829	16462
Coarse Aggregate 2	0	0	-	0	0
Water	257	257	-	178	1600
Air	0	0	-	0.0	0
Σ	3701	3704	-	3704	33338

Figure 3.9 Mixture design spreadsheet used to calculate batch weights on the day of batching.

Once all of the properties have been entered into the spreadsheet, a final SSD mixture design is given. Batch weights adjusted for free moisture are also given so that batching tolerances can be monitored.

4. BRIDGE DECK PRODUCTION AND CONSTRUCTION DOCUMENTATION

4.1 Introduction

This chapter provides documentation of the production and construction of the four internally cured, high-performance concrete bridge decks cast in Indiana in 2013. This document reflects the records obtained by the Purdue research team in coordination with the Indiana Department of Transportation. The Purdue research team was present for a trial batch for each bridge deck mixture and attended the deck pour for bridges #2, #3, and #4 while attending the railing pour for bridge #1. A generalized description of the events that occurred at the trial batch and deck pour are provided in the following paragraphs in order to lend context to the readers for following sections.

For each IC-HPC mixture, a trial batch was held a minimum of 28 days prior to the date of construction. The trial batch was held as an effort for each producer to demonstrate the ability to produce an internally cured, high-performance concrete that performed to the Standard Specification set by the INDOT (2014a). In addition, the trial batch served as a forum for the ready-mix producer to interact with the DOT, the lightweight aggregate suppliers, and Purdue researchers to address any scientific, technical, or procedural questions and/or issues prior to the date of construction. On the day of the trial batch, representatives from the INDOT Office of Materials Management (OMM), the INDOT district testing personnel, the lightweight aggregate supplier, and the Purdue research team would join the ready-mix producer in quality control testing necessary for producing the IC HPC. Upon arrival, a loader operator would provide a sample pile of each aggregate in accordance with Indiana Testing Method (ITM) No. 207-08T. It should be noted that prior to this time, the lightweight aggregate pile would have been soaked for a minimum of 48 hours and allowed to drain for a minimum of 12 hours prior to testing. In general, the total moisture of the fine and coarse aggregate would be determined by the ready-mix producer in accordance with ASTM C 566 and checked against results obtained by INDOT district testing. The absorption, specific gravity, and total moisture of the lightweight aggregate was determined by the INDOT OMM following the procedure outlined in Appendix B of ACI 211.2 (ACI, 1998), where the LWA was spun at 500 rpm for 20 minutes to reach a pre-wetted surface dry condition. The Purdue research team independently ran each of these tests on two samples, with the exception in that the centrifuge method was employed at 2000 rpm for 3 minutes (Miller, Barrett, et al., 2014) (a procedure that has since been adopted (with a slight

modification of sample size) as the standard practice in Indiana Testing Method (ITM) 222). With the aggregate moisture corrections determined, the INDOT OMM personnel would then explain (sometimes in excess of 1 hour) to the ready-mix producer how the concrete mixture design sheet (CMDS) (a document developed by the INDOT for the use of producing IC HPC) functioned. During this period of time, the CMDS would be updated with the free moisture adjustments and finalized batching weights would then be set by the INDOT OMM.

Together, the INDOT OMM personnel and the ready-mix producer would then work to batch a trial truck of concrete containing 3 cubic yards of the IC HPC. Due to restrictions on batching tolerances outlined in the Standard Specification ($\pm 1\%$ of target weight), three of the four producers elected to perform this batching manually (i.e., not utilizing their automated system). This highlights one issue with the current trial batch procedure. It is recommended by the research team that the automated system be used to ensure that the producer is prepared to produce concrete in a similar fashion to the way it will be produced on the day of production.

To batch the concrete, the mixture design (SSD lb/yd³ of each constituent material), the aggregate specific gravities, absorptions, and total moistures, and the admixture dosages needed to be input into the producer's batching software. This is the step in the process where issues with the batching software first arise and should be addressed. Common problems include limits on maximum absorption being exceeded when using lightweight aggregate, surface moisture corrections being calculated incorrectly, and incorrect target batch weights computed by the software. At this point, one of a multitude of "tricks" (discussed in Chapter 2) may be implemented in order to reach agreement between the batching computer and the target batch weights set by the INDOT OMM. Once the batching system is set, manual hopper controls would be used to weigh out target batch weights of each of the constituent materials. Once the materials are batched within tolerance, a truck would be loaded, allowed to mix for a short period of time, and then tested for by the producer to get an initial indication of the fresh properties of the concrete (slump, air content, and unit weight). At this time, adjustments to the admixture dosages may be made by the producer through manual addition to the truck. The truck would then continue to agitate the mixture for a period of time roughly equivalent to the estimated haul time to the bridge deck site, after which the truck would be tested a second time by the producer. If at this point the producer found the fresh properties of the IC HPC to conform to the Standard Specifications, the district INDOT personnel and Purdue researchers would separately test the fresh properties and procure samples for hardened testing at later ages. If however, after the simulated haul time, the fresh properties of the IC HPC do not meet the specification, the concrete in the truck would be discarded and the batching and testing procedure would be repeated

with a second truck after adjustments to correct the mixture (typically admixture dosage rates) are made.

On the day of a deck cast, the aforementioned parties involved in the trial batch would arrive at the ready mix plant at an agreed upon amount of time (typically three hours, established by the INDOT) prior to the requested time of batching for the first truck. During this period, quality control tests for the coarse, fine, and lightweight aggregates would be performed to determine the surface moisture adjustments for each, the absorption of the lightweight aggregate, and the specific gravity of the lightweight aggregate. The final moisture adjustments, determined and agreed upon by the ready-mix producer and the INDOT, would then be used to determine a finalized mixture design for that day of production. The producer and the DOT then together assured that this information was entered correctly into the automated batching system. The first truck would then be batched, allowed to mix briefly, and tested at the plant by the producer for an initial indication of the slump, air content, and unit weight (relative yield). The truck would then be sent to the bridge deck while full production ensued. At this time, a representative of the INDOT OMM, materials testing personnel from the INDOT district office, a quality control manager for the ready-mix producer, and representatives from the Purdue research team would then travel to the construction site. Once at the bridge deck, the contractor would begin placing, vibrating, screeding, and finishing the deck. Generally after every 50 cubic yards of concrete is placed, the INDOT district testing personnel would test the fresh properties of the concrete at the point of placement (i.e., after the concrete is placed, it would be removed from the deck and tested elsewhere) to verify whether the material met the Standard Specification. Upon completion of the deck casting, the contractor would cover the deck with an approved curing system (typically wet burlap and plastic). It should be noted that due to the use of internal curing, the INDOT removed the requirement for the bridge deck to be coated with a commercial sealant product.

After the bridge deck casting, the Purdue research team would then return to the ready-mix plant and order two trucks, batched with 3 cubic yards of concrete each. The first truck would contain the exact mixture that had been sent to the bridge deck that day (i.e., IC HPC) while the second truck would be a modification of the IC HPC where the lightweight aggregate was replaced with fine aggregate. This would in effect be a non-internally cured, high-performance concrete, which in this study will be simply referred to as a high-performance concrete (HPC). A series of samples would be cast from each truck and allowed to cure for at least two days prior to transportation to the laboratory for testing.

This chapter will present notes, aggregate moisture properties, mixture design and analysis, and experimental data obtained from the trial batch and the day of production for each bridge deck in the study. In an effort to quantify variation in mixtures produced at

the trial batch and on the day of the deck pour, compressive strength and sealed resistivity measurements on field produced samples will be presented up to an age of 28 days. This represents a window of data that may have been available to the producer and the DOT prior to the deck pour (i.e., the results from the trial batch mixture) while establishing a benchmark for which the concrete used during production may be evaluated against.

This chapter is organized sequentially by the order in which the bridge decks were cast; this order coincides with the order presented in Chapter 1. The results of the testing for this chapter and all following chapters will be labeled by the type of concrete mixture followed by the bridge deck number the mixture corresponds to. For example, the first bridge deck material will be indicated as “IC HPC 1” and it will be compared to a reference (non-internally cured) material indicated as “HPC 1.” The results from the trial batch for each IC HPC will be indicated as “Trial” followed by the corresponding bridge number (e.g., “Trial 1” corresponds to “IC HPC 1”). For each bridge deck, a brief overview of the project will be given, the as-batched mixture proportions will be summarized, observations about the trial batch and deck pour made by the Purdue research team will be given, and experimental results of compressive strength and sealed resistivity will be shown.

4.2 Bridge #1

The first bridge deck in this study is North-Bound I-69 over Little Black Creek, located in Grant County, Indiana. The original bridge design was approved in 1962 with approved plans for deck reconstruction dated in 1984 and 1995 prior to the 2013 deck reconstruction. This corresponds to in service periods of the bridge decks of approximately 22, 11, and 18 years. According to the 2013 National Bridge Inventory (NBI) report (bridge inspection data made available by the Federal Highway Administration (FHWA)) the last inspection of the bridge was performed in October of 2012, where the bridge was given a sufficiency rating of 63.3% with the present deck condition being rated at 5 (defined as “Fair Condition” characterized where “all primary structural elements are sound but may have minor section loss, cracking, spalling, or scour.”). The bridge was deemed “structurally deficient” due to the superstructure condition.

The structural design of the bridge utilizes a continuous reinforced concrete slab supporting three spans of 21 ft, 28 ft, and 21 ft in the direction of travel. The deck thickness for this bridge is 15.5 in, with 2.5 in of top cover and 1 in of bottom cover for the outermost reinforcing layers. In the longitudinal direction, #8 bars were spaced at 6 in on center for both the top and bottom layers of reinforcement. The transverse reinforcing steel in the deck were #4 bars in the top and #6 bars in the bottom both spaced at 12 in on center. The reinforcing steel utilized in this project was epoxy coated. The annual average daily traffic (AADT)

TABLE 4.1
Concrete mixture design and as-batched proportions for bridge #1 [lb/yd³]. Admixtures are provided in [oz/cwt].

	Approved Design	Trial Batch	Deck Pour	Purdue, IC HPC 1	Purdue, HPC 1
W/CM	0.406	0.405	—	0.405	0.428
Cement	395	398	—	395	398
Fly Ash	125	130	—	125	125
GGBFS	—	—	—	—	—
Silica Fume	25	25	—	25	25
Coarse Aggregate	1835	1846	—	1825	1834
Fine Aggregate	765	780	—	744	1221
Lightweight Aggregate	325	319	—	329	—
Air Entrainer	0.5–3.0	1.71	—	1.20	1.70
HRWRA	10–15	13.33	—	15.00	13.25
MRWRA	—	—	—	—	—
Retarder	2-8	3.79	—	1.99	3.77
Air Content [%]	6.5	6.1	—	7.3	7.1
Slump [in]	2.5–5.5	3.5	—	3.5	6.0
Unit Weight [lb/ft ³]	136.7	139.79	—	137.3	142.1
Paste Content [%]	24.09	24.46	—	24.07	24.95

*Indicates measures not conforming to limits set within INDOT specifications for IC HPC (INDOT, 2014a).

measured in 2007 was 27,450 with 40% of this traffic volume being trucks.

4.2.1 Mixture Design and As-Batched Mixture Proportions

The approved mixture design and as-batched mixture proportions from the trial batch and the two concrete trucks purchased by the Purdue research team for the first bridge deck can be seen in Table 4.1. Mixture proportions for the deck pour are not reported as they were not able to be collected by the Purdue research team and copies of tickets containing mixture proportions were not collected during construction by the INDOT. It can be seen that the trial batch, IC HPC 1, and HPC 1 mixtures conformed to the limitations set in the specifications. The calculated relative yield of the IC HPC 1 mixture was however out of tolerance, at 1.026, likely a repercussion of the addition of aggregate (as agreed upon the INDOT OMM and the producer) to the approved mixture design to correct for under-yielding at the trial batch.

The aggregate moisture properties used on the day of production for the IC HPC 1 and HPC 1 mixtures are reported in Table 4.2. The specific gravity in the saturated surface dry condition (SG_{SSD}) and the design absorption for the coarse and fine aggregates

were provided by the concrete producer and are assumed constant. The design absorption for the lightweight aggregate was determined in the laboratory by the INDOT using an approach outlined in ACI 211 (1998). The total, surface, and batch absorption for the coarse and fine aggregates were determined by the Purdue research team in accordance with ASTM C 566 (ASTM, 2013a). The moisture properties for the LWA were also measured by the Purdue research team; this testing was performed in accordance with the procedure outlined by Miller and colleagues, with the recommended testing procedure provided in Appendix B of this report (Miller, Barrett, et al., 2014). In regards to the LWA, it can be seen that the batch absorption exceeded the design absorption, ensuring that more than the minimum amount of water was available for internal curing.

4.2.2 Trial Batch

The trial batch for the first bridge deck followed the general procedure outlined in the introduction of this chapter. A particular point of interest beyond these general procedures was the role of the LWA supplier. The following paragraph is an excerpt from the special provisions set by the INDOT (see Appendix A for full document).

TABLE 4.2
Aggregate moisture properties on the day of bridge #1 construction.

	SG_{SSD} (N/A)	Design Absorption (%)	Total Moisture (%)	Surface Moisture (%)	Batch Absorption (%)
Coarse Aggregate	2.638	1.79	3.96	2.17	1.79
Fine Aggregate	2.649	1.12	5.93	4.81	1.12
Lightweight Aggregate	1.753	13.74	29.67	8.69	19.3

A representative from the lightweight aggregate supplier shall be present for the trial batch. This representative shall have the necessary test equipment and technical expertise to measure the properties of lightweight fine aggregate for use in structural concrete. The representative shall provide testing, guidance and direction in proportioning the IC concrete per ACI 211.2.

This first trial batch is the only instance of this project (trial batch or otherwise for each of the four bridge decks) in which a technician from the LWA supplier attempted to characterize the moisture state of their LWA in the field. Further, the technician was insistent on use of the drained unit weight of the LWA as well as the use of the so-called paper towel test as described in ASTM C 1761 to determine these moisture states (ASTM, 2013b). These methods have been shown to produce results with greater variability than those from the centrifuge method (Miller, Barrett, et al., 2014) (the experimentally determined variability of each of these tests have reported in Appendix C). It should also be noted that the guidance of the specification refers to ACI 211.2, a document on standard practices for structural lightweight concrete. The authors mention that ACI 211.2 may be inappropriate for the production of internally cured concrete and readers are encouraged to follow proportioning procedures outlined in ASTM C 1761 (ASTM, 2013b), field testing procedures for LWA outlined by Miller and colleagues (Miller, Barrett, et al., 2014), and recommendations made within this report. In addition, it should be highlighted that the recommendations within ASTM C 1761 advocate the use of a 72-hour absorption value for the lightweight aggregate when designing the mixture, however the authors recommend the method implemented in this study where the mixture design was based on a 24-hour absorption value and the absorption on the day of production was required to meet or exceed this design value. This method is preferable to the recommendations of ASTM C 1761 as it is considered to be a conservative design method as well as being more easily specifiable.

Two batched trucks were necessary for the ready-mix supplier to pass the trial batch. Upon batching of the first truck, it was concluded by the INDOT that the mixture was below acceptable targets for the air content and slump and the mixture was not yielding appropriately. This truck was utilized to determine better admixture dosages for the second truck, and at the recommendation of the INDOT, the mixture was adjusted to correct the yield by adding additional coarse and fine aggregate. The second truck batched for the trial was accepted with a measure slump of 3.5," net air content of 6.1%, and a unit weight of 139.79 lb/cyd. It should be noted that the mixture was described as "harsh" by many of the participants at the trial batch, the extent of which being best exhibited by the wetted coarse aggregate which preceded the homogenous concrete mixture upon discharge of the concrete from the truck.

4.2.3 Deck Pour

The Purdue research team was not notified of the deck pour and was therefore not present for the bridge deck pour. A photograph of the finished bridge deck can be seen in Figure 4.1. It is the authors' understanding that the bridge was cast with the mixture that was appropriately adjusted for the aggregates moistures for the first half of the deck. The ready-mix supplier then batched one or more trucks for a different project, and resumed batching trucks for the IC HPC bridge deck. Upon resuming the work, the mixture design from the trial batch (i.e., not corrected for the aggregate moistures measured that day) was used for the completion of the deck. On the first half of the deck, the mixture was not properly consolidated and resulted in honeycombing (see Figure 4.2) at the bottom of the deck (it was presumed by the INDOT that the 1" clearance for the bottom layer of reinforcing steel may not have been suitable for a mixture with low workability and high-coarse aggregate contents). In an informal interview with the construction crew after the bridge deck had been constructed, the crew expressed displeasure with IC HPC mixture's placeability. These concerns came from the inability of the crew to properly vibrate the deck as well as the need for conveyors during placement (i.e., the mixture was not able to be pumped). It should be noted that the



Figure 4.1 Photograph of bridge deck #1 taken approximately 2 months after casting.



Figure 4.2 Photograph of the underside of bridge deck #1 approximately 2 months after casting. The voids seen are primarily due to consolidation issues and were later patched with an INDOT approved filler material.

designed paste volume of the IC HPC 1 mixture was near 24% and was likely too low to provide sufficient workability to ensure proper consolidation.

In order to obtain samples for laboratory testing, the Purdue research team attended the railing pour for the first bridge deck. Upon completion of the rail pour, two trucks containing three cubic yards of concrete were ordered. The first truck was intended to be the same mixture that was sent to the rail pour, however due to over-batching of the fly ash, this truck was rejected. The second truck contained the same mixture sent to the bridge (batched within tolerance) while the third truck contained concrete where the LWA was replaced with fine aggregate (while all other proportions remained unchanged). The official temperature for the day as

reported by the National Oceanic and Atmospheric Administration (NOAA) were a high of 29.4 °C with a low of 14.4 °C (84.9 and 57.9 °F, respectively). The day was partly cloudy with no precipitation. The mixture proportions for the IC HPC 1 mixture and the HPC 1 mixture can be seen in Table 4.1. Due to discrepancies in the measured moisture content of the fine and lightweight aggregate surface moisture contents, the HPC 1 mixture was produced at a slightly elevated w/cm. A corresponding increase in the measured slump was observed.

4.2.4 Experimental Results

Cylindrical specimens were cast at the trial batch and from each of the trucks ordered by the research team at the railing pour. These samples were cured then transported to the laboratory for testing. Figure 4.3 shows the evolution of the compressive strength (ASTM, 2012a) of the mixture accepted at the trial batch compared to the mixtures produced on the day of the railing pour. Figure 4.4 shows the evolution of the sealed resistivity (i.e., not corrected for changes in degree of saturation (DOS)) of these mixtures (Spragg et al., 2013). It can readily be seen that the mixtures exceed the strength requirement within the first week of hydration and additionally the Trial 1 and IC HPC 1 mixtures show consistency after one week of testing. These results are reflected equally by the sealed resistivity method, which can be correlated to quantify microstructural development of the mixture. In comparison of the IC HPC and the HPC mixtures, it can be noticed that the strength of the internally cured mixture was higher which can likely be attributed to differences in w/cm. Due to the dependence of the resistivity method on degree of saturation as well as degree of hydration of the concrete, a direct comparison of this data may not

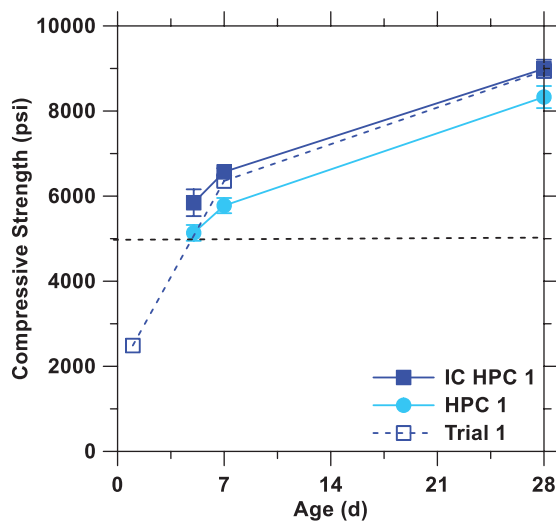


Figure 4.3 Compressive strength of samples produced from the first bridge deck mixtures compared to a reference mixture. The dashed line indicates the minimum acceptable limit as per the specifications.

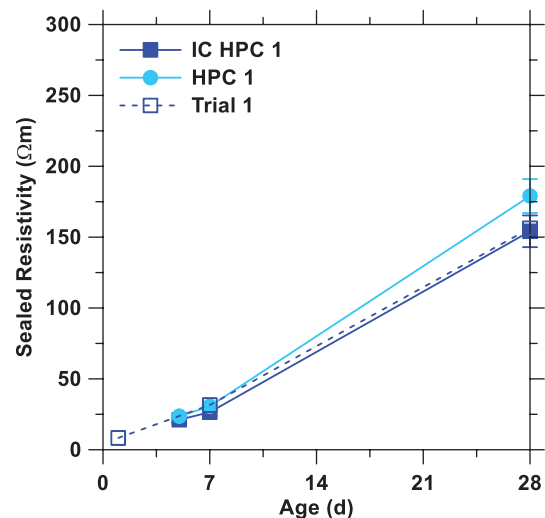


Figure 4.4 Sealed resistivity measurements of samples produced from the first bridge deck mixtures compared to a reference mixture.

be appropriate (Spragg, 2013). Rather, this method is presented to provide a comparison between two mixtures that are intended to be the same (i.e., the trial batch and the IC HPC 1 mixture can be compared) where it can be seen that the two mixtures behave similarly. An in depth comparison of the IC HPC 1 and HPC 1 mixtures will be presented in the following chapter.

4.3 Bridge #2

The second bridge deck in this study is US 150 over Lost River, located in Orange County, Indiana. The original bridge design was approved in 1963 with approved plans for deck reconstruction dated in 1980 prior to the 2013 deck replacement. This corresponds to in service periods of the bridge decks of approximately 17 and 33 years. According to the 2013 NBI report the last inspection of the bridge was performed in October of 2012, where the bridge was given a sufficiency rating of 91.5% with the present deck condition being rated at 4 (defined as “Poor Condition” characterized by, “advanced section loss, deterioration, spalling, or scour”). This bridge was deemed “structurally deficient” due to the poor condition of the bridge deck.

The structural design of the bridge utilizes a continuous, composite steel beam design supporting three spans of 69.75 ft, 84.5 ft, and 69.75 ft in the direction of travel. The deck thickness for this bridge is 8 in, with 2.5 in of top cover and 1 in of bottom cover for the outermost reinforcing layers. In the longitudinal direction, #5 bars were spaced at 8 in on center for both the top and bottom layers of reinforcement. The transverse reinforcing steel in the deck were #5 bars in the top and bottom both spaced at 8 in on center. The reinforcing steel utilized in this project was epoxy coated. The AADT measured in 2011 was 1,900 with 16% of this traffic volume being trucks.

4.3.1 Mixture Design and As-Batched Mixture Proportions

The approved mixture design and as-batched mixture proportions from the trial batch and the two concrete trucks purchased by the Purdue research team for the second bridge deck can be seen in Table 4.3. Mixture proportions for the deck pour were not collected by the Purdue research team or the INDOT for this bridge deck. It can be seen that the trial batch, IC HPC 2, and HPC 2 mixtures conformed to the limitations set in the specifications with the only exception being measured slump values greater than 5". The calculated relative yield of the IC HPC 2 mixture was within 1% tolerance.

The aggregate moisture properties measured on the day of production for the IC HPC 2 and HPC 2 mixtures are reported in Table 4.4. In regards to the LWA, it can be seen that the batch absorption exceeded the design absorption, ensuring that more than the minimum amount of water was available for internal curing.

The LWA surface moisture was measured throughout the morning by the Purdue research team and is listed in Table 4.5. It can be seen that the initial surface moisture value of the aggregate is higher than tests at later ages, while the later testing showed reasonably stable results over time. This may occur for two reasons. The first reason is that the initial sample taken at 05:00 was procured by a standardized method utilizing a front end loader to turn a sample pile from three directions to obtain individual samples for testing. This procedure will result in a higher surface moisture content due to the minimization of surface effects. The second reason that the first test resulted in a higher surface moisture content may be related to the drainage period, wherein water on the surface of the aggregate is still draining from the pile. In general this leads to two conclusions: (1) variability of the surface moisture of

TABLE 4.3
Concrete mixture design and as-batched proportions for bridge #2 [lb/yd³]. Admixtures are provided in [oz/cwt].

	Approved Design	Trial Batch	Deck Pour	Purdue, IC HPC 2	Purdue, HPC 2
W/CM	0.406	0.400	—	0.396	0.403
Cement	443	445	—	443	443
Fly Ash	—	—	—	—	—
GGBFS	96	95	—	100	98
Silica Fume	25	25	—	25	25
Coarse Aggregate	1800	1801	—	1802	1802
Fine Aggregate	780	786	—	780	1336
Lightweight Aggregate	332	339	—	346	—
Air Entrainer	0.2–7.5	0.59	—	0.59	0.59
HRWRA	2–8	4.60	—	5.45	5.47
MRWRA	—	—	—	—	—
Retarder	2–10	1.95	—	2.99	3.00
Air Content [%]	6.5	6.0	—	5.1	5.2
Slump [in]	2.5–5.5	2	—	8.0*	7.0*
Unit Weight [lb/ft ³]	137.2	140.2	—	133.9	143.1
Paste Content [%]	24.59	24.43	—	24.43	24.61

*Indicates measures not conforming to limits set within INDOT specifications for IC HPC (INDOT, 2014a).

TABLE 4.4
Aggregate moisture properties on the day of bridge deck #2 construction.

	SG _{SSD} (N/A)	Design Absorption (%)	Total Moisture (%)	Surface Moisture (%)	Batch Absorption (%)
Coarse Aggregate	2.653	1.33	1.57	0.24	1.33
Fine Aggregate	2.609	1.45	3.27	1.82	1.45
Lightweight Aggregate	1.754	14.92	30.42	9.88	18.7

the LWA within the pile is more significant than changes due to environmental conditions that may lead to evaporation and (2) steps should be taken to ensure that the stockpile of LWA achieves a mostly uniform surface moisture state. Such measures include reducing the height of the pile to allow the majority of the surface moisture to drain during the dedicated drainage period (12–15 hours) and working the stockpile prior to loading it in hoppers. An alternative would be to simply account for any changes in moisture content of the LWA by running the centrifuge test (Miller, Barrett, et al., 2014) and updating the mixture design throughout production.

4.3.2 Trial Batch

The trial batch for the second bridge deck followed the general outline described in the introduction of this chapter. A point of particular interest at this trial batch was encountered when entering moisture corrections in the batching software where the required correction for the surface moisture on the lightweight aggregate exceeded the upper limit of the software. As discussed in previous chapters, this is an issue that can typically be worked around by “tricking” the software. In contrast to these methods, at this trial batch the INDOT OMM had the ready-mix producer fill a five gallon bucket of water (using the hose attached to the concrete truck) to establish a rate of flow. The truck was then batched using manual controls and approximately 66 seconds of water was added to the truck via the onboard hose, with official time being kept by the INDOT OMM. This truck was then tested for an initial indication of fresh properties where the net volumetric air content (as measured by the producer) was 10.6%. After 20 minutes of mixing, the net air content was measured to be 6.0%. At this time, approximately one gallon of water was added to the truck and after 5 additional minutes of mixing, the net air content was (again measured by the producer) 7.0%. The Purdue

TABLE 4.5
Surface moisture variability throughout production.

Time	Surface Moisture (%)
05:00	9.88
07:35	7.12
08:45	6.35
09:35	7.17

research team measured a net air content of 6.0% after approximately 30 minutes of testing. This truck was approved by the INDOT for production.

4.3.3 Deck Pour

On the day of the deck pour, the official temperature for the area reported by the NOAA was a maximum of 35.6 °C with a minimum of 22.2 °C (96.1 and 72.0 °F, respectively). On the morning of the pour, the research team was initially informed that they were the lone party requesting to test the fine and coarse aggregate moisture conditions. This later changed when the INDOT informed the producer that they were required to run aggregate moisture tests to determine the appropriate moisture corrections for the IC HPC mixture. Production began shortly after finalizing the mixture design and verifying the initial fresh properties were near their target values. Of specific relation to the production of internally cured concrete, the producer was required to refill the lightweight aggregate hoppers throughout production; this is in contrast to typical production for this specific producer, where the fine and coarse aggregate bins are refilled by a third party since the ready-mix plant is located in an active quarry. For many producers in Indiana this is not the norm and as such the loading of the lightweight aggregate should not be viewed, in the researchers’ opinion, as an added challenge to the production of internally cured concrete.

An image taken at the deck pour of the second bridge deck can be seen in Figure 4.5. The haul time to the bridge deck was approximately 25 minutes on a two lane highway. On the day of construction, other road construction was taking place and at times limited traffic to one lane. This resulted in some trucks having longer haul times, especially as traffic increased near midday. At the bridge deck, the fresh properties were monitored by the INDOT district technicians after every 50 yd³. It was reported that the air content measured at the point of placement was lower than desired, especially during the early stages of production. Figure 4.6 shows a digital composite of two images taken during the first half of the bridge deck pour, where the pump arm can be seen to extend laterally outward followed by significant straight drop to the bridge deck (for reference, the total length of the pump was approximately 100 ft). It is possible that excessive free fall to the point of placement that the pump geometry resulted in may have contributed to issues with air content at the point of placement. In addition,



Figure 4.5 Internally cured bridge deck being placed in 2013 on US 150 over Lost River in Orange County, Indiana.

concerns of “pumpability” were heard both prior to placement and during construction. Again, it may be possible that an excessive free fall and disrupted haul time (resulting at times in infrequent continual pumping) may not have been suitable conditions for the pump to maintain proper back-pressure for smooth pumping. The final concern voiced by the contractor was the ability to finish the material, describing it as “sticky” and attributing this to the presence of silica fume in the mixture.

4.3.4 Experimental Results

The compressive strength of the trial batch and the samples procured on the day of the deck pour can be seen in Figure 4.7 while the sealed resistivity can be seen in Figure 4.8. It can be seen that the mixture produced on the day of the deck pour varied substantially from the mixture approved at the trial batch. This is likely a difference encountered by the accuracy of water addition of the automated system used during production and the hose that was used at the trial batch. The IC HPC 2 mixture does exceed the minimum strength criterion while the resistance to chloride diffusion of the mixture will be discussed in greater detail in the following chapter.

4.4 Bridge #3

The third bridge deck in this study is US 31 over Hutto Creek, located in Scott County, Indiana. The original bridge design was approved in 1940 with approved plans for deck reconstruction dated in 1977 prior to the 2013 deck replacement. This corresponds to in service periods of the bridge decks of approximately 37 and 36 years. According to the 2013 NBI report the last inspection of the bridge was performed in January of 2012, where the bridge was given a sufficiency rating of 94.3% with the present deck condition being rated at



Figure 4.6 Digital composite of two images taken depicting the pump type and technique at the second bridge deck cast.

6 (defined as “Satisfactory Condition” characterized by, “structural elements show some minor deterioration.”). This bridge was deemed “not deficient,” however the report did indicate that the safety measures for the bridge railings, transitions, and approach did not meet currently acceptable standards.

The structural design of the bridge utilizes a composite steel beam design supporting one span of 55 ft in the direction of travel. The deck thickness for this bridge is 8 in, with 2.5 in of top cover and 1 in of bottom cover for the outermost reinforcing layers. In the longitudinal direction, #4 bars were spaced at 8 in on center for the top layer of reinforcement and #5 bars were spaced at 7.5 to 8 in on center in the bottom layer of reinforcement. The transverse reinforcing steel in the deck were #5 bars spaced at 8 in on center in both the top layer and bottom layers. The reinforcing steel utilized in this project was epoxy coated. The AADT measured in 2012 was 12,500 with 6% of this traffic volume being trucks.

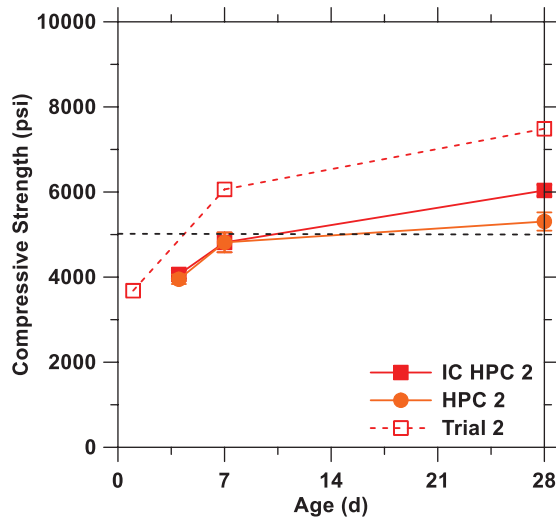


Figure 4.7 Compressive strength of samples produced from the second bridge deck mixtures compared to a reference mixture. The dashed line indicates the minimum acceptable limit as per the specifications.

4.4.1 Mixture Design and As-Batched Mixture Proportions

The approved mixture design and as-batched mixture proportions from the trial batch and the two concrete trucks purchased by the Purdue research team for the third bridge deck can be seen in Table 4.6. A range of mixture proportions observed during the casting of this bridge deck have been summarized here, while the mixture proportions for each individual truck can be seen in Appendix D. It can be seen that the w/cm varies between each mixture, the admixture dosages vary between the deck pour and the trucks procured by

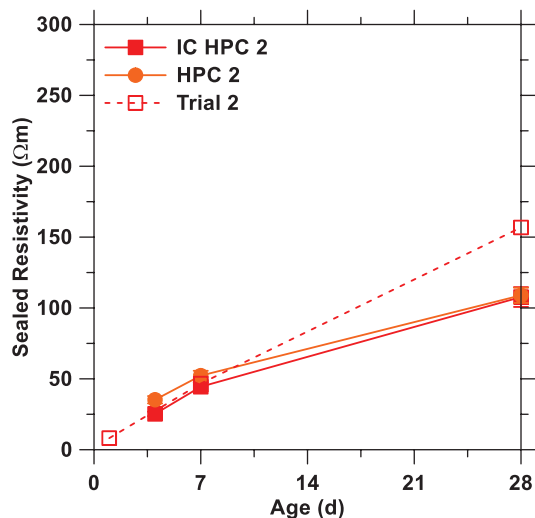


Figure 4.8 Sealed resistivity measurements of samples produced from the second bridge deck mixtures compared to a reference mixture.

the Purdue research team, and as such the fresh properties of the concrete are inconsistent. It should also be noted that the batching tickets from trucks #2, 3, and 7 have boxes marked indicating, “water added by request,” however there is no verifiable way to quantify any additional water that may have been added.

The aggregate moisture properties measured on the day of production for the IC HPC 3 and HPC 3 mixtures are reported in Table 4.7. In regards to the LWA, it can be seen that the batch absorption exceeded the design absorption, ensuring that more than the minimum amount of water was available for internal curing.

4.4.2 Trial Batch

The trial batch for the third bridge deck followed the general procedure outlined in the introduction of this chapter. At this trial, the producer opted to use the automated system to batch the material whereas all other producers involved in this study batched using manual controls. Two trucks were necessary for the trial batch, with the first truck being rejected due to air contents in excess of 11%. The second truck batched had a gross air content of 10.5%, however it was reasoned by the INDOT OMM and the producer that the mixture should have high enough strength to meet the specification with an elevated air content. In addition to admixture dosage issues, the lightweight aggregate for both trucks was under-batched by 3.4% each time; the producer was allowed to weigh out additional lightweight aggregate in a bucket and add the material manually to the truck after batching. It should also be noted that the concrete produced during this trial batch exceeded the maximum RCPT result threshold according to testing performed by the INDOT and was therefore not approved for production. An agreement was reached between the INDOT and the producer to modify the mixture design which reduced the w/cm from 0.400 to 0.396 and the paste volume from 0.400 to 0.396. To achieve this, the cement content was reduced from 443 to 435 lb/yd³, silica fume content was increased from 17 to 25 lb/yd³, and the normal weight fine aggregate was increased from 820 to 825 lb/yd³. The modified approved mixture design is shown under the “Approved Design” column of Table 4.6, and the construction of the bridge deck proceeded without a successful trial batch.

4.4.3 Deck Pour

On the day of the deck pour, the official temperature for the area reported by the NOAA was a maximum of 29.4 °C with a minimum of 15.0 °C (84.9 and 59.0 °F, respectively). On the morning of the deck pour, aggregate moistures were taken by INDOT personnel and the Purdue research team, however the producer was not observed to have performed these tests. Once a finalized mixture design was approved production for the bridge deck began. The estimated haul time for this

TABLE 4.6
Concrete mixture design and as-batched proportions for bridge #3 [lb/yd³]. Admixtures are provided in [oz/cwt].

	Approved Design	Trial Batch	Deck Pour	Purdue, IC HPC 3	Purdue, HPC 3
W/CM	0.396	0.39	0.416-0.419	0.447	0.422
Cement	435	443	434-437	432	432
Fly Ash	115	117	114-116	113	113
GGBFS	—	—	—	—	—
Silica Fume	25	17	17	17	17
Coarse Aggregate	1740	1743	1723-1729	1731	1725
Fine Aggregate	825	821	818-821	818	1338
Lightweight Aggregate	340	331	334	419	—
Air Entrainer	0.1-6.0	1.56	0.99-1.08	0.89	0.95
HRWRA	10-40	9.82	9.54-9.81	9.49	10.08
MRWRA	1.5-5.0	2.95	2.88	1.96	1.90
Retarder	—	—	—	—	—
Air Content [%]	6.5	10.5	5.1-6.7	1.8*	5.9
Slump [in]	2.5-5.5	6	3.5-7.0	2.0	2.0
Unit Weight [lb/ft ³]	137.3	132.6	137.3-141.3	144.1	146.0
Paste Content [%]	24.89	24.76	25.26-25.32*	26.0*	25.17*

*Indicates measures not conforming to limits set within INDOT specifications for IC HPC (INDOT, 2014a).

bridge deck was approximately 40 minutes. Upon arrival of the first truck, it was found that the mixture was not able to be discharged from the truck into the hopper due to site geometry for the pump. A ramp was built by the contractor to aid in solving this issue, however the length of the haul time and the additional time required to build the ramp resulted in the producer opting to not use the truck of material for construction. A portion of this truck was however pumped and placed, resulting in the contractor being required to attempt to remove this material from the deck as best as possible.

Construction of the third bridge deck can be seen in Figure 4.9. The contractor that placed the concrete offered no objections to the IC HPC mixture, admitting they would not have known it was a different mixture had they not been informed midway through construction. The pump operator also had no objections to the “pumpability” of the material, however concern was expressed to the long interval between truck arrivals (batch tickets indicated batching intervals of 30 to 49 minutes between trucks) resulting at one point in the necessity of cycling material in a loop through the pump to prevent clogging. At the completion of the construction of the bridge deck, where the original order was for 36 yd³ of concrete, the final order total

was 54 yd³ with the first truck being recalled by the producer and the sixth truck being unaccounted for. In addition to these challenges, during the procurement of trucks purchased by the Purdue research team, two trucks of IC HPC were produced which did not meet the specification. The second truck was used for this study, despite the mixture not meeting the specified fresh air content, due to material shortages.

4.4.4 Experimental Results

The compressive strength from the trial batch and the samples procured on the day of construction can be seen in Figure 4.10 while the sealed resistivity of these mixtures can be seen in Figure 4.11. It can be readily noticed that the strength of this mixture was much lower than the other IC HPC mixtures in this study and the sealed resistivity reflects this information. The INDOT determined that the performance of this mixture was due to controllable error and approved a modified mixture for construction. The results of the IC HPC 3 mixture can be seen to be on the order of the previous two IC HPC mixtures, however it should be noted that discrepancies in mixture proportions exist between the trucks which were used in construction and those which were purchased by the Purdue research

TABLE 4.7
Aggregate moisture properties on the day of bridge deck #3 construction.

	SG _{SSD} (N/A)	Design Absorption(%)	Total Moisture(%)	Surface Moisture(%)	Batch Absorption(%)
Coarse Aggregate	2.710	1.40	3.44	2.04	1.40
Fine Aggregate	2.610	1.90	4.54	2.64	1.90
Lightweight Aggregate	1.750	13.75	27.89	6.60	20.0



Figure 4.9 Internally cured bridge deck being cast in 2013 on US 31 over Hutto Creek in Indiana.

team on the same day. It should be emphasized that the correction of these discrepancies between the trial batch and the deck pour demonstrate the value of holding a trial batch which may be used as a tool to ensure specifications compliance of the mixture on the day of construction and ultimately result in an improved potential performance of the bridge deck.

4.5 Bridge #4

The fourth bridge deck in this study is SR 933 over Baugo Creek, located in St. Joseph County, Indiana. The original bridge structure design was approved in 1918 (then a steel truss bridge) with reconstruction of the bridge to update the structural design to a steel beam design approved in 1935. Details for repairs (including a deck replacement) to the steel beam bridge were approved in 1973 prior to the 2013 reconstruction. This corresponds to in service periods of the bridge decks of approximately 17, 38, and 40 years. According to the 2013 NBI report the last inspection of the bridge was performed in July of 2012, where the bridge was given a sufficiency rating of 44.1% with the present deck condition being rated at 4 (defined as “Poor Condition” characterized by, “advanced section loss, deterioration, spalling, or scour.”). This bridge was deemed “structurally deficient,” due to its poor deck and substructure condition ratings.

The structural design of the bridge utilizes a continuous composite prestressed concrete bulb-tee beam bridge design supporting two spans of 84.5 ft each. The deck thickness for this bridge is 8 in, with 2.5 in of top cover and 1 in of bottom cover for the outermost reinforcing layers. In the longitudinal direction, #7 and #5 bars were alternated, being spaced at 8 in on center in the top layer of reinforcement in the negative moment region over the pier. The bottom layer of longitudinal reinforcement were #5 bars spaced at 8 in on center. The transverse reinforcing steel in the deck were #5 bars in the top and bottom, being spaced at 6 in

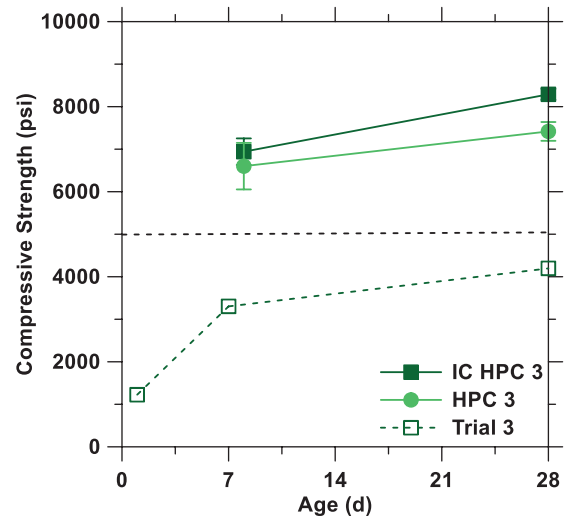


Figure 4.10 Compressive strength of samples produced from the third bridge deck mixtures compared to a reference mixture. The dashed line indicates the minimum acceptable limit as per the specifications.

on center in the top layer and 7 in on center in the bottom layer. The reinforcing steel utilized in this project was epoxy coated. The AADT measured in 2011 was 15,000 with 4% of this traffic volume being trucks.

4.5.1 Mixture Design and As-Batched Mixture Proportions

The approved mixture design and as-batched mixture proportions from the trial batch and the two concrete trucks purchased by the Purdue research team for the fourth bridge deck can be seen in Table 4.8. A range of mixture proportions observed during the casting of this bridge deck have been summarized here, while the mixture proportions for each individual truck can be

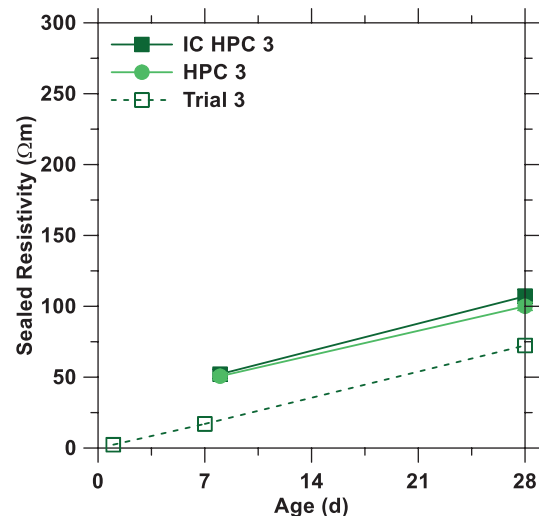


Figure 4.11 Sealed resistivity measurements of samples produced from the third bridge deck mixtures compared to a reference mixture.

seen in Appendix E. Due to a batching error, the IC HPC 4 truck was not within specification and contained an excess of lightweight aggregate.

The aggregate moisture properties measured on the day of production for the IC HPC 4 and HPC 4 mixtures are reported in Table 4.9. In regards to the LWA, it can be seen that the batch absorption exceeded the design absorption, ensuring that more than the minimum amount of water was available for internal curing.

4.5.2 Trial Batch

The trail batch for the fourth bridge deck followed the general procedure outlined in the introduction of this chapter. The trail batch was performed using manual batching controls. The first truck that was batched had a low slump value and was used to determine new admixture dosage rates. A second truck was batched and accepted based upon fresh properties.

4.5.3 Deck Pour

On the day of the deck pour, the official temperature for the area reported by the NOAA was a maximum of 28.3 °C with a minimum of 16.1 °C (82.9 and 61.0 °F, respectively). On the morning of construction, the aggregate moistures were measured, a mixture design was finalized and production began. Of note in this process, this producer was the only one involved in this study that was observed to modify the jog rate of the batching hoppers in order to better control batching tolerances for the lightweight aggregate. The jog rate is a measure of the speed at which the control arms open and close on the hoppers, controlling the amount of material allowed to fall on the batching scale when

approaching the target batch weight. In ready-mix plants equipped for the production of traditional concrete (i.e., no lightweight aggregate used), the jog rates will be set for normal weight fine and coarse aggregate which will fall at different rates than lightweight aggregate in the hoppers. In order to properly control batching tolerances, hoppers containing lightweight aggregate should have an adjusted jog rate. This particular producer had previous experience using lightweight aggregate and thus knew to take appropriate steps to adjust the batching system.

Upon batching of the first truck, the initial measurement of the slump exceeded the upper limit set in the specifications. In addition to this, the mixture exhibited signs of slight segregation and the formation of bubbles at the surface, symptoms common of overdosing high-range water reducing agents. No adjustments were made and full production ensued. The approximate haul time to the construction site was 30 minutes. Figure 4.12 shows the construction of the fourth bridge deck, where it can be seen that the IC HPC mixture was placed using a conveyor. It should be noted that the use of a conveyor was perhaps not necessary with a high-slump material, however the producer chose to use available conveyors as a conservative alternative to pumping.

A final point of emphasis for the construction of the fourth bridge deck concerns conservative engineering judgment. In this case, the choice to produce an overly flowable material and place this material using alternative methods (i.e., not pumping) may have resulted in segregation of the material. When coupled with overuse and misuse of curing compounds during finishing (see Figure 4.13), the resulting bridge deck may be produced inhomogeneously and can lead to unintended issues. In addition, a part of this bridge construction included the casting of an integral pier, where

TABLE 4.8
Concrete mixture design and as-batched proportions for bridge #4 [lb/yd³]. Admixtures are provided in [oz/cwt].

	Approved Design	Trial Batch	Deck Pour	Purdue, IC HPC 4	Purdue, HPC 4
W/CM	0.403	0.389	0.431–0.441	0.465*	0.398
Cement	435	435	435–443	438	458
Fly Ash	—	—	—	—	—
GGBFS	115	115	115–119	120	124
Silica Fume	25	25	25	25	25
Coarse Aggregate	1790	1789	1780–1807	1827	1798
Fine Aggregate	782	779	778–801	852	1384
Lightweight Aggregate	365	376	348–367	507	—
Air Entrainer	0.2–7.5	1.13	0.91–1.29	1.14	1.10
HRWRA	10–15	14.00	11.94–14.93	14.92	14.17
MRWRA	3–5	3.57	3.00–3.77	3.60	3.46
Retarder	—	—	—	—	—
Air Content [%]	6.5	6.4	5.5–7.3	8.1	7.1
Slump [in]	2.5–5.5	3	2.5–8.5*	9.0*	9.0*
Unit Weight [lb/ft ³]	137.3	140.6	139.4–142.9	135.5	144.8
Paste Content [%]	24.92	24.59	25.33–26.25*	24.48	25.00

*Indicates measures not conforming to limits set within INDOT specifications for IC HPC (INDOT, 2014a).

TABLE 4.9
Aggregate moisture properties on the day of bridge deck #4 construction.

	SG _{SSD} (N/A)	Design Absorption (%)	Total Moisture (%)	Surface Moisture (%)	Batch Absorption (%)
Coarse Aggregate	2.763	0.78	2.56	1.78	0.78
Fine Aggregate	2.623	3.31	4.58	3.31	1.27
Lightweight Aggregate	1.782	8.58	30.47	8.58	20.2

over-consolidation and segregation may contribute to additional settlement issues.

4.5.4 Experimental Results

The compressive strength from the trial batch and the samples procured on the day of construction can be seen in Figure 4.14 while the sealed resistivity of these mixtures can be seen in Figure 4.15. It can be seen that the IC HPC 4 mixture has a lower strength than the trial batch mixture and is likely a consequence of elevated w/cm in the IC HPC 4 mixture. The sealed resistivity is higher than the trial batch mixture and may be related to a higher degree of saturation due to excess lightweight aggregate for the purpose of internal curing. Despite differences in performance, both the trial batch and IC HPC 4 mixtures exceed the specified minimum strength and exhibit sealed resistivity values similar to other IC HPC mixtures in this study.

4.6 Summary

This chapter has summarized the construction process of four internally cured, high-performance bridge decks in Indiana during 2013. While avoidable issues during construction have been highlighted, two points should be emphasized. Firstly, four bridge decks utilizing internal curing are now in service. The concrete materials produced for each of the four bridge decks in

this study achieve higher performance in laboratory testing (strength, shrinkage, and chloride resistance) than traditional INDOT Class C bridge deck materials used in Indiana (this is discussed in detail in the following chapters). Second, a mixed specification of prescriptive and performance-based parameters was successfully used to produce these bridge decks. A final consideration for the use of internally cured, high-performance concrete is summarized monetarily in Table 4.10, where the price of the bridge deck concretes procured in this study are listed.

4.7 Conclusions

In 2013, the INDOT commissioned the construction of four internally cured, high-performance concretes. This chapter has summarized the trial batch, production, and construction of these bridge decks. The conclusions of this chapter are summarized as:

1. Four internally cured, high-performance bridge decks were successfully constructed and are now in service.
2. A mixed specification of prescriptive and performance-based measures was successfully implemented in the production of the bridge deck materials produced in this study.
3. Pre-wetted lightweight aggregate can be successfully used in the production of internally cured concrete if the moisture condition of the aggregates are understood, controlled, and accounted for in production.



Figure 4.12 Internally cured bridge deck being cast in 2013 on SR 933 over Baugo Creek in Indiana.



Figure 4.13 Finishing of an internally cured bridge deck with an excess of paste visible at the surface.

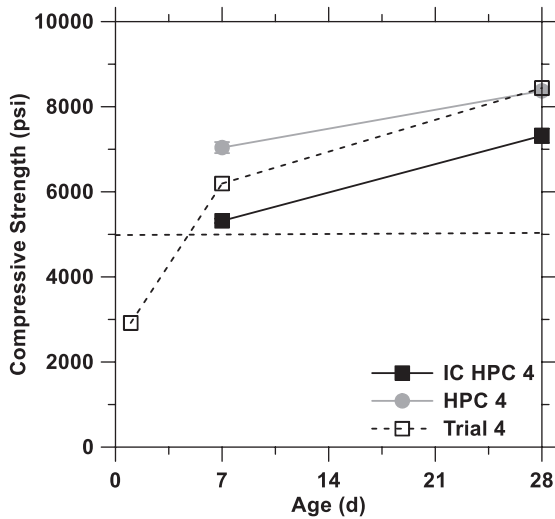


Figure 4.14 Compressive strength of samples produced from the fourth bridge deck mixtures compared to a reference mixture. The dashed line indicates the minimum acceptable limit as per the specifications.

This study implemented a new testing technique that utilizes a centrifuge to rapidly condition the lightweight aggregate to a surface-dry condition and reduces variability in testing over previous testing methods.

- Variability in moisture states within a stockpile of pre-wetted lightweight aggregate should be controlled or monitored and accounted for throughout concrete production.
- Batching issues exist regardless of the concrete mixture proportions, whether the concrete mixtures are internally cured or not, or regardless of the constituent materials used during production. It is the research team's position that these issues are avoidable with additional training and education.

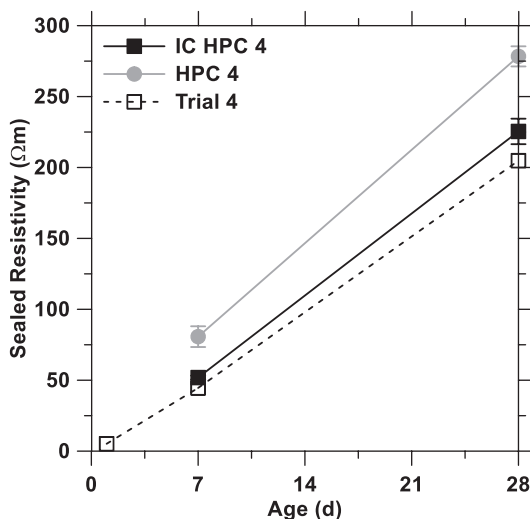


Figure 4.15 Sealed resistivity measurements of samples produced from the fourth bridge deck mixtures compared to a reference mixture.

TABLE 4.10
Price (\$/yd³) for each mixture in this study.

Mixture	1	2	3	4
IC HPC	126	203	116	165
HPC	126	104	116	159

- Pumping issues exist regardless of the concrete mixture proportions, whether the concrete mixtures are internally cured or not, or regardless of the constituent materials used in concrete production and are avoidable with additional training and education.
- Segregation issues existed on one deck that are independent of whether the concrete mixtures are internally cured or not and are avoidable with additional training and education.
- Trial batches should be used to identify and solve potential issues for production prior to date of construction.

5. LABORATORY TESTING OF FIELD PRODUCED SAMPLES: MECHANICAL AND TRANSPORT BEHAVIOR EVALUATION

5.1 Introduction

In the previous chapter, the design, production, and construction of four internally cured high-performance bridge decks was detailed. As a part of this work, samples of the industrially produced IC HPC mixtures were prepared and tested. In addition to these concretes, four corresponding non-internally cured mixtures were also produced as reference materials. This chapter presents an experimental study on the performance of these industrially produced concretes.

5.2 Objectives

The objective of this chapter is to evaluate the performance of the eight industrially produced bridge deck concrete mixtures through a series of standardized laboratory tests. The mechanical behavior will be presented with an emphasis on codified approximations for the evolution of strength and stiffness. The resistance to chloride diffusion of each material as measured by four commonly specified tests will also be presented. The results presented in this chapter are intended to quantify any changes in behavior due to the presence of lightweight aggregate for the purpose of internal curing while also documenting the as-built performance of the four bridge decks discussed in the previous chapter.

5.3 Testing Methods

The following tests were performed to assess the mechanical behavior of the IC HPC mixtures as well as the HPC reference mixtures: compressive strength, Young's elastic modulus, and splitting tensile strength.

In addition to the these tests, the following tests were performed to assess the transport behavior of the IC HPC mixtures as well as the HPC reference mixtures: uniaxial resistivity, rapid chloride permeability test, Nordtest non-steady state chloride migration, and the migration test using Stadium Lab simulation.

5.3.1 Compressive Strength

The compressive strength was determined in accordance with ASTM C39 (2012a). A set of 4 in diameter \times 8 in tall (100 mm \times 200 mm) cylinders were cast to study the compressive strength up to one year of age, with testing ages of 3, 7, 28, 56, 90, and 365 days. The cylinders were cast in two lifts, being rodded 25 times after each lift. After a minimum of 24 hours of field curing, the cylinders were transported to the laboratory where they were stored in their molds (i.e., in the sealed condition) at a temperature of 23 ± 1 °C until tested. For each day of testing, three cylinders were tested to determine the compressive strength of the mixtures. The cylinders were loaded at a rate of 35 ± 2 psi/s in a 700 kip hydraulic compression machine, utilizing neoprene end caps when tested.

5.3.2 Young's Modulus of Elasticity

The static modulus of elasticity (Young's modulus of elasticity) was determined using a procedure similar to that in ASTM C469 (ASTM, 2002). A set of 4 in diameter \times 8 in tall (100 mm \times 200 mm) cylinders were cast to study the modulus of elasticity up to one year of age, with testing ages of 3, 7, 28, 56, 90, and 365 days. The cylinders were cast in two lifts, being rodded 25 times after each lift. After a minimum of 24 hours of field curing, the cylinders were transported to the laboratory where they were stored in their molds (i.e., in the sealed condition) at a temperature of 23 ± 1 °C until tested. Upon testing, the cylinders were fitted with a compressometer equipped with a linear variable differential transformer (LVDT) displacement transducer. The cylinders were then loaded to 40% of their ultimate strength two separate times. The resulting slope of the stress-strain curve from the second loading was taken as the static modulus of elasticity. For each day of testing, two cylinders were tested for every mixture with no cylinder being tested at more than one age.

5.3.3 Splitting Tensile Strength

The splitting tensile strength of each mixture was determined in accordance with ASTM C 496 (ASTM, 2004a). A set of 4 in diameter \times 8 in tall (100 mm \times 200 mm) cylinders were cast to study the tensile strength up to one year of age, with testing ages of 3, 7, 28, 56, 90, and 365 days. The cylinders were cast in two lifts, being rodded 25 times after each lift. After a minimum of 24 hours of field curing, the cylinders were transported to the

laboratory where they were stored in their molds (i.e., in the sealed condition) at a temperature of 23 ± 1 °C until tested. Upon testing, the cylinder was demolded and placed on its side in a hydraulic compression machine. Using thin wood strips to distribute the load, the sample would be loaded at a rate of 35 ± 5 lb/s until failure.

5.3.4 Uniaxial Resistivity

The sealed uniaxial, bulk resistivity of the concrete mixtures was measured in accordance with the testing protocol similar to recommendations by Spragg, Castro, Nantung, Paredes, and Weiss (2012). A set of 4 in diameter \times 8 in tall (100 mm \times 200 mm) cylinders were cast to study the bulk resistivity up to one year of age, with testing ages of 3, 7, 28, 56, 90, and 365 days. The cylinders were cast in two lifts, being rodded 25 times after each lift. After a minimum of 24 hours of field curing, the cylinders were transported to the laboratory where they were demolded, sealed in plastic bags, and stored in an environmental chamber where the temperature was controlled to 23 ± 1 °C and the relative humidity was $98 \pm 2\%$ (to minimize evaporation) until testing. At each age of testing, the cylinders were connected to a resistance meter via metal caps placed on both ends of the cylinder with wet sponges between the cap and cylinder to ensure proper contact (see Figure 5.1). The sealed uniaxial, bulk resistivity was calculated by multiplying the measured resistance by the geometry factor, equal to the area of the cylinder divided by the length of the cylinder. The same samples were tested over the varying ages, being re-sealed in bags and placed back in a 100% RH chamber until the next testing age.

It should be noted that the samples were stored in a sealed condition and cannot be considered to be saturated. This is an important consideration, as previous research has shown that changes in degree of saturation (DOS) change the measured bulk resistivity (Rajabipour, Weiss, Shane, Mason, & Shah, 2005). To address this issue, curing methods utilizing a saturated lime water tank are frequently specified, however recent research has shown that this method may lead to excessive leeching in the samples while not providing a saturated condition for the sample (Spragg et al., 2015). In this research, the samples were stored in their molds (i.e., in a sealed condition) such that the change in degree of saturation should be due to the consumption of water during the hydration reaction alone while also preventing the potential for alkali leeching. It should be emphasized that the sealed resistivity measurements are not a direct measurement of a material property without correcting for changes in degree of saturation and as such comparisons are only applicable to mixtures which are the same (or intended to be similar, as is the case during field production).

The corrected uniaxial resistivity at 91 days is presented in addition to the sealed resistivity curves. These results were calculated by correcting the

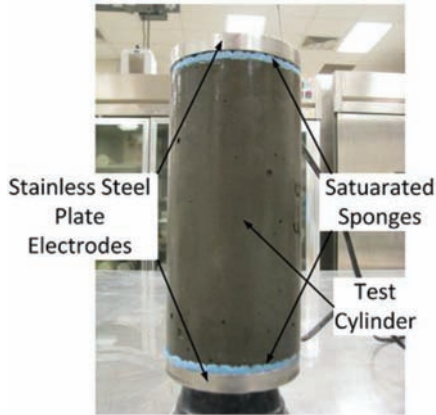


Figure 5.1 A picture schematic of the uniaxial resistivity testing setup (Spragg et al., 2012).

measured sealed resistivity at 91 days with the measured degree of saturation of the sample at that age using a saturation correction function, shown in Equation 5.1, as suggested elsewhere (Spragg, 2013).

$$\rho_{s=1} = \rho_{s \neq 1} \cdot S^n \quad (5.1)$$

where (ρ) is the resistivity at some degree of saturation (S) and (n) describes the non-linear change in resistivity with changes in degree of saturation and is determined experimentally. The saturation correction function of the form (S^n) was developed for non-air-entrained concretes and may require modifications for mixtures which have entrained air, however this subject matter is beyond the scope of this report and as such has been omitted. Due to the need of further research to better understand the relationship between degree of saturation and measured resistivity in air-entrained concretes, the variability in the corrected uniaxial resistivity measurements has also been omitted. For reference to the readers, a study has been performed which assessed the coefficient of variation of the resistivity test and was found to be similar to the established variation observed in the testing of compressive strength (12.0% versus 10.6% single laboratory precision index for resistivity and compressive strength, respectively) (Spragg et al., 2012; Spragg, Villani, et al., 2013). Finally, the corrected resistivity can may be used to directly calculate the formation factor (a material property describing the microstructural development) if the pore solution conductivity is known. To determine this, the authors recommend the use of a free online calculation tool available from the National Institute of Standards and Technology available at the following website: <http://concrete.nist.gov/poresolncalc.html>. These calculations were performed for the mixtures tested in this study using the mixture proportions and material chemistry that may be found in Appendix F.

5.3.5 Rapid Chloride Permeability Test

The rapid chloride permeability test (RCPT) was performed following the procedure outlined in ASTM C 1202 (ASTM, 2012b). A set of 4 in diameter \times 8 in tall (100 mm \times 200 mm) cylinders were cast to study the chloride migration, with a testing age of 90 days. The cylinders were cast in two lifts, being rodded 25 times after each lift. After a minimum of 24 hours of field curing, the cylinders were transported to the laboratory where they were stored in their molds (i.e., in the sealed condition) at a temperature of 23 ± 1 °C until tested. Upon testing, the cylinder was demolded and samples of 50 ± 1 mm length were cut out of the interior of the cylinder. These samples were epoxied on the side, leaving the two cut faces exposed, then vacuum saturated with water using an industrial vacuum pump regulated to 6 ± 3 tor. The samples were allowed to absorb water for a minimum of 18 hours after vacuum saturation, at which point they were tested. The saturated samples were placed in the apparatus shown in Figure 5.2, where the sample is sealed between two solution reservoirs containing either 3% NaCl by mass or 0.3 normal NaOH. An electrical potential of 60 ± 1 V was then applied across the sample for 6 hours, causing the chloride ions to migrate through the sample. The current was measured automatically in 5 minute intervals throughout testing and upon completion was integrated to determine the result of the test, reported as total charge passed measured in Coloumbs.

5.3.6 Nordtest Non-Steady-State Chloride Migration

The Nordtest was performed in accordance with NT Build 492 (Nordtest, 1999). A set of 4 in diameter \times 8 in tall (100 mm \times 200 mm) cylinders were cast to study the chloride migration at an age of 90 days. The cylinders were cast in two lifts, being rodded 25 times after each lift. After a minimum of 24 hours of field curing, the cylinders were transported to the laboratory where they were stored in their molds (i.e., in the sealed

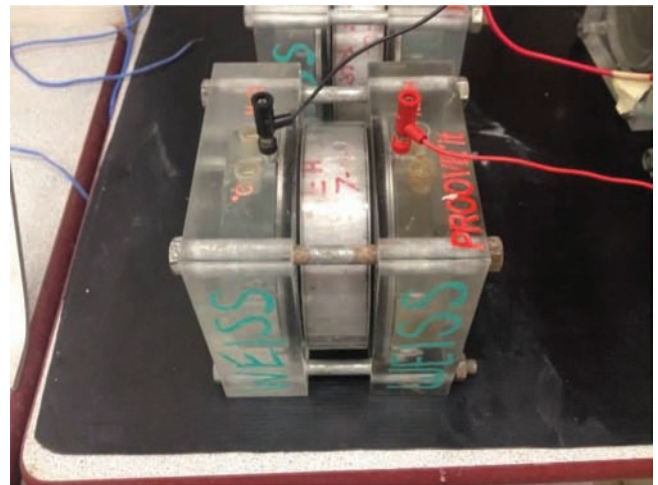


Figure 5.2 A picture of the RCPT test during operation.

condition) at a temperature of 23 ± 1 °C until tested. Upon testing, the cylinder was demolded and samples of 50 ± 1 mm length were cut out of the interior of the cylinder. These samples were epoxied on the side, leaving the two cut faces exposed, then vacuum saturated with $\text{Ca}(\text{OH})_2$ using an industrial vacuum pump regulated to 6 ± 3 tor. The samples were allowed to absorb $\text{Ca}(\text{OH})_2$ for a minimum of 18 hours after vacuum saturation, at which point they were tested. The saturated samples were placed in the apparatus shown in Figure 5.3 where the top of the sample was exposed to 0.3 N NaOH while the reservoir was filled with 10% NaCl solution. The applied voltage and duration of testing was determined using Appendix 2 of the testing specification.

5.3.7 Migration Cell and Stadium Lab

The diffusion coefficients for ionic species were measured using Stadium Lab and a migration cell. The test method is a modified version of ASTM C1202 (ASTM, 2012b) (see Figure 5.4), where the intensity of electrical current passed through a 4 in diameter by 2 in thick (100 mm \times 50 mm) cylindrical specimen is monitored over a 14-day period (SIMCO Technologies, Inc., 2013). The samples used for this test were cut from a set of field cast, 4 in diameter by 8 in long concrete cylinders that were sealed and placed in a chamber at 100% RH and 23 ± 2 °C for 90 days. After the samples were cut, the sides of the samples were sealed with an epoxy after which they were vacuum saturated with 0.3 M NaOH for approximately 18 hours. Once saturated, the samples were mounted between a cell filled with 0.3 M NaOH solution (downstream) and a cell filled with 0.5 M NaCl + 0.3 M NaOH solution (upstream). A constant DC potential of 20V was maintained across the specimen for 14 days while the voltage, current, and temperature were measured and recorded at 15 minute intervals.

In conjunction with the migration cell testing, the volume of permeable voids of the samples was

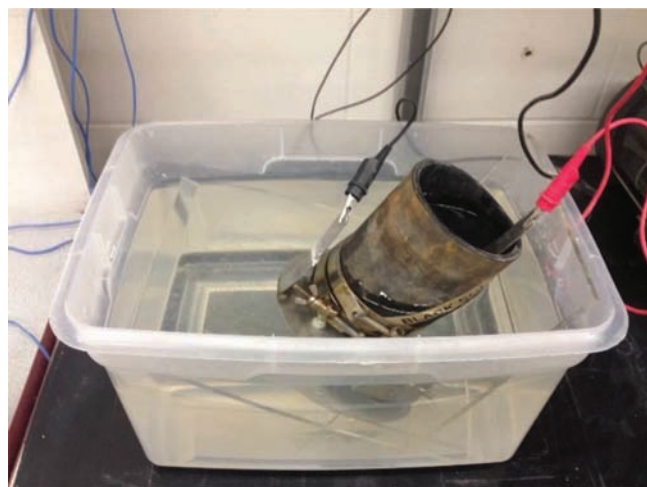


Figure 5.3 A picture of the Nordtest during operation.

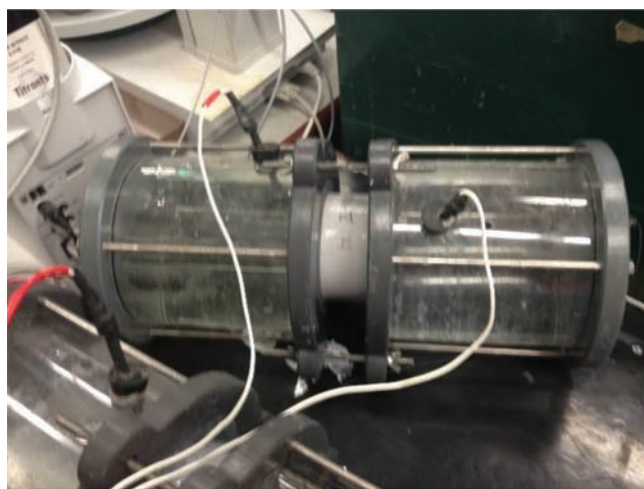


Figure 5.4 A picture of the Stadium migration test during operation.

determined in accordance with ASTM C642 (ASTM, 2006) (with the exception that boiling was replaced with vacuum saturation). For this test, additional 4 in diameter by 2 in thick samples were cut from 4 in diameter by 8 in tall cylinders at an age of 90 days, sealed on the lateral sides, and placed in an environmental chamber at 50 %RH and 23 °C. The mass change of the samples was monitored until a mass equilibrium of $\pm 0.5\%$ was reached, at which point the samples were oven dried then vacuum saturated. Using the oven dry mass, saturated mass, buoyant mass, and conditioned mass, the volume of permeable voids was able to be determined. The results from the migration cell and the volume of permeable voids were entered into STADIUM Lab software to evaluate the ion diffusion coefficients and the tortuosity of the samples (Samson, Marchand, & Snyder, 2003).

5.4 Results

The results for each mixture has been grouped by the same naming convention outlined in the previous chapter. The results will be presented for each of the tests described in the previous section in the same order for each of the bridges that were involved in the study (i.e., bridges 1 through 4) with the IC HPC mixtures being shown in the same plot or table as the HPC mixtures for comparison.

5.4.1 Bridge Deck #1

The results of the testing performed on samples procured on the day of construction of the first bridge deck railing are shown in the following section.

5.4.1.1 Compressive Strength. The compressive strength of the IC HPC 1 and HPC 1 mixtures are shown in Figure 5.5. It can be seen that both of these mixtures exceed the minimum specified strength of 5000 psi after approximately 7 days of hydration. It can

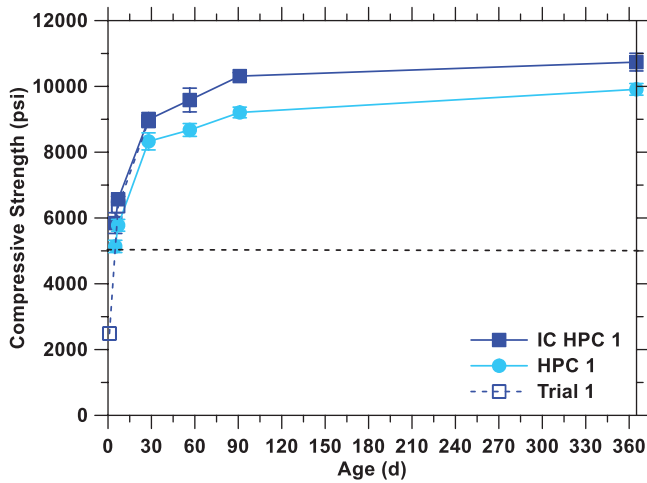


Figure 5.5 Compressive strength evolution of samples procured on the day of construction of the first bridge deck. The dashed line indicates the minimum required strength at 28 days as outlined in the special provisions (INDOT, 2014a).

also be seen that the IC HPC 1 mixture had a measured increase in compressive strength relative to the HPC 1 mixture of approximately 10%. This increase can be due in part to the increased hydration due to internal curing as well as the reduction in strength due to increased w/cm in the HPC 1 mixture, discussed in the previous chapter.

5.4.1.2 Young's Elastic Modulus. The evolution of Young's elastic modulus for the samples produced on the day of construction of the railing on the first bridge deck is shown in Figure 5.6. It can be seen that the IC HPC 1 mixture has no change in rate of stiffness development and the presence of the LWA in the mixture results in a stiffness reduction of approximately 5% in comparison to the HPC 1 mixture. Figure 5.7 shows the elastic modulus of the mixtures plotted as a function of the square root of compressive strength,

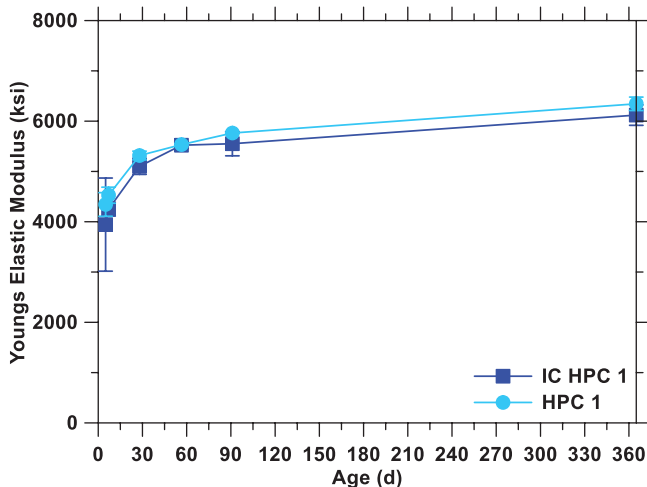


Figure 5.6 Evolution of Young's elastic modulus of samples procured on the day of construction of the first bridge deck railing.

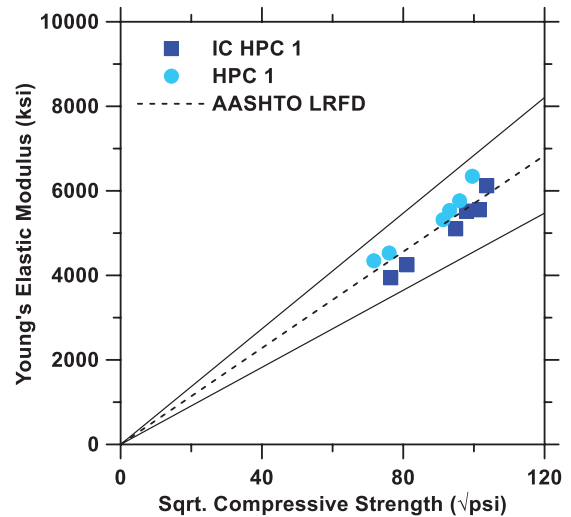


Figure 5.7 Young's elastic modulus of samples procured on the day of construction of the first bridge deck railing plotted as a function of the square root of the corresponding measured compressive strength. The dashed line indicates the result from AASHTO, Section C5.4.2.4 for normal weight concrete while the solid line indicates $\pm 20\%$ (AASHTO, 2012).

where this relationship is approximately linear and has been codified in ACI (2011) and adopted by the AASHTO LRFD Bridge Design Specifications (AASHTO, 2012). This figure shows that the codified equation for normal weight concrete (indicated by the dashed line) closely estimates the elastic modulus, with all of the data falling within the published accuracy of the codified equation ($\pm 20\%$, as indicated by the solid lines in Figure 5.7).

5.4.1.3 Splitting Tensile Strength. The splitting tensile strength of the mixtures procured at the construction of the first bridge deck railing can be seen in Figure 5.8. It can be seen that, similar to the compressive strength, the tensile strength of the IC HPC 1 mixture is

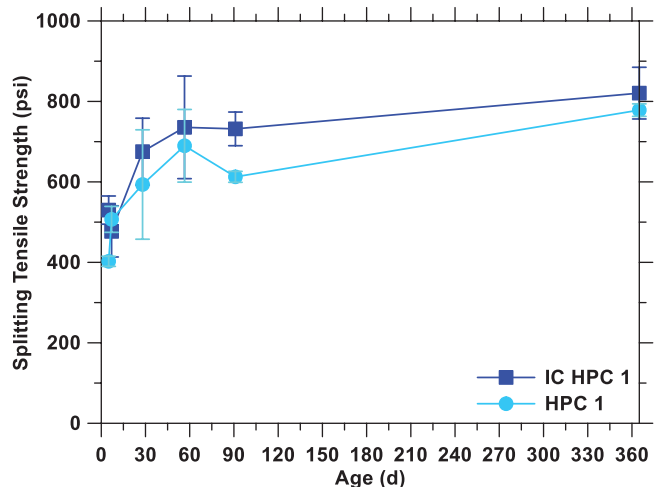


Figure 5.8 Evolution of splitting tensile strength of samples procured on the day of construction of the first bridge deck railing.

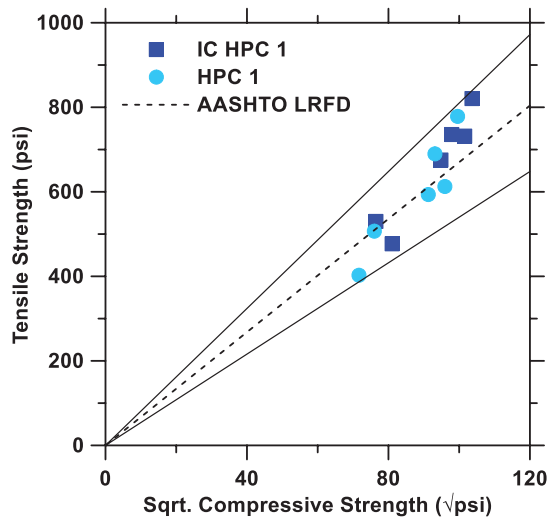


Figure 5.9 Splitting tensile strength of samples procured on the day of construction of the first bridge deck plotted as a function of the square root of the corresponding measured compressive strength. The dashed line indicates the result from AASHTO, Section 5.8.2.2 while the solid line indicates $\pm 20\%$ (AASHTO, 2012).

approximately 10% higher than the HPC 1 mixture. Again, this is likely attributable to the increased w/cm in the HPC 1 mixture as well as the extended degree of hydration in the IC HPC 1 mixture. Figure 5.9 shows this data plotted as a function of the square root of the corresponding compressive strength. In the figure, the dashed line indicates the predicted relationship as suggested in ACI 318, R8.6.1 and Section 5.8.2.2 in the AASHTO LRFD Bridge Design Specifications. This figure shows that the codified equation closely estimates the splitting tensile strength, with all of the data falling within $\pm 20\%$, as indicated by the solid lines in Figure 5.9.

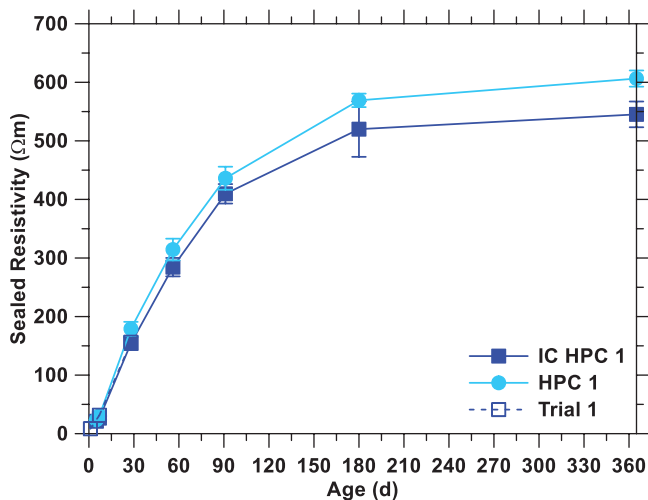


Figure 5.10 Evolution of the sealed uniaxial resistivity of samples procured on the day of construction of the first bridge deck railing.

5.4.1.4 Sealed Uniaxial Resistivity. The sealed uniaxial resistivity of the samples procured on the day of casting of the first bridge railing are shown in Figure 5.10. The results indicate that the HPC 1 mixture exhibited approximately 5 to 15% higher sealed resistivity over the first year, however as was discussed in the description of the testing procedure, this comparison may not be appropriate as the measured degree of saturation of the IC HPC 1 mixture was 66% at 91 days while that of the HPC 1 mixture was 58% at the same age.

5.4.1.5 RCPT, Nordtest, Stadium Lab, and Uniaxial Resistivity. The results from the RCPT test, the Nordtest, the Stadium Lab simulation using migration testing, and the uniaxial resistivity test performed on samples that had been cured for 91 days can be seen in Table 5.1. The results from each of these tests are reported in the units defined by the data reduction method outlined in the respective testing methods. It can readily be seen that without further interpretation the results of these tests cannot be directly compared due to the incompatibility of units. For the purposes and intents of this report, focus can be given to the RCPT test, where the charge passed for both the IC HPC 1 and HPC 1 mixtures were below the specified maximum charge passed of 1500 C (INDOT, 2014a). The results of the remaining tests may be used as reference values for alternative testing methods that may be used in performance-based specifications. Consideration should be given to inherent conditions of different testing methods that may introduce variations in measurements such as exposed lightweight aggregate on cut faces in the migration tests (Di Bella, 2012), chloride binding in the RCPT and Nordtest, and the filling of air voids during the preparation of samples for each test (Bu, 2014). These considerations will not be discussed in depth herein.

It should be noted here that the result of the stadium migration test is derived from an average of two samples tested while the standard deviation associated with this test (not provided herein) is still an active area of research (Conciatori, Grégoire, Samson, Marchand, & Chouinard, 2014). Similarly, the uncertainty in the resistivity method is not yet defined and has been omitted herein. It should be highlighted that the resistivity values presented in Table 5.1 are the corrected uniaxial resistivity (i.e., the resistivity in a saturated sample at 91 days) while the formation factor (equal to the resistivity of a saturated sample divided by the resistivity of the pore solution) is provided in parenthesis following the uniaxial resistivity.

5.4.2 Bridge Deck #2

The results of the testing performed on samples procured on the day of construction of the second bridge deck are shown in the following section.

TABLE 5.1

Results of chloride migration tests and resistivity test for the samples procured on the day of construction of the first bridge deck railing. The results of each test are presented in the corresponding units used in the calculation of results of each test.

Mixture	Test	Result	Standard Deviation	Unit
IC HPC 1	RCPT	420	± 10	C
HPC 1		435	± 65	C
IC HPC 1	NORD	2.1	± 0.3	(10 ⁻¹² m ² /sec)
HPC 1		3.5	± 0.8	(10 ⁻¹² m ² /sec)
IC HPC 1	Stadium Migration	0.96	—	(10 ⁻¹¹ m ² /sec)
HPC 1		1.32	—	(10 ⁻¹¹ m ² /sec)
IC HPC 1	Uniaxial Resistivity	88.0 (733)	—	(Ω·m)
HPC 1	(Formation Factor)	76.7 (841)	—	(Ω·m)

Note: All samples tested at an age of 91 days.

5.4.2.1 Compressive Strength. The compressive strength of the mixtures produced on the day of construction of the second bridge deck can be seen in Figure 5.11. It can be seen that the IC HPC 2 mixture exhibited an approximate increase in compressive strength of 5 to 10% over the first year. As the mixture proportions and fresh properties of these mixtures were very similar (discussed in the previous chapter) this small increase in compressive strength is likely associated with increased hydration due to internal curing and is consistent with previous research (Schlitter, Henkensiefken, et al., 2010). Irrespective of the slight differences in strength, both mixtures surpass the specified minimum strength requirement after two weeks of curing. It can be noticed that the samples from the trial batch were significantly stronger than those produced on the day of the deck pour, however due to the method of water addition at the trial batch (discussed in the previous chapter) no quantifiable statement can be made about this difference.

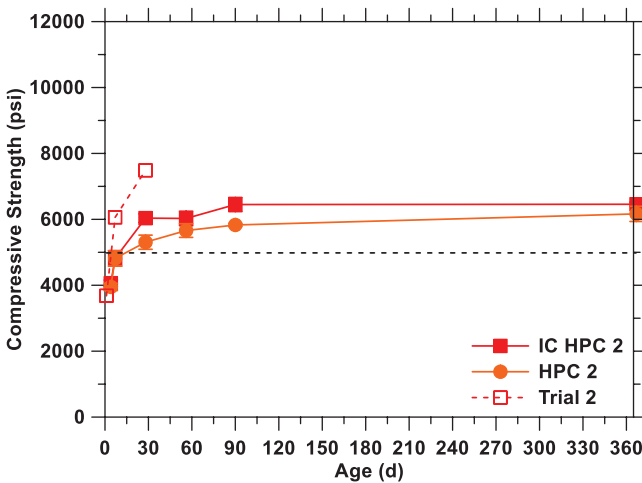


Figure 5.11 Compressive strength evolution of samples procured on the day of construction of the second bridge deck. The dashed line indicates the minimum required strength at 28 days as outlined in the special provisions (INDOT, 2014a).

5.4.2.2 Young’s Elastic Modulus. The evolution of the Young’s modulus of elasticity for the samples procured on the day of construction of the second bridge deck can be seen in Figure 5.12 while Figure 5.13 shows this data presented as a function of the square root of compressive strength. Figure 5.12 shows close agreement of the modulus of elasticity for the IC HPC 2 and HPC 2 mixtures, with the IC HPC 2 mixture having a reduction of approximately 5 to 10% during the first year. Figure 5.13 shows that the codified equations closely estimate the elastic modulus using the measured compressive strength, with the majority of the data for these mixtures falling within ± 20% (outliers are conservatively estimated with the codified equation).

5.4.2.3 Splitting Tensile Strength. The splitting tensile strength of the samples procured on the day of construction of the second bridge deck can be seen in Figure 5.14 while Figure 5.15 shows this data plotted as a function of the square root of the corresponding

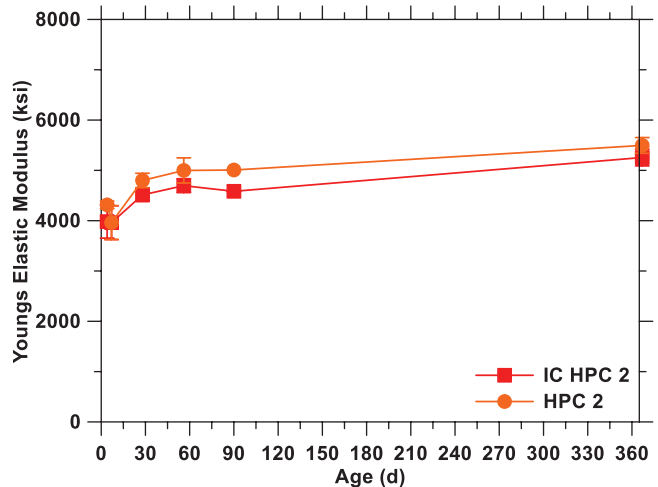


Figure 5.12 Evolution of Young’s elastic modulus of samples procured on the day of construction of the second bridge deck railing.

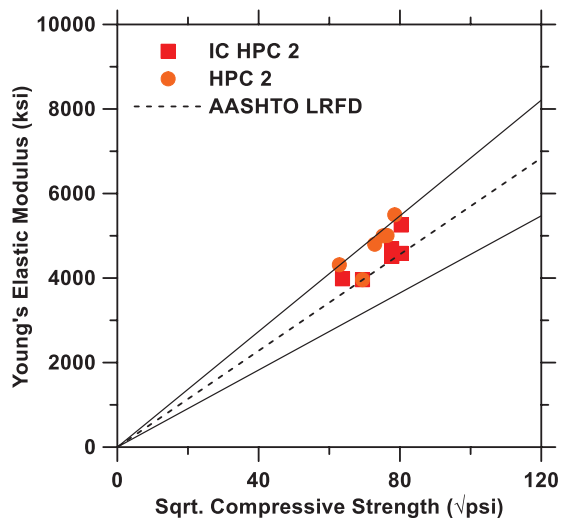


Figure 5.13 Young's elastic modulus of samples procured on the day of construction of the second bridge deck plotted as a function of the square root of the corresponding measured compressive strength. The dashed line indicates the result from AASHTO, Section C5.4.2.4 for normal weight concrete while the solid line indicates $\pm 20\%$ (AASHTO, 2012).

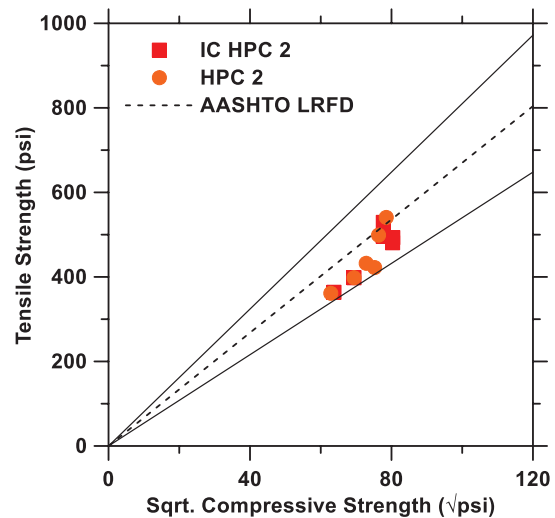


Figure 5.15 Splitting tensile strength of samples procured on the day of construction of the first bridge deck plotted as a function of the square root of the corresponding measured compressive strength. The dashed line indicates the result from AASHTO, Section 5.8.2.2 while the solid line indicates $\pm 20\%$ (AASHTO, 2012).

compressive strength. Figure 5.14 shows that the tensile strength of the two mixtures are similar at later ages, with the IC HPC 2 mixture showing an approximate increase of 15 to 20% at 28 and 56 days. Figure 5.15 shows that the codified equation for splitting tensile strength shows good agreement with the measured data, especially at later ages, with all of the data within $\pm 20\%$ of the predicted result.

5.4.2.4 Sealed Uniaxial Resistivity. The sealed uniaxial resistivity of the samples procured on the day of construction of the second bridge deck can be seen in Figure 5.16. In general, the results of the IC HPC 2 and HPC 2 mixtures show close agreement over the first year. The measured degree of saturation of the IC HPC

2 mixture was 70% and 74% for the HPC 2 mixture (indicating that the correction for the degree of saturation would be similar for each mixture). Due to this higher degree of saturation, these results are not directly comparable to those from the first bridge deck as the correction necessary for these materials is substantially different. To make such a comparison, these results would need to be corrected for degree of saturation and pore solution conductivity (Spragg, 2013). For this reason, the sealed resistivity should only be used for the purposes of comparing two mixtures of the same intended design (i.e., having the same mixture proportions) to detect variability in production and should not be used directly as a quality assurance measure.

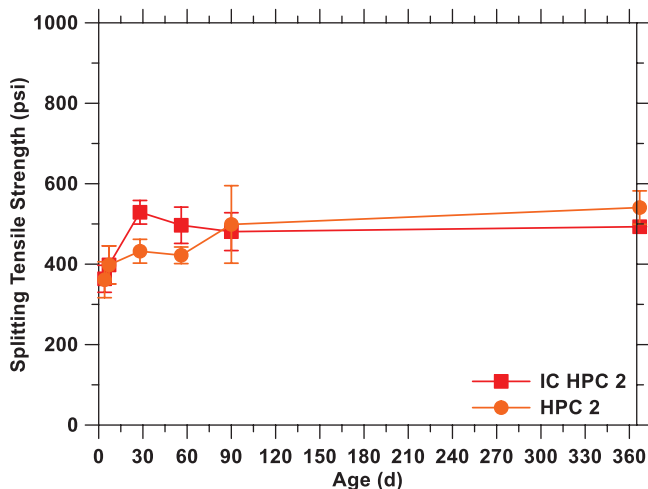


Figure 5.14 Evolution of splitting tensile strength of samples procured on the day of construction of the first bridge deck railing.

5.4.2.5 RCPT, Nordtest, Stadium Lab, and Uniaxial Resistivity. The results from the RCPT test, the Nordtest, the Stadium Lab simulation using migration testing, and the uniaxial resistivity test performed on samples that had been cured for 91 days can be seen in Table 5.2. The results of the RCPT indicate that both the IC HPC 2 and HPC 2 mixtures have a measured charge passed lower than the specified 1500 C. A comparison of the chloride diffusion coefficients of the two mixtures indicates that the IC HPC 2 mixture has an increased resistance to chloride penetration compared to the HPC 2 mixture (i.e., a lower RCPT value) and is likely associated with improved consolidation in the IC HPC 2 mixture. Additional considerations that may have resulted in an improved resistance to chloride migration in the IC HPC mixtures include an increased degree of hydration as well as enhanced depercolation of the interfacial

TABLE 5.2

Results of chloride migration tests and resistivity test for the samples procured on the day of construction of the second bridge deck. The results of each test are presented in the corresponding units used in the calculation of results of each test.

Mixture	Test	Result	Standard Deviation	Unit
IC HPC 2	RCPT	1105	± 1410	C
HPC 2		1410	± 605	C
IC HPC 2	NORD	5.1	± 0.4	(10 ⁻¹² m ² /sec)
HPC 2		7.6	± 0.9	(10 ⁻¹² m ² /sec)
IC HPC 2	Stadium Migration	2.38	—	(10 ⁻¹¹ m ² /sec)
HPC 2		4.83	—	(10 ⁻¹¹ m ² /sec)
IC HPC 2	Uniaxial Resistivity	52.7 (496)	—	(Ω·m)
HPC 2	(Formation Factor)	50.3 (520)	—	(Ω·m)

Note: All samples tested at an age of 91 days.

zones between the lightweight aggregate and the surrounding matrix (Castro, 2011).

5.4.3 Bridge Deck #3

The results of the testing performed on samples procured on the day of construction of the third bridge deck are shown in the following section.

5.4.3.1 Compressive Strength. The evolution of the compressive strength of the samples procured on the day of construction of the third bridge deck can be seen in Figure 5.17. As can be seen, the IC HPC 3 mixture exhibits an increased compressive strength of approximately 5 to 10% in comparison to the HPC 3 mixture, similar to the results from the first two bridge decks. Both mixtures exceeded the minimum specified strength after 7 days of curing. The lower strength of the trial batch material was discussed in the previous chapter and the higher strength of the IC HPC 3 material gives an indication that these issues were resolved.

5.4.3.2 Young’s Elastic Modulus. The evolution of the Young’s modulus of elasticity for the samples procured

on the day of construction of the third bridge deck can be seen in Figure 5.18 while Figure 5.19 shows this data plotted as a function of the square root of the measured compressive strength of corresponding samples. Figure 5.18 shows that the modulus of elasticity of the IC HPC 3 mixtures is approximately 5% greater than that of the HPC 3. This trend may be related to the lower air content of the IC HPC 3 mixture (1.8%), however the difference is small and the impact on practice is negligible. Figure 5.19 shows that the measured modulus of elasticity of the IC HPC 3 and HPC 3 mixtures is estimated closely by the codified equation.

5.4.3.3 Splitting Tensile Strength. The evolution of the splitting tensile strength of the samples procured on the day of construction of the third bridge deck can be seen in Figure 5.20 while Figure 5.21 shows this data plotted as a function of the square root of measured compressive strength of corresponding samples. Figure 5.20 shows that at any given age, there is statistically not a significant difference in the tensile strength of the IC HPC 3 and HPC 3 mixtures. Figure 5.21 shows that this data agrees well with the

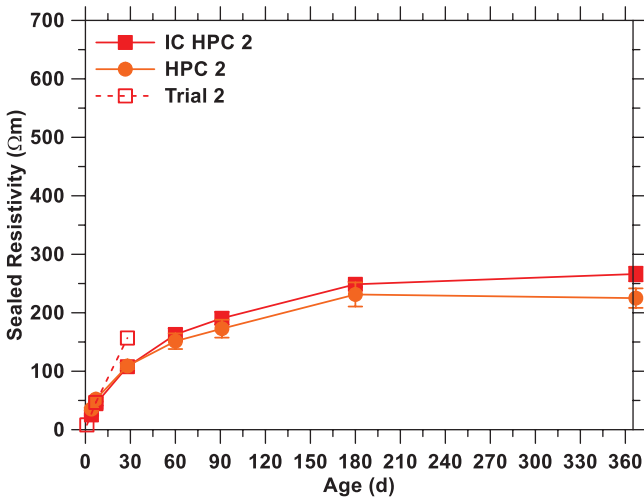


Figure 5.16 Evolution of the sealed uniaxial resistivity of samples procured on the day of construction of the first bridge deck railing.

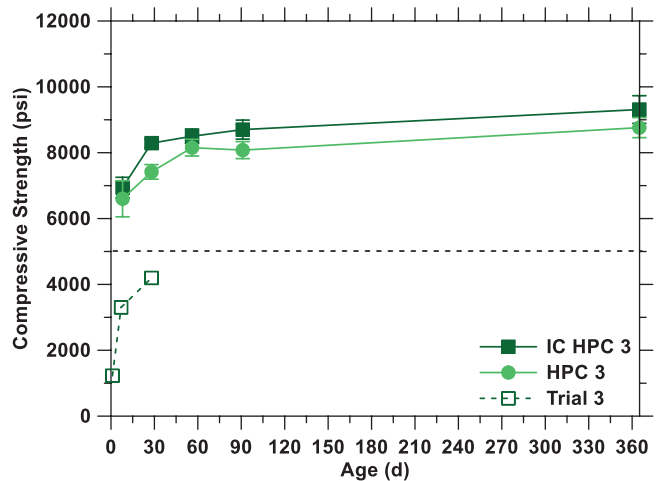


Figure 5.17 Compressive strength evolution of samples procured on the day of construction of the third bridge deck. The dashed line indicates the minimum required strength at 28 days as outlined in the special provisions (INDOT, 2014a).

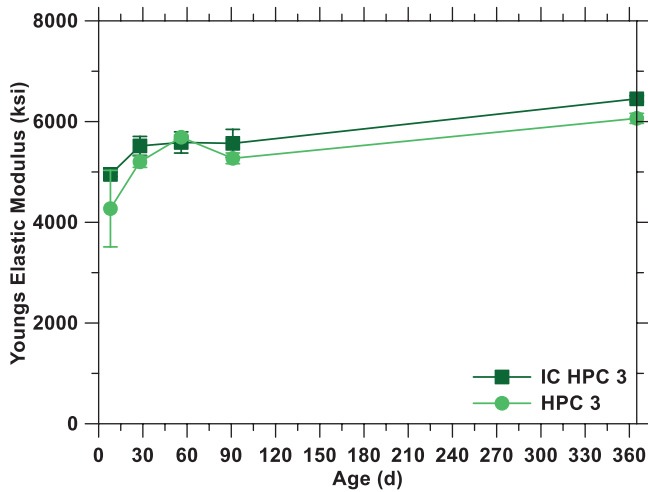


Figure 5.18 Evolution of Young's elastic modulus of samples procured on the day of construction of the third bridge deck railing.

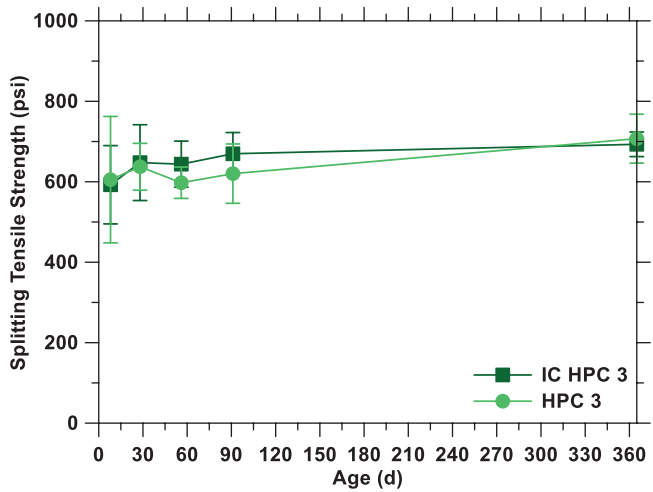


Figure 5.20 Evolution of splitting tensile strength of samples procured on the day of construction of the third bridge deck.

result of the codified equation for the splitting tensile strength of concrete.

5.4.3.4 Sealed Uniaxial Resistivity. The evolution of the sealed uniaxial resistivity of the samples procured on the day of construction of the third bridge deck can be seen in Figure 5.22. It can be seen that the IC HPC 3 mixture exhibited an increased sealed resistivity of up to 20% at one year of age while the degree of saturation of the IC HPC 3 mixture was measured to be 83% at 91 days while the HPC 3 mixture was measured at 73%.

5.4.3.5 RCPT, Nordtest, Stadium Lab, and Uniaxial Resistivity. The results from the RCPT, the Nordtest, the Stadium Lab simulation using migration testing, and the uniaxial resistivity test performed on samples that had been cured for 91 days can be seen in Table 5.3. The results of the RCPT indicate that both the IC HPC 3 mixture and the HPC 3 mixture are below the specified maximum charge passed of 1500 C. A comparison of diffusion coefficients indicates that the IC HPC 3 mixture had an improved resistance to chloride migration in comparison with the HPC 3 mixture. This result is likely a consequence of better consolidation that was achieved in the IC HPC 3 mixture during production.

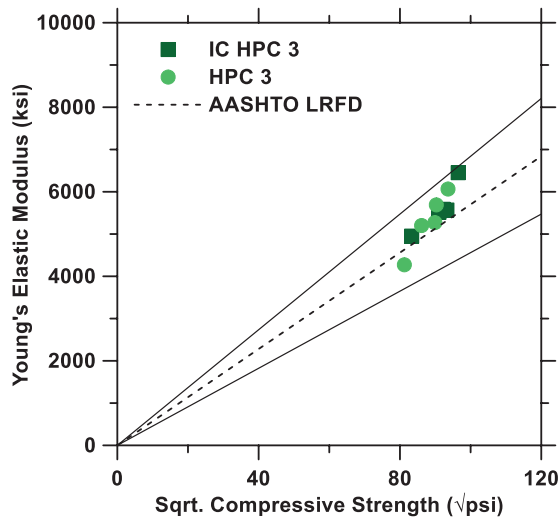


Figure 5.19 Young's elastic modulus of samples procured on the day of construction of the third bridge deck plotted as a function of the square root of the corresponding measured compressive strength. The dashed line indicates the result from AASHTO, Section C5.4.2.4 for normal weight concrete while the solid line indicates $\pm 20\%$ (AASHTO, 2012).

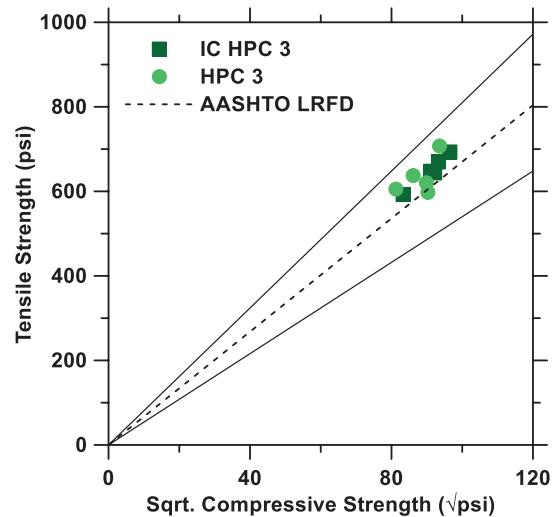


Figure 5.21 Splitting tensile strength of samples procured on the day of construction of the third bridge deck plotted as a function of the square root of the corresponding measured compressive strength. The dashed line indicates the result from AASHTO, Section 5.8.2.2 while the solid line indicates $\pm 20\%$ (AASHTO, 2012).

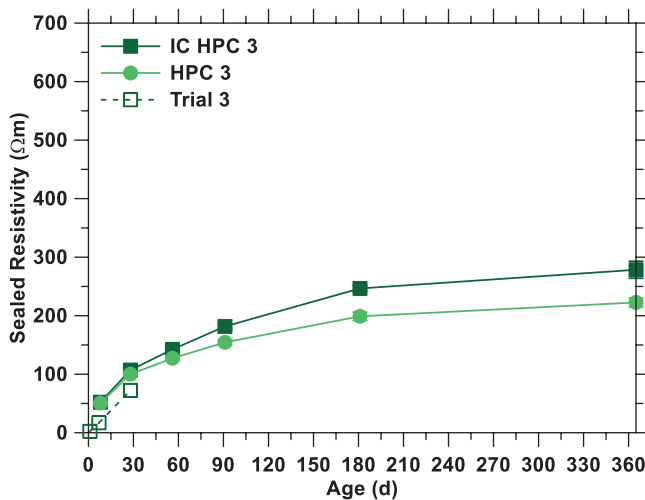


Figure 5.22 Evolution of the sealed uniaxial resistivity of samples procured on the day of construction of the third bridge deck.

5.4.4 Bridge Deck #4

The results of the testing performed on samples procured on the day of construction of the fourth bridge deck are shown in the following section.

5.4.4.1 Compressive Strength. The evolution of the compressive strength of samples procured on the day of construction of the fourth bridge deck can be seen in Figure 5.23. In contrast to the previous bridge decks, the IC HPC 4 mixture exhibited compressive strengths approximately 15% lower at later ages than that of the HPC 4 mixture. This was likely a consequence of elevated w/cm in the IC HPC 4 mixture due to a batching error. The practical implications of this reduction in strength are insignificant, as both the IC HPC 4 and HPC 4 mixtures exceeded the minimum required strength after 7 days of curing.

5.4.4.2 Young's Elastic Modulus. The evolution of the Young's modulus of elasticity of samples procured on the day of construction of the fourth bridge deck can be seen in Figure 5.24 while Figure 5.25 shows this data

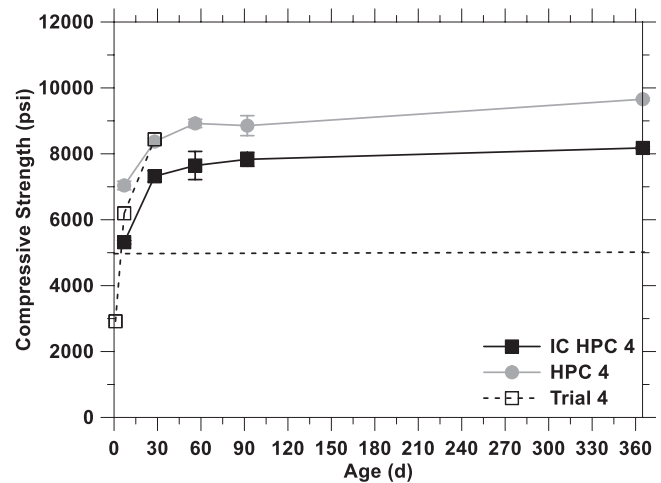


Figure 5.23 Compressive strength evolution of samples procured on the day of construction of the fourth bridge deck. The dashed line indicates the minimum required strength at 28 days as outlined in the special provisions (INDOT, 2014a).

plotted as a function of the square root of measured compressive strength of corresponding samples. Figure 5.24 shows a similar trend as seen in the compressive strength, where the HPC 4 mixture had an increased modulus of elasticity of 15 to 30%. Part of this reduction in the modulus of elasticity in the IC HPC 4 mixture is likely related to the elevated w/cm, while an additional reduction was observed due to the presence of lightweight aggregate, as was seen in the data from previous bridge decks. Figure 5.25 shows that for the mixtures from the fourth bridge deck, the codified equation conservatively estimates the stiffness of the mixtures, with the IC HPC 4 mixture falling within +20% of the predicted values.

5.4.4.3 Splitting Tensile Strength. The evolution of the splitting tensile strength of samples procured on the day of construction of the fourth bridge deck can be seen in Figure 5.26 while Figure 5.27 shows this data plotted as a function of the square root of the measured compressive strength of corresponding samples. Figure 5.26 shows that at early ages there is statistically little difference in the tensile strength of the IC HPC 4

TABLE 5.3
Results of chloride migration tests and resistivity test for the samples procured on the day of construction of the third bridge deck. The results of each test are presented in the corresponding units used in the calculation of results of each test.

Mixture	Test	Result	Standard Deviation	Unit
IC HPC 3	RCPT	945	± 130	C
HPC 3		1420	N/A	C
IC HPC 3	NORD	3.6	± 0.3	(10 ⁻¹² m ² /sec)
HPC 3		7.1	± 1.7	(10 ⁻¹² m ² /sec)
IC HPC 3	Stadium Migration	1.43	—	(10 ⁻¹¹ m ² /sec)
HPC 3		3.32	—	(10 ⁻¹¹ m ² /sec)
IC HPC 3	Uniaxial Resistivity	67.5 (648)	—	(Ω·m)
HPC 3	(Formation Factor)	74.9 (719)	—	(Ω·m)

Note: All samples tested at an age of 91 days.

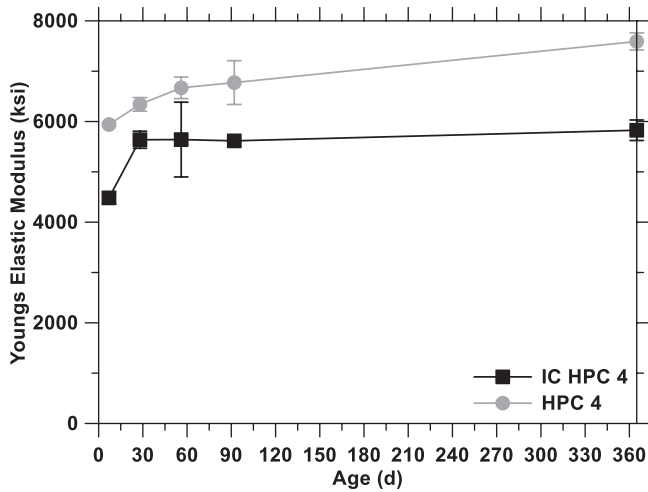


Figure 5.24 Evolution of Young's elastic modulus of samples procured on the day of construction of the fourth bridge deck railing.

and HPC 4 mixtures with an increase of approximately 20% at later ages which can likely be attributed to the elevated w/cm in the IC HPC 4 mixture. Figure 5.27 shows that this data is in close agreement with the codified equation which predicts the splitting tensile strength of the concrete.

5.4.4.4 Sealed Uniaxial Resistivity. The evolution of the sealed uniaxial resistivity of the samples procured on the day of construction of the fourth bridge deck can be seen in Figure 5.28. The measured degree of saturation of was measured to be 60% for the IC HPC 4 mixture and 59% for the HPC 4 mixture. Due to differences in w/cm, a direct comparison of these

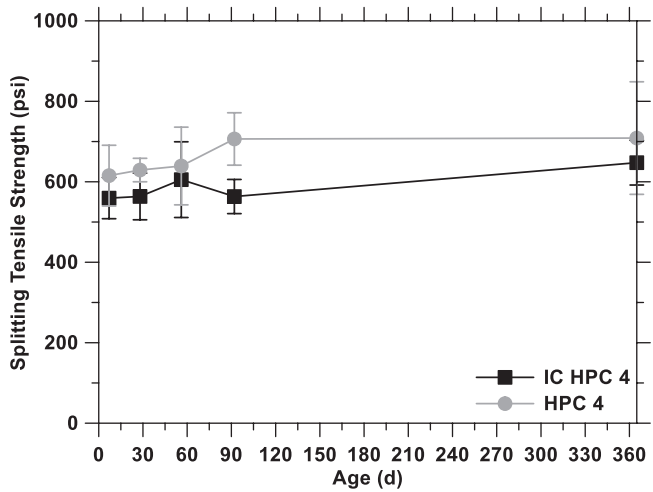


Figure 5.26 Evolution of splitting tensile strength of samples procured on the day of construction of the fourth bridge deck.

mixtures may not be significant, however the sealed resistivity is in reasonable agreement for the two mixtures and is on the same order of magnitude as the first bridge deck materials.

5.4.4.5 RCPT, Nordtest, Stadium Lab, and Uniaxial Resistivity. The results from the RCPT test, the Nordtest, the Stadium Lab simulation using migration testing, and the uniaxial resistivity test performed on samples that had been cured for 91 days can be seen in Table 5.4. The results of the RCPT for the IC HPC 4 and HPC 4 mixtures indicate that the charge passed in these samples were well below the maximum specified allowable charge passed of 1500 C. A comparison of the

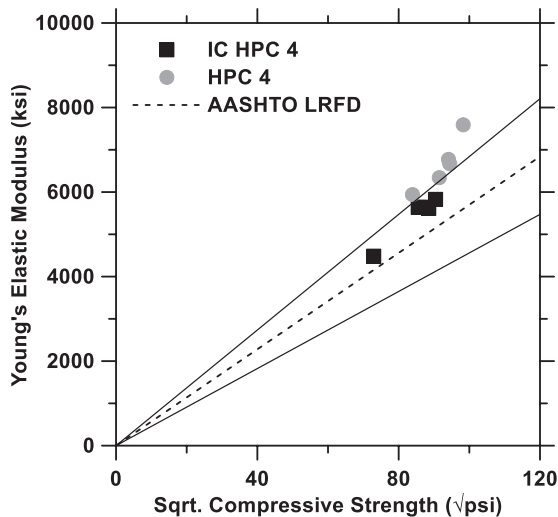


Figure 5.25 Young's elastic modulus of samples procured on the day of construction of the fourth bridge deck plotted as a function of the square root of the corresponding measured compressive strength. The dashed line indicates the result from AASHTO, Section C5.4.2.4 for normal weight concrete while the solid line indicates $\pm 20\%$ (AASHTO, 2012).

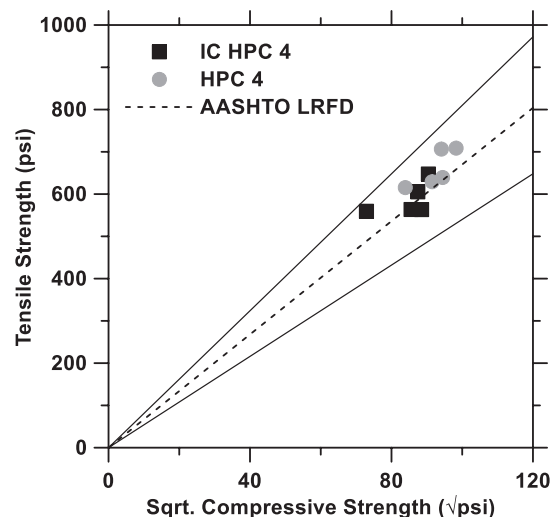


Figure 5.27 Splitting tensile strength of samples procured on the day of construction of the fourth bridge deck plotted as a function of the square root of the corresponding measured compressive strength. The dashed line indicates the result from AASHTO, Section 5.8.2.2 while the solid line indicates $\pm 20\%$ (AASHTO, 2012).

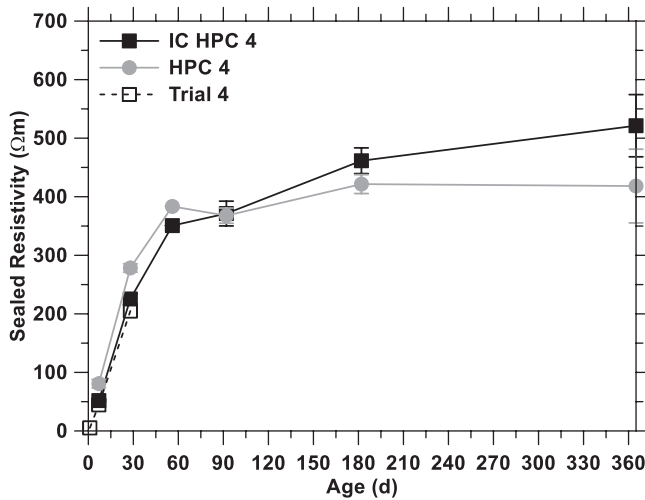


Figure 5.28 Evolution of the sealed uniaxial resistivity of samples procured on the day of construction of the fourth bridge deck.

measured diffusion coefficients indicates a resistance to chloride penetration similar to that of the first bridge deck materials.

5.5 Conclusions

In 2013, the INDOT commissioned the construction of four internally cured, high-performance concretes using a performance-based specification. This chapter has summarized the experimental results obtained from laboratory testing of samples procured on the day of construction of each of these bridge decks. The conclusions of this chapter are summarized as:

1. Each of the samples tested exceeded the minimum specified 28-day strength of 5 ksi within two weeks. Additionally, the mixtures from the first and fourth bridge decks reached strengths near 10 ksi after one year.
2. The modulus of elasticity of the IC HPC mixtures is similar to HPC mixtures, with results generally falling within $\pm 5\%$.
3. The splitting tensile strength of IC HPC mixtures are similar to HPC mixtures, with the results from each mixture generally falling within the standard deviation of the test relative to the corresponding mixture.

TABLE 5.4

Results of chloride migration tests and resistivity test for the samples procured on the day of construction of the fourth bridge deck. The results of each test are presented in the corresponding units used in the calculation of results of each test.

Mixture	Test	Result	Standard Deviation	Unit
IC HPC 4	RCPT	550	± 35	C
HPC 4		560	± 15	C
IC HPC 4	NORD	2.3	± 0.7	$(10^{-12} \text{ m}^2/\text{sec})$
HPC 4		3.0	± 0.4	$(10^{-12} \text{ m}^2/\text{sec})$
IC HPC 4	Stadium Migration	1.32	—	$(10^{-11} \text{ m}^2/\text{sec})$
HPC 4		1.18	—	$(10^{-11} \text{ m}^2/\text{sec})$
IC HPC 4	Uniaxial Resistivity	76.6 (750)	—	$(\Omega\cdot\text{m})$
HPC 4	(Formation Factor)	109.8 (1075)	—	$(\Omega\cdot\text{m})$

Note: All samples tested at an age of 91 days.

4. The codified equations for predicting the modulus of elasticity (E_c) and the splitting tensile strength (f_{ct}) using the square root of the measured compressive strength show good agreement with experimental data within the tolerance of the estimation ($\pm 20\%$). The equations have been provided here:

$$E_c = 1,820 \sqrt{f'_c (\text{ksi})} \quad \text{AASHTOC5.4.2.4.1}$$

$$f_{ct} = \frac{1}{4.7} \sqrt{f'_c (\text{ksi})} \quad \text{AASHTO5.8.2.2}$$

5. Each of the samples tested in the rapid chloride permeability test exhibited a charge passed that was below the maximum threshold of 1500 C.
6. Each of the IC HPC samples tested exhibited a lower charge passed in the RCPT compared to the reference HPC mixtures.

6. SERVICE LIFE ESTIMATION

6.1 Introduction

In 2013, the Indiana Department of Transportation (INDOT) commissioned the construction of four bridge decks to be made with a new class of internally cured, higher performance concrete (IC HPC). In an effort to improve upon the standard bridge deck concrete which achieves an estimated service life of approximately 18 years (Weiss, Bu, Di Bella, & Villani., 2013), a ternary blended cementitious system made at moderate water-to-cementitious-materials ratios (w/cm), of less than 0.43. It has been shown that materials made at lower w/cm utilizing large amounts of supplementary cementitious materials can have an increased susceptibility to cracking (Bentur, 2003; Weiss, 1999). To address this, internal curing was implemented.

The IC HPC bridge decks that were cast were made by four separate producers, located in four different INDOT districts. The projects were supervised by four different district construction units. The bridges had varying span lengths (maximum span lengths ranged from 8.5 m to 26 m) and varying structural configurations (single span composite with steel girders, three span continuous composite with steel girders, and two span continuous composite with prestressed concrete beams with an integrally cast pier).

6.2 Objectives

This chapter presents an experimental investigation of the four internally cured bridge deck concretes that were cast in the state of Indiana in 2013. In addition, these same mixtures were reproduced without internal curing at the local production facilities using the same approach used for the IC HPC (henceforth referred to as simply higher performance concrete (HPC)). The service life was then estimated for these 8 bridge deck concretes using a fundamental approach which accounts for the measured permeability, diffusion, and mixture proportions of each material. The service life of each of these mixtures will then be compared to the service life of the traditional bridge deck concrete mixture in Indiana. Finally, one of the IC HPC bridge decks was inspected after approximately 6 months of service for shrinkage cracking.

6.3 Experimental Investigation

The specimens obtained in this study were produced on the same day that each bridge deck was cast using the same mixture proportions, batching and mixing system, and aggregate moisture adjustments as was used for the bridge deck. Upon completion of the deck pour, two separate concrete trucks were ordered at each producer's facility, containing 2.3 m³ (three cubic yards) of concrete each. The first truck contained the IC HPC as batched that morning while the second truck contained the equivalent HPC, where the LWA in the mixture was replaced with normal weight fine aggregate.

6.3.1 Materials

The cementitious materials used in the study include Type I ordinary portland cement, Class C fly ash or ground granulated blast furnace slag (GGBFS), and densified silica fume. The aggregate consisted of a

normal weight natural fine aggregate and a normal weight limestone conforming to INDOT gradation 9 (INDOT, 2014b). To achieve internal curing, an expanded shale lightweight fine aggregate was used to replace a portion of the normal fine aggregate. The LWA stockpiles were required to be soaked with water using an approved sprinkler system for a minimum of 48 hours, followed by a draining period of 12 to 15 hours immediately prior to production. The moisture state of the LWA was determined using the centrifuge method (Miller, Barrett, et al., 2014) where, at the time of batching, the measured absorption ranged from 18.7 to 20.2% for all mixtures. The measured surface moisture contents of the LWA for all mixtures ranged between 6.6 to 9.9%.

6.3.2 Mixture Proportions

The as-batched mixture proportions of the concretes used in this study can be seen in Table 6.1. The naming convention of each mixture is denoted by the concrete mixture type (IC HPC or HPC) and a numeral indicating the base mixture for each bridge deck in no particular order. Concrete mixtures IC HPC 1 and HPC 1 were made using the same mixture proportions with the only difference being the replacement of fine aggregate with LWA for the purposes of internal curing. The design mixture proportions were specified to have a w/cm between 0.36 and 0.43, contain 20 to 25% replacement of cement by fly ash (by mass) or alternatively 15 to 20% of GGBFS (by mass), and a 3 to 7% replacement of cement by silica fume. Additionally, the mixtures were specified to have a paste content below 25%, contain 6.5% of entrained air by volume, and achieve a slump of 63.5 mm to 139.7 mm (INDOT, 2014a). Air entrainer, high-range water reducing agents (HRWRA), mid-range water reducing agent (MRWRA), and retardant admixtures were added at the discretion of each producer in order to meet these

TABLE 6.1
Concrete mixture proportions as batched.

	IC HPC 1	HPC 1	IC HPC 2	HPC 2	IC HPC 3	HPC 3	IC HPC 4	HPC 4	
W/CM	0.405	0.428	0.396	0.403	0.447	0.422	0.465	0.398	
Cement	394	398	443	443	432	432	438	458	
Fly Ash	125	125	—	—	113	113	—	—	
GGBFS	—	—	99	98	—	—	120	125	
Silica Fume	[lb/cyd]	25	25	25	17	17	25	25	
Coarse Aggregate	1825	1834	1802	1802	1731	1724	1827	1798	
Fine Aggregate	745	1222	780	1335	819	1338	851	1384	
Lightweight Aggregate	329	—	346	—	420	—	507	—	
Air Entrainment	1.20	1.70	0.59	0.59	0.89	0.95	1.14	1.10	
HRWRA	[oz/cwt]	15.00	13.25	5.45	5.47	9.49	10.08	14.92	14.17
MRWRA	—	—	—	—	1.96	1.90	3.60	3.46	
Retarder	1.99	3.77	2.99	3.00	—	—	—	—	
Measured Air Content	[%]	6.5	7.1	5.1	5.2	1.8*	5.9	8.1	7.1
Slump	[in]	3.5	6.0	8.0*	7.0*	2.0	2.0	9.0*	9.0*
Paste Content	[%]	24.0	25.0	24.4	24.6	26.0*	25.2*	24.5	25.3*

*Indicates measures not conforming to limits set within INDOT specifications for IC HPC (INDOT, 2014a).

specifications. In mixtures which were internally cured, a volume of lightweight aggregate was used to replace normal fine aggregate at a rate such that the LWA supplied approximately 7.2 kg of water/kg of cementitious materials, following the approach set forth by Bentz and Snyder (1999).

6.3.3 Methods

The permeability associated with the loss of water vapor of each mixture was determined through the use of drying tests on cylindrical samples. At an age of 91 days, a set of six specimens obtained by cutting field cast 4 in diameter by 8 in tall cylinders to 4 in diameter by 0.4 in tall and 2 in tall from (three samples of each height). The samples were then submerged in water until they reached a mass equilibrium, considered in this case to be the “saturated” condition. The “saturated” surface dry weight was then taken (as well as the buoyant weight) then the samples were introduced to a drying environment of 50% relative humidity (RH) at 23 ± 2 °C (73 ± 4 °F). The mass change of the samples was monitored for a minimum of 6 months for each mixture. Upon completion of the drying tests, the samples were oven dried in order to obtain the porosity (ASTM, 2006).

The diffusion coefficients for ionic species were measured using the Stadium Lab simulation technique and a migration cell. The test method is a modified version of ASTM C1202 (ASTM, 2012d), where the intensity of electrical current passed through a 4 in diameter by 2 in thick cylindrical specimen is monitored over a 14-day period (SIMCO Technologies, Inc., 2013). The samples used for this test were cut from a set of 4 in diameter by 8 in tall concrete cylinders that were sealed and placed in a chamber at $98 \pm 2\%$ RH and 23 ± 2 °C (73 ± 4 °F) for 90 days. After the samples were cut, the sides of the samples were sealed with an epoxy after which they were vacuum saturated with 0.3 M NaOH for approximately 18 hours using an industrial vacuum chamber regulated 6 ± 3 tor. Once saturated, the samples were mounted between a cell filled with 0.3 M NaOH solution (downstream) and a cell filled with 0.5 M NaCl + 0.3 M NaOH solution (upstream). A constant DC potential of 20V was maintained across the specimen for 14 days while the voltage, current, and temperature were measured and recorded at 15 minute

intervals (Di Bella, 2012). The results from the migration cell and the volume of permeable voids were then used in Stadium Lab software to evaluate the ionic diffusion coefficients and the tortuosity of the samples (Samson et al., 2003).

The results from the permeability tests and ionic diffusion tests, as well as mixture proportions and material compositions were then used in the Stadium simulation package to estimate the service life of the bridge deck materials; this method follows the outlined procedure in the Stadium technical guide (SIMCO Technologies, Inc., 2010). To be consistent, the exposure condition for each bridge deck mixture was simulated for Indianapolis, Indiana, where the exposure temperature cycled about an average temperature of 11 °C with an amplitude of 13 °C (52 ± 23 °F) over the course of each year. The average exposure RH for the materials was set to be 70.5% while exposure to sodium chloride was set for a period of 45 days with a maximum concentration of 400 mmol/L. The simulations were carried out for 120 years, with a time step of 24 hours. Detailed inputs including the cementitious compositions of each mixture used in these simulations are available in Appendix F.

6.4 Results and Discussion

The results from the permeability test can be seen in Table 6.2. In general, it can be noticed that the measured volume of permeable voids is greater in internally cured mixtures, however this is likely an artifact of the testing method in which the porous lightweight aggregates are exposed when the samples are cut. Further evidence of this phenomenon can be seen by estimating the desorption isotherm as calculated by Equation 6.1, where the water content, w , is estimated as a function of relative humidity, H . The parameters β and δ are fitted from the drying test described previously and ϕ is the measured volume of permeable voids. Figure 6.1 shows a comparison of the estimated isotherms for IC HPC 4 and HPC 4, where it can be noticed that in general, the difference in volume of pores exists largely at the highest relative humidities. Using the Kelvin-Laplace equation to estimate the size of the voids that would be emptying at these high RH, it becomes clear that these are the largest pores in the system (Barrett et al., 2014), which is consistent with drying occurring in the larger pores of the exposed lightweight aggregates.

TABLE 6.2
Results from moisture desorption testing for water vapor permeability.

	IC HPC 1	HPC 1	IC HPC 2	HPC 2	IC HPC 3	HPC 3	IC HPC 4	HPC 4
Volume of permeable voids, ϕ [%]	13.0	11.7	12.8	11.9	15.0	12.5	13.8	11.7
Permeability [E-22 m ²]	18.0	14.8	19.8	34.7	12.0	18.2	10.1	3.31
β Parameter	-145.0	-156.9	-163.2	-176.6	-89.2	-111.8	-100.1	-89.40
δ Parameter	0.10	0.11	0.10	0.10	0.11	0.11	0.11	0.10

Note: Average coefficient of variation for permeability measurements is 20.6% (Conciatori et al., 2014).

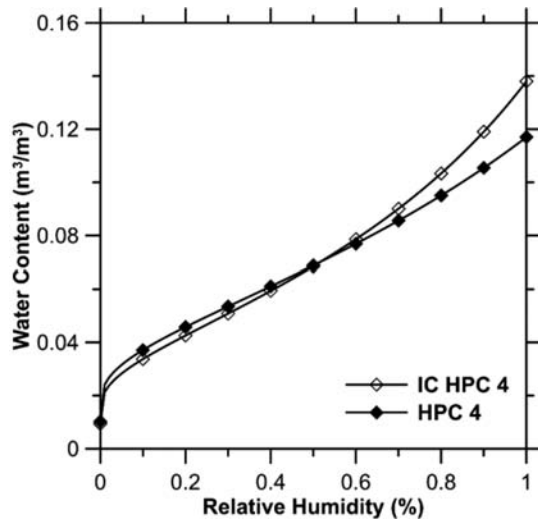


Figure 6.1 Estimated desorption isotherm for IC HPC 4 and HPC 4.

Inspection of the permeability coefficients of each mixture yields no general trend between IC HPC and HPC, with the internally cured mixtures having lower permeability in the second and third series while it is higher in the first and fourth. Additionally, there seems to be no correlation between the magnitudes of the permeability in relation to w/cm or mixture proportions. It is perhaps worth noting that the volume of entrained air was lower for IC HPC 2 and 3 in comparison to IC HPC 1 and 4, which may have resulted in the lower permeability for these mixtures in reference to their non-internally cured counterparts, as water occupying this space would be lost easier resulting in higher permeabilities.

$$w = \frac{\phi}{\beta \phi + (H^{\beta} - 1) + 1} \quad (3.1)$$

The results of the migration cell testing can be seen in Table 6.3. It should first be noted that the method presented here differs from similar migration methods in that the diffusion coefficients are calculated over the pore volume and not the bulk of the sample. In addition, the calculations assume a linear relationship between diffusion coefficients and tortuosity, hence the relative differences hold for both measures. It can be seen that the tortuosity of IC HPC 1, 2, and 3 are significantly lower than their non-internally cured counterparts, with reductions of 28%,

51%, and 56% respectively. This reduction in tortuosity (and chloride diffusion) can be attributed to the extended degree of hydration due to the additional water from internal curing and the densification of the matrix adjacent to the lightweight aggregates, as is consistent with previous findings (Bentz & Stutzman, 2008; Castro, 2011). For IC HPC 4, a 12% increase in tortuosity is observed and is likely attributable to the increase in w/cm in relation to HPC 4. In comparison to a recent study performed on the traditional bridge deck mixtures (i.e., Class C concrete), the magnitude of the chloride diffusion coefficients of the mixtures presented here are 1.75 to 8 times lower (with the Class C concrete having a chloride diffusion coefficient reported as $7.67E-11 \text{ m}^2/\text{s}$ at 91 days) (Weiss et al., 2013).

The results of the service life simulations for the eight bridge deck materials can be seen in Figure 6.2, where the total chloride content of each mixture at the depth of the reinforcing bar is plotted as a function of time. The dashed line on the plot indicates a critical threshold for the initiation of the corrosion of the reinforcing steel, set at 0.5% as suggested by Stadium and based upon research conducted by the Federal Highway Administration (McDonald, Pfeifer, & Sherman, 1998). The estimated service life of IC HPC 2 and 3 is approximately 60 years, while IC HPC 4 achieves a service life of 73 years and IC HPC 1 reaches 92 years before the initiation of corrosion. The HPC 2 and 3 mixtures achieve lower service lives of 30 to 35 years, which may be associated with the higher permeability and greater connectivity of the pore structure (i.e., higher tortuosity) of the HPC 3 mixture. HPC 1 and 4 are both estimated to achieve longer service lives than their internally cured counterparts, however it should be acknowledged that this model does not account for the potential for cracking, the presence of which would expedite deterioration (Bentz et al., 2013; Pease, Geiker, Stang, & Weiss, 2011; Raoufi & Weiss, 2012). Perhaps the most important takeaway from this service life estimation however is the relative comparison to the standard bridge deck mixture used in Indiana which has an estimated service life (using the same methodologies presented here) of 18 years. The bridge deck materials in this study achieve a corrosion-based life cycle of nearly 2 to 5 times longer than the standard Class C mixture, with the internally cured mixtures showing 3 to 4.5 times longer life

TABLE 6.3
Calculated chloride diffusion coefficients and associated tortuosity from migration cell testing.

	IC HPC 1	HPC 1	IC HPC 2	HPC 2	IC HPC 3	HPC 3	IC HPC 4	HPC 4
Cl ⁻ Diffusion Coefficient [e-11 m ² /s]	0.96	1.32	2.38	4.83	1.43	3.32	1.32	1.18
Tortuosity	0.0047	0.0065	0.0117	0.0238	0.0071	0.0163	0.0065	0.0058

Note: Average coefficient of variation for ionic diffusion coefficients is 11.1% (Conciatori et al., 2014).

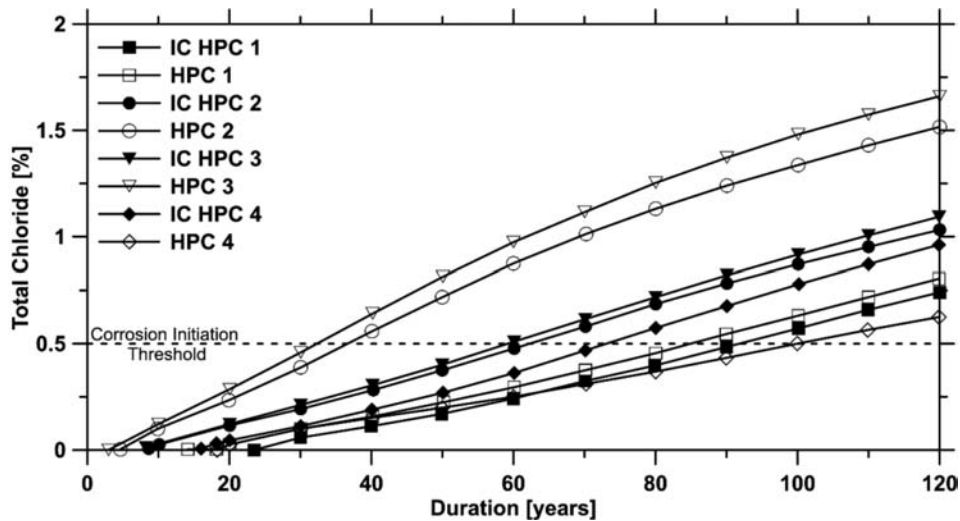


Figure 6.2 Total chloride content versus time for each mixture. (Corrosion initiation threshold for reinforcing steel indicated by dashed line at 0.5%).

cycles while also addressing the potential for cracking through internal curing.

After approximately six months of service, a visual inspection for cracking was performed on the bridge deck which consisted of the material referred to as IC HPC 4 herein. A picture from this inspection can be seen in Figure 6.3. Upon inspection, it was found that two cracks were present in the bridge deck, located directly above the integrally placed pier (at either edge of the pier), while no other signs of cracking was identified. Due to the structural configuration of this bridge (two continuous spans cast compositely with prestressed beams) it is likely that these cracks are due to the restraint provided by the integral pier and the negative moment induced in the bridge deck above this pier from traffic loading. Evidence of transverse cracking that is consistent with shrinkage cracking in higher performance concretes used in bridge decks was not found (Frosch & Aldridge, 2008). Further observations of this bridge deck and the others involved in this study will be made, however it is believed that the use of internal curing has effectively reduced the potential for shrinkage cracking due to volumetric changes in the concrete material used to construct the decks. These findings are similar to field observations made in which an internally cured Class C concrete bridge deck showed no cracking during inspection after 20 months of service, while a second bridge made during the same week which consisted of standard Class C concrete contained two transverse cracks (Di Bella, Schlitter, Carboneau, & Weiss, 2012).

6.5 Summary and Conclusions

This chapter presented data from internally cured commercial concrete used in field structures to estimate the service life of reinforced concrete bridge decks by

using a methodology of which accounts for the mixture proportions, the permeability, and the intrinsic chloride diffusion of a concrete mixture while simulating the regional field exposure conditions of a bridge deck made with these materials. The conclusions of this chapter are summarized as:



Figure 6.3 Field inspection of IC HPC bridge deck on State Road 933 over Baugo Creek, Indiana, USA.

1. The results indicate that the measured permeability of IC HPC mixtures is similar to corresponding HPC mixtures, with small variations existing due to a measured increase in the volume of voids present from exposed lightweight aggregate surfaces (an artefact of the testing method).
2. Internal curing generally results in a significant reduction in the tortuosity of the concrete, due in part to the extended degree of hydration and the densification of the interfacial regions around the LWA.
3. The IC HPC concretes cast in the state of Indiana in 2013 achieve an estimated service life improvement of 3 to 4.5 times that of the conventional bridge deck concrete specified.
4. A field inspection of one of these bridges indicated no visible shrinkage cracking after six months of service.

7. LABORATORY MEASUREMENTS OF SHRINKAGE BEHAVIOR

7.1 Introduction

In the previous chapters, the construction, performance, and service life of industrially produced bridge deck concretes was discussed. As an effort to reduce shrinkage, internal curing was used in these mixtures to address the early age shrinkage that may occur in higher performance concretes, however few standardized methods for the field measurement of autogenous shrinkage exist. In order to assess the shrinkage behavior of the IC HPC and HPC mixtures involved in this study laboratory measurements are needed.

7.2 Objectives

This chapter presents an experimental investigation of the shrinkage behavior of the IC HPC mixtures specified and produced as a part of this research. These mixtures were recreated in the laboratory using constituent materials obtained on the day of construction of each of the four bridge decks described in this report. In an effort to assess the impact of internal curing (a technology

implemented specifically to address the autogenous shrinkage of higher performance concretes) the linear autogenous shrinkage of IC HPC mixtures will be compared to the HPC mixtures. Using the dual ring test, the stress generated due to autogenous shrinkage of each mixture will also be assessed. In addition, the total shrinkage due to drying and autogenous deformations will be measured for each mixture.

7.3 Mixture Proportions and Mixing Procedure

The mixture proportions used to produce samples for evaluating the shrinkage of the IC HPC and HPC mixtures are shown in Table 7.1. The IC HPC mixture designs are based on the approved mixtures for production of the bridge decks. The HPC mixtures use the corresponding IC HPC mixture as a base design for proportioning with an adjustment being made to replace the lightweight aggregate with an equivalent volume of normal weight fine aggregate. The admixture dosage rates were unchanged in order to provide an indication of impact on fresh properties due to the presence of lightweight aggregate for internal curing. The measured slump and air content of each mixture is also provided in Table 7.1, where it can be seen that (for different combinations of commercially available admixtures) the presence of lightweight aggregate has minor effects on these fresh properties.

The laboratory mixtures were mixed in a dual action pan mixer with the aggregates being prepared in the open dry state. For the mixtures which contained fine lightweight aggregate for the purposes of internal curing, the aggregate was soaked in the mixing water for an amount of time necessary to achieve the design absorption (based on a 24-hour absorption value determined by the Indiana Department of Transportation Office of Materials Management, as reported in Chapter 4). At the time of production, the fine aggregate, coarse aggregate, and lightweight fine aggregate (if any) were added to

TABLE 7.1
Mixture proportions of samples created to study the shrinkage of IC HPC and HPC concretes.

	IC HPC1	HPC1	IC HPC2	HPC2	IC HPC3	HPC3	IC HPC4	HPC4
W/CM	0.406	0.429	0.406	0.403	0.396	0.396	0.403	0.403
Cement	395	398	443	443	435	435	435	435
Fly Ash	125	125	—	—	115	115	—	—
GGBFS	—	—	96	98	—	—	115	115
Silica Fume	25	25	25	25	25	25	25	25
Coarse Aggregate	1825	1834	1800	1802	1740	1740	1790	1790
Fine Aggregate	744	1221	780	1336	825	1341	782	1335
Lightweight Aggregate	329	—	332	—	340	—	365	—
Air Entrainer	0.6	0.6	0.2	0.2	0.3	0.3	0.4	0.4
HRWRA	4.4	4.4	1.8	1.82	3.36	3.36	4.72	4.72
MRWRA	—	—	—	—	0.6	0.6	1.2	1.2
Retarder	1.3	1.3	1.0	1.0	—	—	—	—
Air Content [%]	9.8	10.6	9.6	7.3	4.6	5.5	6.5	6.0
Slump [in]	1.5	1.5	2.0	1.0	0.5	1.5	2.5	1.5
Unit Weight [lb/ft ³]	138.6	137.2	133.3	143.3	141.3	144.5	139.2	147.9
Paste Content [%]	24.09	24.98	24.59	24.61	24.89	24.89	24.92	24.92

a “battered” mixing pan and a small amount of mixing water was added to control dust. For the IC HPC mixtures, the excess mixing water was decanted from the lightweight aggregate prior to addition to the pan. The cementitious materials would then be added and mixed until blended homogeneously, at which point the remaining mixing water would be added. Admixtures were added after the complete addition of mixing water. The concrete was mixed for a period of three minutes, allowed to rest for three minutes, then mixed for an additional two minutes prior to casting.

7.4 Testing Methods

The following tests were performed to assess the shrinkage behavior of the IC HPC mixtures as well as the HPC reference mixtures: linear drying shrinkage test, linear autogenous shrinkage test, and the dual ring test for evaluating the restrained shrinkage behavior due to autogenous shrinkage.

7.4.1 Linear Drying Shrinkage Prisms

The total shrinkage due to drying and autogenous shrinkage was determined using a procedure similar to ASTM C 157 for concrete (ASTM, 2008). A series of 3 in tall \times 3 in deep \times 11.25 in long, prismatic specimens were cast to study the length change over time for a drying condition of $50 \pm 1\%$ RH at 23 ± 1 °C. Each sample was cast in two lifts, being rodded and vibrated after each lift. After 24 hours of curing in the molds, the samples were demolded and sealed with two layers of aluminum foil tape over the ends and two opposite sides resulting in unidirectional drying. The length change over time was measured using a digital comparator with a precision of ± 0.0001 in. The mass of each sample was also measured throughout the duration of testing.

7.4.2 Linear Autogenous Shrinkage Tubes

The linear autogenous shrinkage was measured using a modified procedure for concrete similar to the method outlined in ASTM C 1698 (ASTM, 2009), as pictured in Figure 7.1. Concrete was placed vertically in a 3 in



Figure 7.1 Picture of the linear autogenous “tube” shrinkage test during operation.

diameter by 12 in long corrugated tube being vibrated and rodded throughout casting to ensure the filling of each rib of the corrugated tube. The ends of the tube were sealed using metal caps, and the tube was placed horizontally on a metal frame for the entirety of the test. Linear voltage differential transformer (LVDT) displacement transducers were mounted to the frame which automatically measured the length change of the sample in five minute intervals over the duration of the test.

7.4.3 Restrained Autogenous Shrinkage

The dual ring test was used to quantify the stress generated due to autogenous deformations. The dual ring testing device (shown in Figure 7.2) consists of two instrumented concentric invar restraining rings on a circulating-water cold plate base that operates in an insulated chamber (Schlitter, Bentz, & Weiss, 2011; Schlitter, Senter, et al., 2010). In this test, a concrete specimen was cast between the inner and outer rings in two lifts, being rodded and vibrated after each lift then trowel finished upon completion. After casting, the experimental setup is placed in an insulated housing where the cold plate base is connected to a circulating water bath to maintain a constant temperature for 7 days. After 7 days of near isothermal conditions, the temperature of the sample was reduced at a rate of 2 °C/hour in an attempt to induce a thermal shrinkage crack. Strain measurements from the rings were automatically recorded at 5 minute intervals and were used to determine the stress generated in the sample.

7.5 Results

The results for each mixture have been presented using the same naming convention outlined in the previous

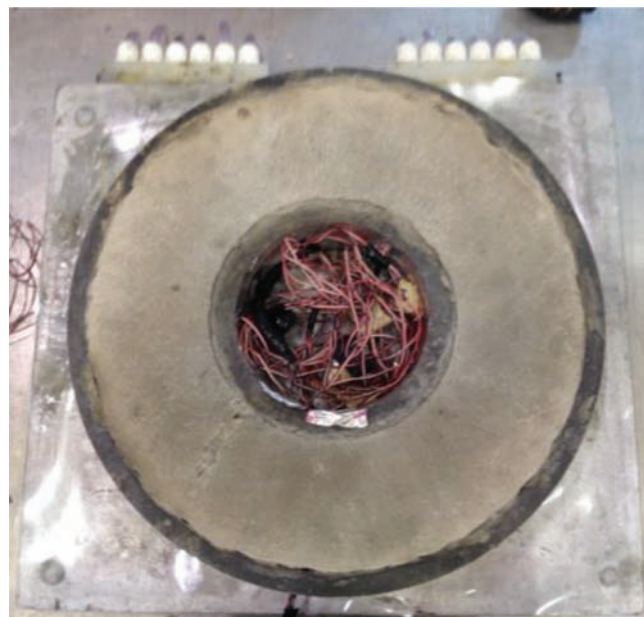


Figure 7.2 Picture of the concrete dual ring test upon completion of the test.

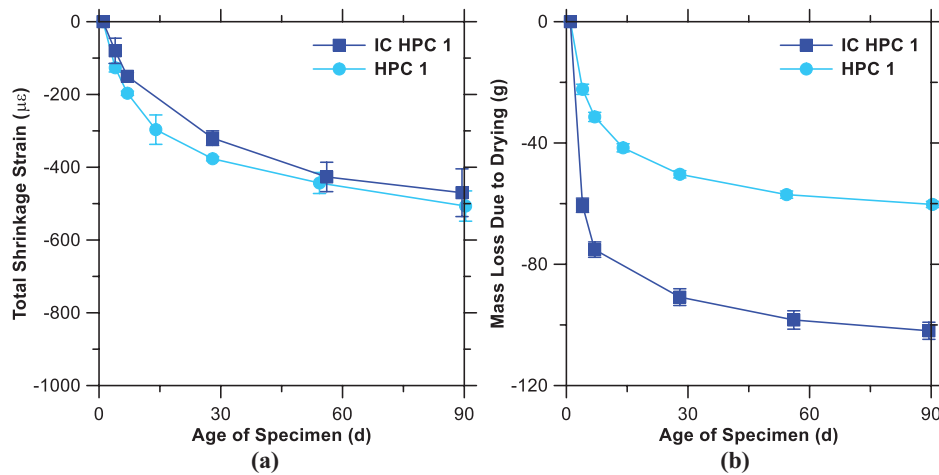


Figure 7.3 (a) Total strain due to drying and autogenous deformations and (b) total mass loss of IC HPC 1 and HPC 1 mixtures.

chapters. The results will be presented for each of the tests described in the previous section in the same order for each of the bridges that were involved in the study (i.e., bridges 1 through 4) with the IC HPC mixtures being shown in the same plot as the HPC mixtures for comparison.

7.5.1 Bridge Deck #1

The results of the testing performed on samples replicating the mixtures produced at the first bridge deck are shown in the following section.

7.5.1.1 Linear Drying Shrinkage Prisms. The results of the drying shrinkage test performed on mixtures which reproduced the concretes procured on the day of construction for the first bridge deck can be seen in Figure 7.3. It can be seen that the total shrinkage of the IC HPC 1 and HPC 1 mixtures is similar throughout the duration of testing, a finding that is consistent with previous research (Henkensiefken et al., 2009). It should be noted however that these measurements are zeroed after 24 hours of hydration has occurred and therefore do not include any autogenous strains that occurred over this period of time. The total strain measured in the test after 90 days is approximately 500 $\mu\epsilon$.

The difference between the behavior of the IC HPC 1 and HPC 1 mixtures can be seen in a comparison of the mass loss during the test, where the IC HPC 1 mixture loses approximately twice the mass of water relative to the HPC 1 mixture. This behavior is a consequence of specifying a testing condition of 50% RH, which fixes a critical pore size where any larger pores will empty due to drying. In internally cured mixtures where water may still be in the lightweight aggregate during testing (as is the likely scenario in this test where the w/cm is moderate and the testing is occurring at low degrees of hydration) this water will be lost due to drying since the pores of the LWA are larger than the critical pore size. This result is again consistent with previous research (Radlinska et al., 2008) and it should be emphasized that the excess water

in the IC HPC 1 mixture available for evaporation due to drying can act to mitigate plastic shrinkage cracking although this is not the designed intent (Henkensiefken, Briatka, Bentz, Nantung, & Weiss, 2010).

7.5.1.2 Linear Autogenous Shrinkage Tubes. The results of the linear autogenous shrinkage test performed on mixtures which reproduced the concretes procured on the day of construction for the first bridge deck can be seen in Figure 7.4. In the presentation of the results, a negative strain indicates shrinkage in the sample while a positive strain indicates a measured expansion. The results of the IC HPC 1 and HPC 1 mixtures indicate that expansions occurred throughout the duration of the testing period. This result is not uncommon in internally cured mixtures (Schlitter, Henkensiefken, et al., 2010) however the expansion present in the HPC 1 mixture likely indicates that expansive reactions are present during the first week of hydration in this cementitious system.

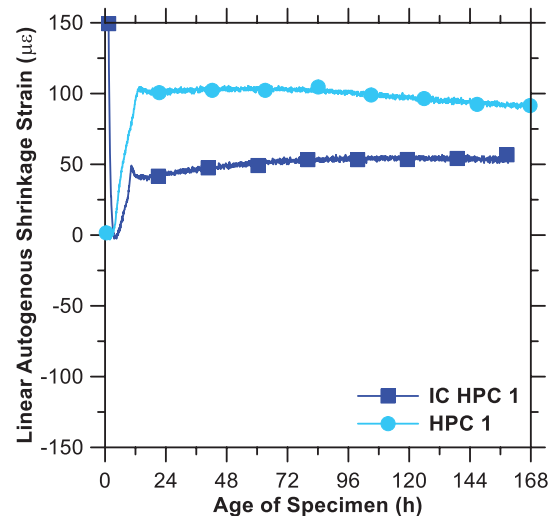


Figure 7.4 Linear autogenous shrinkage of IC HPC 1 and HPC 1 mixtures.

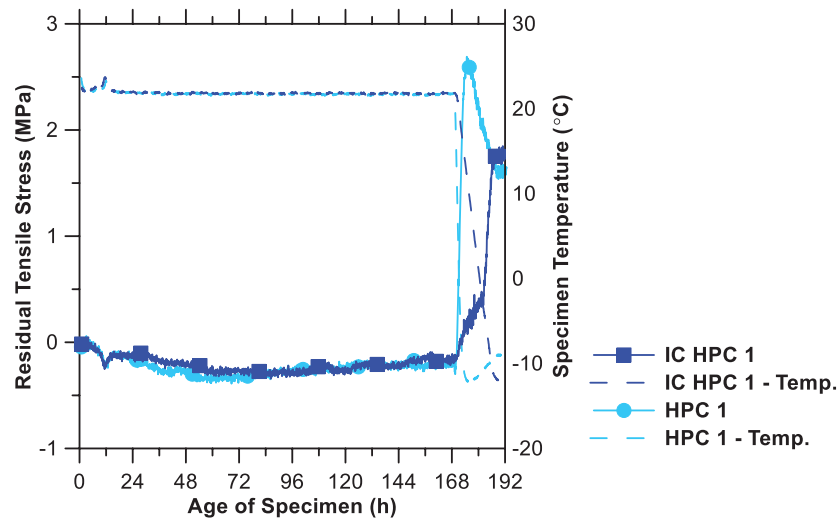


Figure 7.5 Residual stress developed in the dual ring test for IC HPC 1 and HPC 1 mixtures.

7.5.1.3 Dual Ring Test. The results of the dual ring test performed on mixtures which reproduced the concretes procured on the day of construction for the first bridge deck can be seen in Figure 7.5. It can be seen that expansive stresses (i.e., compression in the sample) developed over the first seven days in both the IC HPC 1 and HPC 1 mixtures, consistent with the results from the autogenous shrinkage test. Upon reduction of the temperature after seven days, neither sample cracked however inspection of the results shows a reduction in the peak thermally induced stress in the IC HPC 1 mixture of approximately 25%. This reduction in thermally induced stress is largely a consequence of a lower coefficient of thermal expansion (COTE) in internally cured concretes (Wyrzykowski & Lura, 2013). An additional effect of the presence of LWA can be seen in the slope of the induced thermal stress, where the rate of stress development in the IC HPC 1 mixture is lower due to the more compliant nature of the IC HPC 1 mixture (Barrett et al., 2011; Raoufi, Schlitter, Bentz, & Weiss, 2011; Schlitter et al., 2013).

7.5.2 Bridge Deck #2

The results of the testing performed on samples replicating the mixtures produced at the second bridge deck are shown in the following section.

7.5.2.1 Linear Drying Shrinkage Prisms. The results of the drying shrinkage test performed on mixtures which reproduced the concretes procured on the day of construction for the second bridge deck can be seen in Figure 7.6. It can be seen that the IC HPC 2 and HPC 2 mixtures exhibit similar total shrinkage strains while the IC HPC 2 mixture loses approximately 50% more mass (i.e., moisture) due to drying. The total shrinkage strain is approximately 600 $\mu\epsilon$ after 91 days and in general these results follow the same trends as those seen from the first bridge deck.

7.5.2.2 Linear Autogenous Shrinkage Tubes. The results of the linear autogenous shrinkage test performed on mixtures which reproduced the concretes

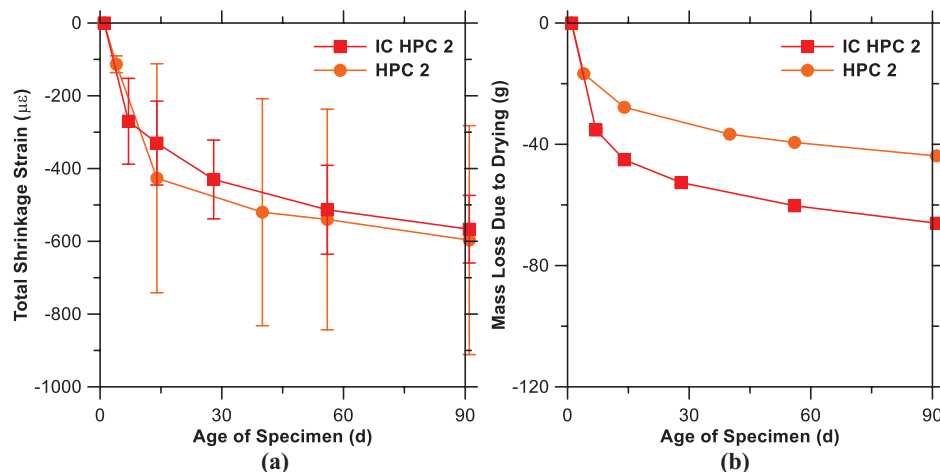


Figure 7.6 (a) Total strain due to drying and autogenous deformations and (b) total mass loss of IC HPC 2 and HPC 2 mixtures.

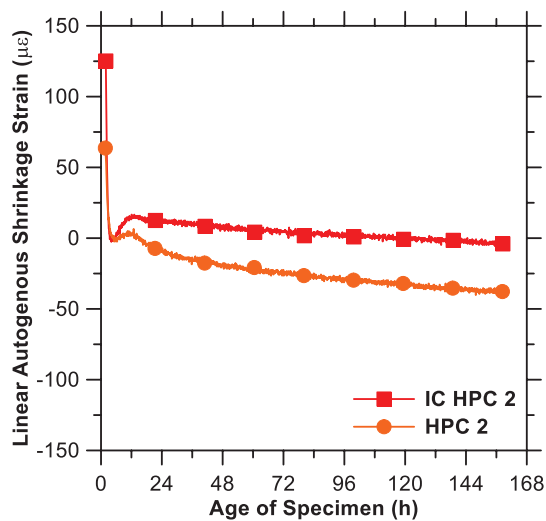


Figure 7.7 Linear autogenous shrinkage of IC HPC 2 and HPC 2 mixtures.

procured on the day of construction for the second bridge deck can be seen in Figure 7.7. It can be seen that the IC HPC 2 mixture exhibits a reduction of approximately 90% compared to HPC 2, with a total measured autogenous strain of $5 \mu\epsilon$ after 7 days of hydration. These results are consistent with previous research, indicating that an appropriate amount of lightweight aggregate was provided to supply a volume of water sufficient to mitigate early age autogenous deformations (Schlitter, Henkensiefken, et al., 2010). It should be noted that the mixtures produced in the field (i.e., those discussed in previous chapters and presently in service at each bridge) was designed with the same volume of water provided for internal curing, however during production this amount of water was allowed to be exceeded, resulting in more water being available for internal curing in the field produced mixtures. It is therefore

anticipated that the results presented in Figure 7.7 represent the upper bound of autogenous shrinkage occurring in the field mixtures.

7.5.2.3 Dual Ring Test. The results of the dual ring test performed on mixtures which reproduced the concretes procured on the day of construction for the second bridge deck can be seen in Figure 7.8. The results indicate that the IC HPC 2 mixture reduced the residual tensile stress due to restrained autogenous shrinkage by 80% compared to HPC 2, with a total stress generated of 0.1 MPa (14.5 psi) at 7 days. After reducing the temperature of each sample no cracks were induced, however the peak stress induced in the sample was reduced by 45% in the IC HPC 2 mixture. Additionally, the rate of stress development in the IC HPC 2 mixture was reduced. Collectively, these results indicate that the presence of internal curing reduces the residual tensile stress due to autogenous shrinkage to a negligible quantity while also providing a more robust response to thermal loading at early ages.

7.5.3 Bridge Deck #3

The results of the testing performed on samples replicating the mixtures produced at the third bridge deck are shown in the following section.

7.5.3.1 Linear Drying Shrinkage Prisms. The results of the drying shrinkage test performed on mixtures which reproduced the concretes procured on the day of construction for the third bridge deck can be seen in Figure 7.9. It can be seen from the shrinkage strain that the IC HPC 3 mixture exhibited a lower total shrinkage than the HPC 3 mixture, a result that may be consistent with a larger amount of underlying autogenous shrinkage. In the IC HPC 3 mixture this autogenous shrinkage should be reduced substantially resulting in

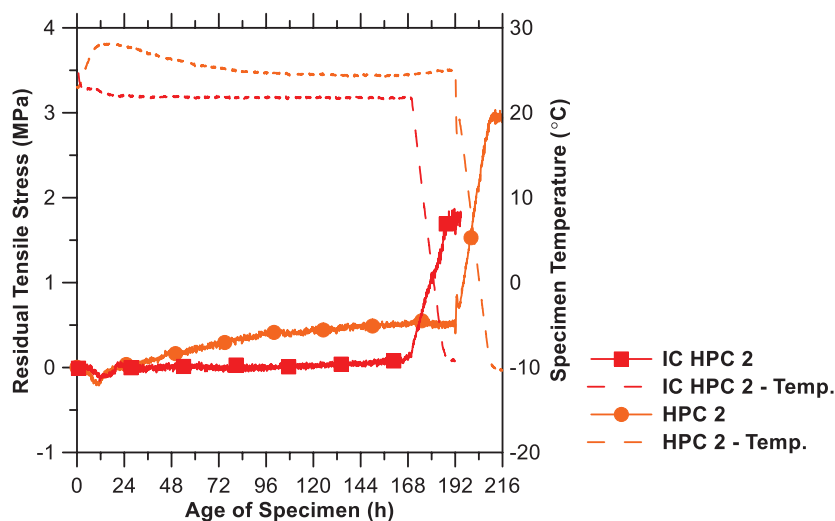


Figure 7.8 Residual stress developed in the dual ring test for IC HPC 2 and HPC 2 mixtures.

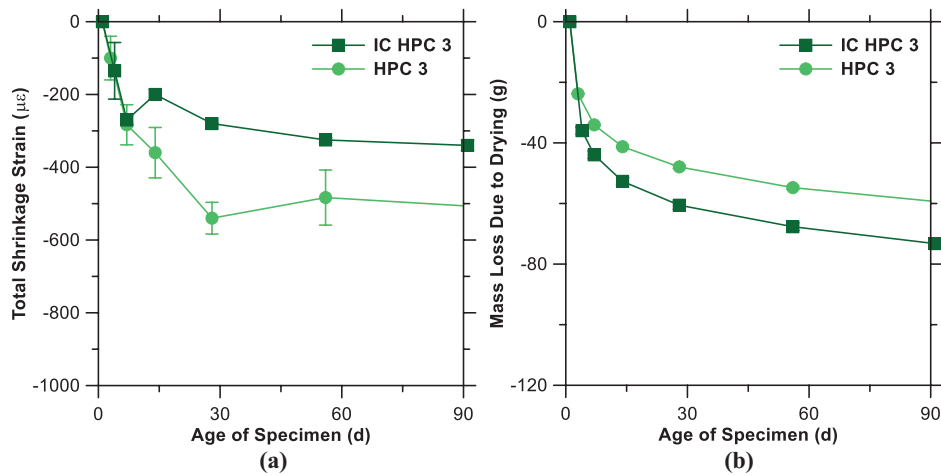


Figure 7.9 (a) Total strain due to drying and autogenous deformations and (b) total mass loss of IC HPC 3 and HPC 3 mixtures.

the observed reduction of total shrinkage strain compared to a non-internally cured mixture (i.e., HPC 3). The self-desiccation occurring in the IC HPC 3 mixture would also result in the migration of more water from the LWA to refill the smaller pores in the matrix and manifests in the mass loss results shown in Figure 7.9b where the total mass of water lost in the IC HPC 3 mixture is similar to that of HPC 3 in comparison to the previous two bridge decks.

7.5.3.2 Linear Autogenous Shrinkage Tubes. The results of the linear autogenous shrinkage test performed on mixtures which reproduced the concretes procured on the day of construction for the third bridge deck can be seen in Figure 7.10. It can be seen that the autogenous shrinkage in the IC HPC 3 mixture is reduced by approximately 70% in comparison to HPC 3, with a total shrinkage strain of 27 $\mu\epsilon$ at 7 days. Again, it should be emphasized that these laboratory results represent the upper bound of autogenous

shrinkage expected in the field produced concrete for the third bridge deck.

7.5.3.3 Dual Ring Test. The results of the dual ring test performed on mixtures which reproduced the concretes procured on the day of construction for the third bridge deck can be seen in Figure 7.11. It can be seen that the residual tensile stress in the IC HPC 3 sample due to autogenous shrinkage has been reduced by approximately 80% at 7 days compared to HPC 3. The peak stress induced by thermal shrinkage was reduced by 55%, while the rate of generation of this stress was reduced by approximately 50%. Collectively, these results indicate that the presence of internal curing reduces the residual tensile stress due to autogenous shrinkage to a negligible quantity while also providing a more robust response to thermal loading at early ages.

7.5.4 Bridge Deck #4

The results of the testing performed on samples replicating the mixtures produced at the fourth bridge deck are shown in the following section.

7.5.4.1 Linear Drying Shrinkage Prisms. The results of the drying shrinkage test performed on mixtures which reproduced the concretes procured on the day of construction for the fourth bridge deck can be seen in Figure 7.12. It can be seen that the IC HPC 4 and HPC 4 mixtures exhibit similar total shrinkage strains while the loss of mass due to drying is also similar after 28 days of testing. These trends are consistent with the results from previous mixtures.

7.5.4.2 Linear Autogenous Shrinkage Tubes. The results of the linear autogenous shrinkage test performed on mixtures which reproduced the concretes procured on the day of construction for the fourth

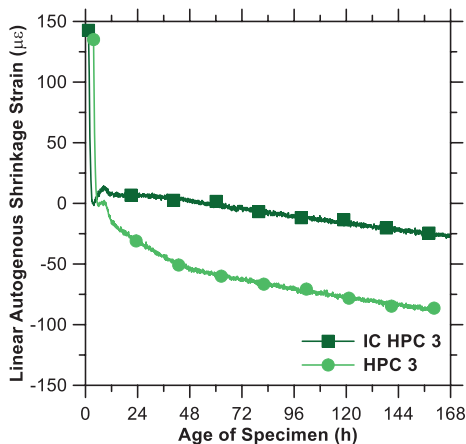


Figure 7.10 Linear autogenous shrinkage of IC HPC 3 and HPC 3 mixtures.

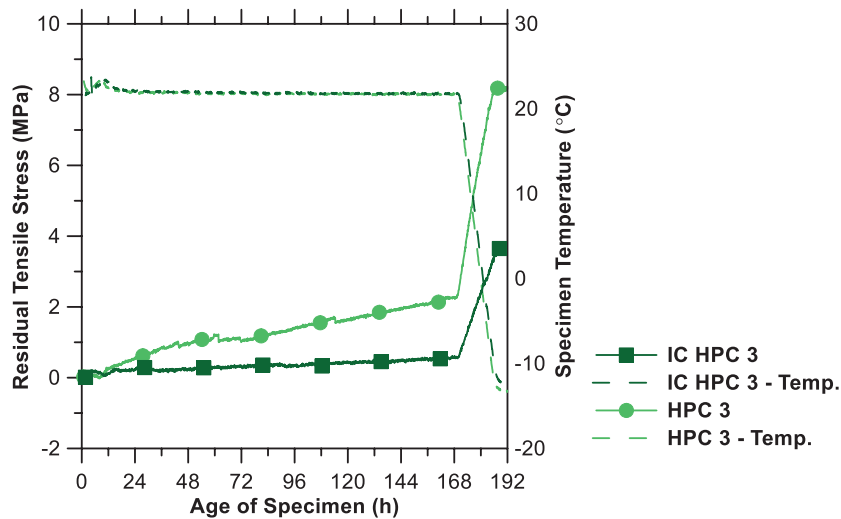


Figure 7.11 Residual stress developed in the dual ring test for IC HPC 3 and HPC 3 mixtures.

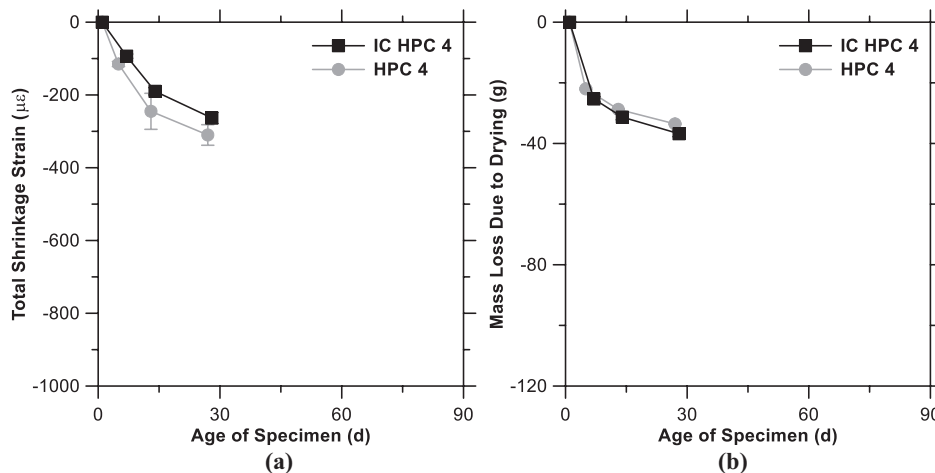


Figure 7.12 (a) Total strain due to drying and autogenous deformations and (b) total mass loss of IC HPC 4 and HPC 4 mixtures.

bridge deck can be seen in Figure 7.13. It can be seen that the autogenous shrinkage in the IC HPC 4 mixture is reduced by approximately 70% in comparison to

HPC 4, with a total shrinkage strain of $20 \mu\epsilon$ at 7 days. Again, it should be emphasized that these laboratory results represent the upper bound of autogenous shrinkage expected in the field produced concrete for the fourth bridge deck.

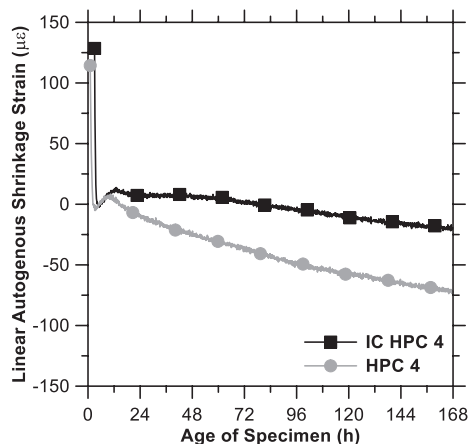


Figure 7.13 Linear autogenous shrinkage of IC HPC 4 and HPC 4 mixtures.

7.5.4.3 Dual Ring Test. The results of the dual ring test performed on mixtures which reproduced the concretes procured on the day of construction for the fourth bridge deck can be seen in Figure 7.14. It can be seen that the residual tensile stress in the IC HPC 4 sample due to autogenous shrinkage has been reduced by approximately 100% at 7 days compared to HPC 4 (the results of the test indicate induced expansion in the IC HPC 4 mixture). The peak stress induced by thermal shrinkage was reduced by 50%, while the rate of generation of this stress was reduced by approximately 65%. Collectively, these results indicate that the presence of internal curing reduces the residual tensile stress due to autogenous shrinkage to a negligible quantity while also providing a more robust response to thermal loading at early ages.

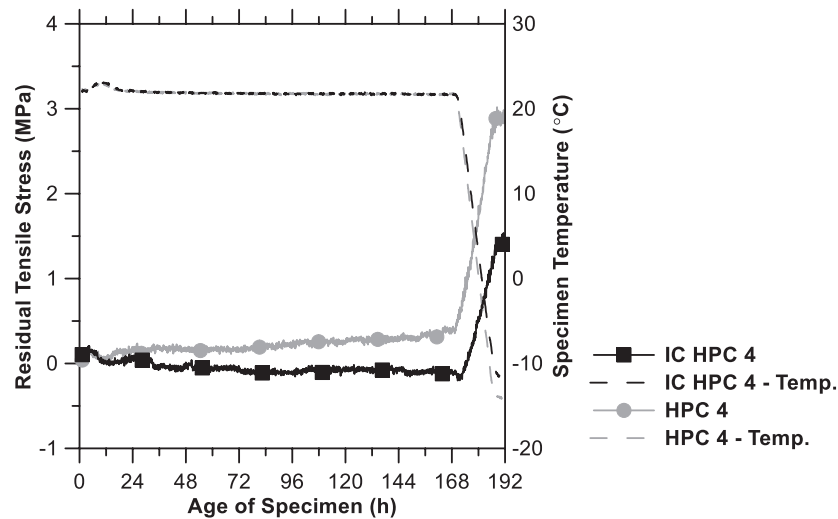


Figure 7.14 Residual stress developed in the dual ring test for IC HPC 4 and HPC 4 mixtures.

7.6 Conclusions

This chapter has summarized the experimental results of laboratory made concretes which reproduced the mixtures used in the production of the four bridge decks discussed in previous chapters. While recreating the field mixtures exactly is not possible, the mixtures presented here represent an upper bound of shrinkage behavior that may be anticipated in the field produced mixtures. The conclusions of this chapter are summarized as:

1. The total strain of IC HPC mixtures due to combined autogenous and drying shrinkage is similar to or lower than that of comparable mixtures which are not internally cured. Further, such tests that begin measurements after 24 hours of hydration may not be the most appropriate measurement to assess the impact of internal curing.
2. The IC HPC mixtures exhibited a reduction in measured linear autogenous shrinkage strain of 70 to 90%, with the maximum measured strain of any IC HPC sample at 7 days being 27 $\mu\epsilon$.
3. The IC HPC mixtures exhibited a reduction in measured residual tensile stress due to autogenous shrinkage of 80% or more with the maximum measured stress of any IC HPC sample at 7 days being 0.5 MPa (72 psi), or approximately 10% of the available tensile strength.
4. The IC HPC mixtures exhibited a reduction in measured peak induced thermal stress of 25 to 55% and is likely associated with a reduction in the COTE of the internally cured mixtures.
5. The IC HPC mixtures exhibited a reduction up to 50% in the rate of induced stress due to temperature reduction and is likely associated to the more compliant nature of the internally cured mixtures.

Collectively, these results indicate that the presence of internal curing reduces the residual tensile stress due to autogenous shrinkage to negligible quantities while also providing a more robust response to thermal loading at early ages.

8. SUMMARY AND CONCLUSIONS

8.1 Introduction

The Indiana Department of Transportation constructed four bridge decks utilizing internally cured high-performance concrete during the summer of 2013. These decks are being considered as one method to reduce cracking and to improve durability based on research findings from the research presented in the FHWA/IN/JTRP-2010/10 report (<http://dx.doi.org/10.5703/1288284314262>) (Schlitter, Henkensiefken, et al., 2010). The objective of this research was to document the construction of the four IC HPC bridge decks that were constructed in Indiana during 2013 and to quantify the properties and performance of these decks. The documentation provided in this project focused on three main areas:

1. Documentation of construction and measurement of the constituent materials, variability, and fresh concrete properties.
2. Documentation of the properties that influence long-term service life, including chloride diffusion and other transport properties.
3. Documentation of the shrinkage and cracking resistance with a comparison of IC HPC and reference (non-internally cured) mixtures.

8.2 Summary of Conclusions

The conclusions of each chapter are summarized in the following sections.

8.2.1 Chapter 2: Background and Introduction

This chapter presented a literature review on internal curing, providing the necessary background for understanding the science of this approach toward mitigating autogenous shrinkage and putting the technique in the context of field application. Comments were made on

the use of a new testing technique which utilizes a centrifuge to determine the moisture state of the lightweight aggregate. An example was then provided to instill the importance for determining the moisture states of all the aggregates if a higher performance concrete truly is desired. Finally, comments on the field preparation of LWA stockpiles were offered.

8.2.2 Chapter 3: Mixture Proportioning

This chapter served to discuss how to use developed spreadsheets to calculate properties of lightweight aggregate and how to implement these properties into the mixture design process for internally cured concrete. The properties of the lightweight aggregate that are important for design are absorption, desorption, and relative density. To make an initial design, these properties should be determined after a 24-hour soaking period. Once the properties are obtained, any existing mixture can be internally cured using the mixture proportion design sheet provided with this report. It is then necessary to repeat testing using the same worksheets on the day of batching in the field to make sure that the mixture is produced as designed. The absorption needs to be checked to make sure that it is equal to or higher than the 24-hour absorption used in the original design and the surface moisture (free moisture) must be calculated correctly to achieve the design w/c. Finally, the relative density must be tested again in the field to adjust the additional absorbed moisture. This will allow the volume of lightweight aggregate to remain constant and will prevent the mixture from under-yielding. Once all of the properties have been entered into the spreadsheet, a final SSD mixture design is given. Batch weights are adjusted for free moisture are also given so that batching tolerances can be monitored. It is emphasized that this technique differs from design recommendations provided in ASTM C 1761 (ASTM, 2013b) and the authors believe that the methods presented herein provide an easily specifiable yet conservative method for producing internally cured concrete in the field.

8.2.3 Chapter 4: Bridge Deck Production and Construction Documentation

This chapter has summarized the construction process of four internally cured, high-performance bridge decks in Indiana during 2013. While avoidable issues during construction have been highlighted, two points should be emphasized. First, four bridge decks utilizing internal curing are now in service. The concrete materials produced for each of the four bridge decks in this study achieve higher performance in laboratory testing (strength, shrinkage, and chloride resistance) than traditional INDOT Class C bridge deck materials used in Indiana (this is discussed in detail in the following chapters). Second, a mixed specification of prescriptive and performance-based parameters was successfully used to produce these bridge decks. A final consideration for

the use of internally cured, high-performance concrete is summarized monetarily in Table 8.1, where the price of the bridge deck concretes procured in this study are listed.

This chapter has summarized the trial batch, production, and construction of these bridge decks. The conclusions of this chapter are summarized as:

1. Four internally cured, high-performance bridge decks were successfully constructed and are now in service.
2. A mixed specification of prescriptive and performance-based measures was successfully implemented in the production of the bridge deck materials produced in this study.
3. Pre-wetted lightweight aggregate can be successfully used in the production of internally cured concrete if the moisture condition of the aggregates are understood, controlled, and accounted for in production. This study implemented a new testing technique that utilizes a centrifuge to rapidly condition the lightweight aggregate to a surface-dry condition and reduces variability in testing over previous testing methods.
4. Variability in moisture states within a stockpile of pre-wetted lightweight aggregate should be controlled or monitored and accounted for throughout concrete production.
5. Batching issues were observed which would be present regardless of the concrete mixture proportions, whether the concrete mixtures are internally cured or not, or regardless of the constituent materials used during production. It is the research team's position that additional training and education for batch plant operators to fully understand how to make moisture adjustments and change scale jog rates when producing mixtures containing lightweight aggregates may serve to avoid potential issues.
6. Pumping issues were observed which would be present regardless of the concrete mixture proportions, whether the concrete mixtures are internally cured or not, or regardless of the constituent materials used in concrete production and are avoidable with additional training and education.
7. Segregation issues were observed on one deck that are independent of whether the concrete mixtures are internally cured or not and are avoidable with additional training and education.
8. Trial batches should be used to identify and solve potential issues for production prior to date of construction, as exemplified by the third bridge deck in this study.

8.2.4 Chapter 5: Laboratory Testing of Field Produced Samples: Mechanical and Transport Behavior Evaluation

This chapter has summarized the experimental results obtained from laboratory testing of samples procured on the day of construction of each of these

TABLE 8.1
Price [$\$/\text{yd}^3$] for each mixture in this study.

Mixture	1	2	3	4
IC HPC	126	203	116	165
HPC	126	104	116	159

bridge decks. The conclusions of this chapter are summarized as:

1. Each of the samples tested exceeded the minimum specified 28-day strength of 5 ksi within two weeks. Additionally, the mixtures from the first and fourth bridge decks reached strengths near 10 ksi after one year.
2. The modulus of elasticity of the IC HPC mixtures is similar to HPC mixtures, with results generally falling within $\pm 5\%$.
3. The splitting tensile strength of IC HPC mixtures are similar to HPC mixtures, with the results from each mixture generally falling within the standard deviation of the test relative to the corresponding mixture.
4. The codified equations for predicting the modulus of elasticity (E_c) and the splitting tensile strength (f_{ct}) using the square root of the measured compressive strength show good agreement with experimental data within the tolerance of the estimation ($\pm 20\%$). The equations have been provided here: $E_c = 1,820\sqrt{f'_c(\text{ksi})}$ AASHTO C5.4.2.4-1 $f_{ct} = \frac{1}{4.7}\sqrt{f'_c(\text{ksi})}$ AASHTO 5.8.2.2.
5. Each of the samples tested in the rapid chloride permeability test exhibited a charge passed that was below the maximum threshold of 1500 C.
6. Each of the IC HPC samples tested exhibited a lower charge passed in the RCPT compared to the reference HPC mixtures.

8.2.5 Chapter 6: Service Life Estimation

This chapter presented experimental results obtained from laboratory testing of samples procured on the day of construction of each bridge deck involved in this study which were used to estimate the diffusion-based service life of each reinforced concrete bridge deck. The methodology implemented accounts for the mixture proportions, permeability, and the intrinsic chloride diffusion of each concrete mixture while simulating the regional field exposure conditions of each bridge deck made with these materials. The conclusions of this chapter are summarized as:

1. The results indicate that the measured permeability of IC HPC mixtures is similar to corresponding HPC mixtures, with small variations existing due to a measured increase in the volume of voids present from exposed lightweight aggregate surfaces (an artefact of the testing method).
2. Internal curing generally results in a significant reduction in the tortuosity of the concrete, due in part to the extended degree of hydration and the densification of the interfacial regions around the LWA.
3. The IC HPC concretes cast in the state of Indiana in 2013 achieve an estimated service life improvement of 3 to 4.5 times that of the conventional Class C bridge deck concrete that is specified in Indiana.
4. A field inspection of one of these bridges indicated no visible shrinkage cracking after six months of service.

8.2.6 Chapter 7: Laboratory Measurements of Shrinkage Behavior

This chapter summarized the experimental results of laboratory made concretes which reproduced the

mixtures used in the production of the four bridge decks discussed in previous chapters. While recreating the field mixtures exactly is not possible, the mixtures presented here represent an upper bound of shrinkage behavior that may be anticipated in the field produced mixtures. The conclusions of this chapter are summarized as:

1. The total strain of IC HPC mixtures due to combined autogenous and drying shrinkage is similar to or lower than that of comparable mixtures which are not internally cured. Further, such tests that begin measurements after 24 hours of hydration may not be the most appropriate measurement to assess the impact of internal curing.
2. The IC HPC mixtures exhibited a reduction in measured linear autogenous shrinkage strain of 70 to 90%, with the maximum measured strain of any IC HPC sample at 7 days being 27 $\mu\epsilon$.
3. The IC HPC mixtures exhibited a reduction in measured residual tensile stress due to autogenous shrinkage of 80% or more with the maximum measured stress of any IC HPC sample at 7 days being 0.5 MPa (72 psi), or approximately 10% of the available tensile strength.
4. The IC HPC mixtures exhibited a reduction in measured peak induced thermal stress of 25 to 55% and is likely associated with a reduction in the COTE of the internally cured mixtures.
5. The IC HPC mixtures exhibited a reduction up to 50% in the rate of induced stress due to temperature reduction and is likely associated to the more compliant nature of the internally cured mixtures.

Collectively, these results indicate that the presence of internal curing reduces the residual tensile stress due to autogenous shrinkage to negligible quantities while also providing a more robust response to thermal loading at early ages.

8.3 Final Recommendations

The conclusions of this report and the findings presented in the FHWA/IN/JTRP-2010/10 report (<http://dx.doi.org/10.5703/1288284314262>) (Schlitter, Henkensiefken, et al., 2010) and the CDOT-2014-3 report (Jones et al., 2014) indicate that internal curing is a practice-ready, engineered solution that may lead to the production of higher performance concretes which have a reduced potential for cracking. To aid in the implementation of internal curing in practice, spreadsheets which automate calculations necessary for quality control for lightweight aggregates, mixture proportioning, and moisture adjustments have been made available as a part of this report (see Appendix G and Appendix H). The authors emphasize that the implementation of such technologies alone does not guarantee higher performance however, as the production of such concrete requires a degree of technical competence in design, production, and construction of concrete materials. As is the case with the production of any concrete, internally cured or not, performance will be directly tied to the careful accounting of water, be it on the surface of aggregates, in the mixing drum after

washing, or elsewhere. Special attention should be paid to the proper operation of batching systems, while placement techniques should be reviewed to minimize unwanted effects, and proper finishing and curing techniques must always be practiced. Only after performing the basics of concrete production properly will the full benefits of internal curing be actualized.

REFERENCES

- AASHTO. (2007). *Standard test method for electrical indication of concrete's ability to resist chloride ion penetration*. Washington, DC: American Association of State Highway and Transportation Officials.
- AASHTO. (2012). *AASHTO LRFD bridge design specifications*. Washington, DC: American Association of State Highway and Transportation Officials.
- ACI. (1998). *Standard practice for selecting proportions for structural lightweight concrete (ACI 211.2-98)*. Farmington Hills, MI: American Concrete Institute.
- ACI. (2011). *Building code requirements for structural concrete (ACI 318-11)*. Farmington Hills, MI: American Concrete Institute.
- ASTM. (2002). *Standard test method for static modulus of elasticity and Poisson's ratio of concrete in compression (ASTM Standard C469)*. West Conshohocken, PA: ASTM International.
- ASTM. (2004a). *Standard test method for splitting tensile strength of cylindrical concrete specimens (ASTM Standard C496/C496M)*. West Conshohocken, PA: ASTM International.
- ASTM. (2004b). *Standard test method for determining age at cracking and induced tensile stress characteristics of mortar and concrete under restrained shrinkage (ASTM Standard C1581)*. West Conshohocken, PA: ASTM International.
- ASTM. (2006). *Standard test method for density, absorption, and voids in hardened concrete (ASTM Standard C642)*. West Conshohocken, PA: ASTM International.
- ASTM. (2008). *Standard test method for length change of hardened hydraulic-cement mortar and concrete (ASTM Standard C157/C157M)*. West Conshohocken, PA: ASTM International.
- ASTM. (2009). *Standard test method for autogenous strain of cement paste and mortar (ASTM Standard C1698-09)*. West Conshohocken, PA: ASTM International.
- ASTM. (2012a). *Standard test method for compressive strength of cylindrical concrete specimens (ASTM Standard C39/C39M)*. West Conshohocken, PA: ASTM International.
- ASTM. (2012b). *Standard test method for electrical indication of concrete's ability to resist chloride ion penetration (ASTM Standard C1202)*. West Conshohocken, PA: ASTM International.
- ASTM. (2012c). *Standard test method for chemical shrinkage of hydraulic cement paste (ASTM Standard C 1608-12)*. West Conshohocken, PA: ASTM International.
- ASTM. (2012d). *Standard test method for electrical indication of concrete's ability to resist chloride ion penetration (ASTM Standard C 1202-12)*. West Conshohocken, PA: ASTM International.
- ASTM. (2013a). *Standard test method for total evaporable moisture content of aggregate by drying (ASTM Standard C566-13)*. West Conshohocken, PA: ASTM International.
- ASTM. (2013b). *Standard specification for lightweight aggregate for internal curing of concrete (ASTM Standard C1761-13-B)*. West Conshohocken, PA: ASTM International.
- Barrett, T., Miller, A., & Weiss, J. (2014). Reducing shrinkage cracking with internal curing: From theory to practice. *The Indian Concrete Journal*, 88(4), 61–71.
- Barrett, T. J., De La Varga, I., Schlitter, J. & Weiss, W. J. (2011). *Reducing the risk of cracking in high volume fly ash concrete by using internal curing*. Paper presented at the World of Coal Ash Conference, May 9–12, 2011, Denver, CO. Retrieved from <http://www.flyash.info/2011/131-DelaVarga-2011.pdf>
- Barrett, T. J., De La Varga, I. & Weiss, W. J. (2012). Reducing cracking in concrete structures by using internal curing with high volumes of fly ash. In J. Carrato & J. Burns (Eds.), *Proceedings: Structures Congress 2012* (pp. 669–707). <http://dx.doi.org/10.1061/9780784412367.063>
- Bentur, A. (2003). Report 25: Early age cracking in cementitious systems—Report of RILEM technical committee TC 181-EAS: Early age cracking shrinkage induced stresses and cracking in cementitious systems (Vol. 25). RILEM Publications.
- Bentur, A., Igarashi, S.-I., & Kovler, K. (2001). Prevention of autogenous shrinkage in high-strength concrete by internal curing using wet lightweight aggregates. *Cement and Concrete Research*, 31, 1587–1591.
- Bentz, D. P. (1997). Three-dimensional computer simulation of portland cement hydration and microstructure development. *Journal of the American Ceramic Society*, 80, 3–21.
- Bentz, D. P., Garboczi, E. J., Lu, Y., Martys, N., Sakulich, A. R., & Weiss, W. J. (2013). Modeling of the influence of transverse cracking on chloride penetration into concrete. *Cement and Concrete Composites*, 38, 65–74.
- Bentz, D. P., Garboczi, E. J., & Quenard, D. A. (1998). Modelling drying shrinkage in reconstructed porous materials: Application to porous vycor glass. *Modelling and Simulation in Materials Science and Engineering*, 6, 211–236.
- Bentz, D. P., & Jensen, O. M. (2006). Mitigation strategies for autogenous shrinkage cracking. *Cement and Concrete Composites*, 26, 677–685.
- Bentz, D. P., Lura, P., & Roberts, J. W. (2005). Mixture proportioning for internal curing. *Concrete International*, 27, 35–40.
- Bentz, D. P., & Snyder, K. A. (1999). Protected paste volume in concrete: Extension to internal curing using saturated lightweight fine aggregate. *Cement and Concrete Research*, 29, 1863–1867.
- Bentz, D. P., & Stutzman, P. E. (2008). Internal curing and microstructure of high-performance mortars. In D. Bentz & B. Mohr (Eds.), *ACI SP-256, Internal curing of high-performance concretes: Laboratory and field experiences* (pp. 81–90). Farmington Hills, MI: American Concrete Institute.
- Bentz, D. P., & Weiss, W. J. (2011). *Internal curing: A 2010 state of the art review*. Gaithersburg, MD: National Institute of Standards and Technology, U.S. Department of Commerce.
- Bu, Y. (2014). *Service life prediction of concrete: considerations of specimen conditioning and testing methods on the measurement of porosity and diffusion coefficient of chloride* (Doctoral dissertation). West Lafayette, IN: Purdue University. Retrieved from <http://docs.lib.purdue.edu/dissertations/AAI3635801/>
- Byard, B. E., Schindler, A. K., & Barnes, R. W. (2014). Cracking tendency of lightweight aggregate bridge deck concrete. *ACI Materials Journal*, 111(2), 179–188.

- Capitol Scientific. (2015). Corning® 70581-1L PYREX® VISTA™ 1000mL Economy Class B Volumetric Flask with Blue PE Snap-Cap [Image]. Retrieved from <http://www.capitolscientific.com/Corning-70581-1L-PYREX-VISTA-1000mL-Economy-Class-B-Volumetric-Flask-with-Blue-PE-Snap-Cap>
- Castro, J. (2011). *Moisture transport in cement based materials: Application to transport tests and internal curing* (Doctoral dissertation). West Lafayette, IN: Purdue University. Retrieved from <http://docs.lib.purdue.edu/dissertations/AAI3475407/>
- Conciatori, D., Grégoire, É., Samson, É., Marchand, J., & Chouinard, L. (2014). Statistical analysis of concrete transport properties. *Materials and Structures*, 47, 89–103.
- Cusson, D., & Hoogveen, T. (2008). Internal curing of high-performance concrete with pre-soaked fine lightweight aggregate for prevention of autogenous shrinkage cracking. *Cement and Concrete Research*, 38, 757–765.
- De La Varga, I., Castro, J., Weiss, J., & Brameshuber, W. (2010). Preliminary findings from research to extend internal curing concepts to mixtures with higher volumes of fly ash. In W. Brameshuber (Ed.), *International RILEM conference on material science* (pp. 141–153). Bagnaux, France: RILEM Publications.
- Di Bella, C. (2012). *Chloride transport and shrinkage of plain and internally cured concrete* (Master's thesis). West Lafayette, IN: Purdue University. Retrieved from <http://docs.lib.purdue.edu/dissertations/AAI1529635/>
- Di Bella, C., Schlitter, J., Carboneau, N., & Weiss, J. (2012). *Documenting the construction of a plain concrete bridge deck and an internally cured bridge deck* (Indiana Local Technical Assistance Program Technical Reports Publication No. INLTAP-TR-1-2012). West Lafayette, IN: Purdue University. Retrieved from <http://docs.lib.purdue.edu/inltaptechs/2>
- Frosch, R. J., & Aldridge, T. S. (2008). *High-performance concrete bridge decks: A fast-track implementation study—Volume 1: Structural behavior* (Joint Transportation Research Program Publication No. FHWA/IN/JTRP-2008/29-1). West Lafayette, IN: Purdue University. <http://dx.doi.org/10.5703/1288284314308>
- Frosch, R. J., Gutierrez, S., & Hoffman, J. S. (2010). *Control and repair of bridge deck cracking* (Joint Transportation Research Program Publication No. FHWA/IN/JTRP-2010/04). West Lafayette, IN: Purdue University. <http://dx.doi.org/10.5703/1288284314267>
- Geiker, M. (1983). *Studies of Portland cement hydration by measurements of chemical shrinkage and a systematic evaluation of hydration curves by means of the dispersion model*. Lyngby, Denmark: Technical University of Denmark.
- Geiker, M. R., Bentz, D. P., & Jensen, O. M. (2004). Mitigating autogenous shrinkage by internal curing. In J. P. Ries & T. A. Holm (Eds.), *High-performance structural lightweight concrete, Edition: ACI SP-218* (pp. 143–154). Farmington Hills, MI: American Concrete Institute.
- Greenspan, L. (1977). Humidity fixed points of binary saturated aqueous solutions. *Journal of Research of the National Bureau of Standards*, 81, 89–96.
- Haecker, C., Bentz, D., Feng, X., & Stutzman, P. (2003). *Prediction of cement physical properties by virtual testing*. *Cement International*, 1, 86–92.
- Hammer, T. (1999). Test methods for linear measurement of autogenous shrinkage before setting. In E. Tazawa (Ed.), *Autogenous shrinkage of concrete* (pp. 143–154). London, UK: E&FN Spon.
- Henkensiefken, R., Bentz, D., Nantung, T., & Weiss, J. (2009). Volume change and cracking in internally cured mixtures made with saturated lightweight aggregate under sealed and unsealed conditions. *Cement and Concrete Composites*, 31, 427–437.
- Henkensiefken, R., Briatka, P., Bentz, D., Nantung, T., & Weiss, J. (2010). Plastic shrinkage cracking in internally cured mixtures made with pre-wetted lightweight aggregate. *Concrete International*, 32, 49–54.
- Henkensiefken, R., Nantung, T., & Weiss, J. (2011). Saturated lightweight aggregate for internal curing in low w/c mixtures: Monitoring water movement using X-ray absorption. *Strain*, 47(s1), e432–e441. <http://dx.doi.org/10.1111/j.1475-1305.2009.00626.x>
- Hossain, A. B., & Weiss, J. (2004). Assessing residual stress development and stress relaxation in restrained concrete ring specimens. *Cement and Concrete Composites*, 26, 531–540.
- House, M., Di Bella, C., Sun, H., Zima, G., Barcelo, L., & Weiss, W. J. (2014). The influence of slag aggregate production on its potential for use in internal curing. *Transportation Research Record*, 2441, 105–111.
- Igarashi, S.-I., Bentur, A., & Kovler, K. (2000). Autogenous shrinkage and induced restraining stresses in high-strength concretes. *Cement and Concrete Research*, 30, 1701–1707.
- INDOT. (2014a). *Indiana standard specifications: Section 502—Special provisions for internally cured, high performance, structural concrete for bridge deck*. Indianapolis, IN: Indiana Department of Transportation.
- INDOT. (2014b). *Indiana standard specifications: Section 904.03, Table (e)*. Indianapolis, IN: Indiana Department of Transportation.
- Jensen, O. M., & Hansen, P. F. (1996). Autogenous deformation and change of the relative humidity in silica fume-modified cement paste. *ACI Materials Journal*, 93(6), 539–543.
- Jensen, O. M., & Hansen, P. F. (2001a). Autogenous deformation and RH-change in perspective. *Cement and Concrete Research*, 31(12), 1859–1865. [http://dx.doi.org/10.1016/S0008-8846\(01\)00501-4](http://dx.doi.org/10.1016/S0008-8846(01)00501-4)
- Jensen, O. M., & Hansen, P. F. (2001b). Water-entrained cement-based materials: I. Principles and theoretical background. *Cement and Concrete Research*, 31, 647–654.
- Jones, W. A., House, M. W., & Weiss, W. J. (2014). *Internal curing of high performance concrete using lightweight aggregates and other techniques* (Colorado Department of Transportation Report No. CDOT-2014-3). Denver, CO: Colorado Department of Transportation.
- Kennedy, C. T. (1940). The design of concrete mixes. *ACI Journal Proceedings*, 36(2), 373–400.
- Le Chatelier, H. (1900). Sur les changements de volume qui accompagnent le durcissement des ciments. *Bulletin de la Societe d'Encouragement pour l'Industrie Nationale*, (5th series), 54–57.
- Lura, P. (2003). *Autogenous deformation and internal curing of concrete*. Delft, The Netherlands: Delft University Press.
- Lura, P., Bentz, D. P., Lange, D. A., Kovler, K., Bentur, A., & Van Breugel, K. (2006). Measurement of water transport from saturated pumice aggregates to hardening cement paste. *Materials and Structures*, 39, 861–868.
- Lura, P., Jensen, O. M., & Igarashi, S.-I. (2007). Experimental observation of internal water curing of concrete. *Materials and Structures/Materiaux et Constructions*, 40(2), 211–220. <http://dx.doi.org/10.1617/s11527-006-9132-x>
- Lura, P., Jensen, O. M., & Weiss, J. (2009). Cracking in cement paste induced by autogenous shrinkage. *Materials and Structures/Materiaux et Constructions*, 42(8), 1089–1099. <http://dx.doi.org/10.1617/s11527-008-9445-z>

- McDonald, D. B., Pfeifer, D. W., & Sherman, M. R. (1998). *Corrosion evaluation of epoxy-coated, metallic-clad and solid metallic reinforcing bars in concrete*. McLean, VA: Federal Highway Administration.
- Mehta, P. K., & Monteiro, P. J. M. (1993). Durability. In J. P. Skalny (Ed.), *Concrete, microstructure, properties and materials* (2nd ed.) (pp. 113–155). Upper Saddle River, NJ: Prentice-Hall.
- Miller, A., Spragg, R., Antico, F. C., Ashraf, W., Barrett, T., Behnood, A., Tian, Q. (2014). Determining the moisture content of pre-wetted lightweight aggregate: Assessing the variability of the paper towel and centrifuge methods. In J. Olek and J. Weiss (Eds.), *Proceedings of the 4th International Conference on the Durability of Concrete Structures* (pp. 312–316). West Lafayette, IN: Purdue University. Retrieved from <http://docs.lib.purdue.edu/icdcs/2014/materialscharacterization/4/>
- Miller, A. E., Barrett, T. J., Zander, A. R., & Weiss, W. J. (2014). Using a centrifuge to determine moisture properties of lightweight fine aggregate for use in internal curing. *Advances in Civil Engineering Materials*, 3(1). <http://dx.doi.org/10.1520/ACEM20130111>
- Mindess, S., Young, J. F., & Darwin, D. (2003). *Concrete*. Upper Saddle River, NJ: Prentice-Hall.
- Moon, J. H., & Weiss, J. (2006). Estimating residual stress in the restrained ring test under circumferential drying. *Cement and Concrete Composites*, 28, 486–496.
- Nordtest (1999). *Concrete, mortar and cement-based repair materials: Chloride migration coefficient from non-steady-state migration experiments* (NT Build 492). Espoo, Finland: Nordtest. Retrieved from <http://www.nordtest.info/index.php/methods/item/concrete-mortar-and-cement-based-repair-materials-chloride-migration-coefficient-from-non-steady-state-migration-experiments-nt-build-492.html>
- Pease, B., Geiker, M., Stang, H., & Weiss, J. (2011). The design of an instrumented rebar for assessment of corrosion in cracked reinforced concrete. *Materials and Structures*, 44, 1259–1271.
- Persson, B. (1997). Self-desiccation and its importance in concrete technology. *Materials and Structures*, 30, 293–305.
- Popovics, S. (1990). Analysis of concrete strength versus water-cement ratio relationship. *ACI Materials Journal*, 87(5), 517–529. <http://dx.doi.org/10.14359/1944>
- Powers, T. C., & Brownard, T. L. (1946). Studies of the physical properties of hardened Portland cement paste. *ACI Journal Proceedings*, 43(9), 249–336.
- Radlinska, A. (2008). *Reliability-based analysis of early-age cracking in concrete* (Doctoral dissertation). West Lafayette, IN: Purdue University. Retrieved from <http://docs.lib.purdue.edu/dissertations/AAI3344112/>
- Radlinska, A., Rajabipour, F., Bucher, B., Henskensiefken, R., Sant, G., & Weiss, J. (2008). Shrinkage mitigation strategies in cementitious systems: A closer look at differences in sealed and unsealed behavior. *Transportation Research Record*, 2070, 59–67.
- Radlinski, M., & Olek, J. (2010). *High-performance concrete bridge decks: A fast-track implementation study—Volume 2: Materials* (Joint Transportation Research Program Publication No. FHWA/IN/JTRP-2008/29-2). West Lafayette, IN: Purdue University. <http://dx.doi.org/10.5703/1288284314307>
- Rajabipour, F., Weiss, J., Shane, J. D., Mason, T. O., & Shah, S. P. (2005). Procedure to interpret electrical conductivity measurements in cover concrete during rewetting. *Journal of Materials in Civil Engineering*, 17, 586–594.
- Raoufi, K., Schlitter, J., Bentz, D., & Weiss, J. (2011). Parametric assessment of stress development and cracking in internally cured restrained mortars experiencing autogenous deformations and thermal loading. *Advances in Civil Engineering*, 2011. <http://dx.doi.org/10.1155/2011/870128>
- Raoufi, K., & Weiss, W. J. (2012). Corrosion and service life estimates for internally cured concrete. *ACI Special Publication*, 290. <http://dx.doi.org/10.14359/51684180>
- Samson, E., Marchand, J., & Snyder, K. (2003). Calculation of ionic diffusion coefficients on the basis of migration test results. *Materials and Structures*, 36, 156–165.
- Sant, G., Lura, P., & Weiss, J. (2006). A discussion of analysis approaches for determining ‘time-zero’ from chemical shrinkage and autogenous strain measurements in cement paste. In O. M. Jensen, P. Lura, & K. Kovler (Eds.), *International RILEM conference on volume changes of hardening concrete: Testing and mitigation* (pp. 20–23). Bagnaux, France: RILEM Publications. <http://dx.doi.org/10.1617/2351580052.040>
- Schlitter, J., Bentz, D., & Weiss, W. (2011). Quantifying residual stress development and reserve strength in internally cured concrete. *ACI Materials Journal*, 110, 51–55.
- Schlitter, J., Henskensiefken, R., Castro, J., Raoufi, K., Weiss, J., & Nantung, T. (2010). *Development of internally cured concrete for increased service life* (Joint Transportation Research Program Publication No. FHWA/IN/JTRP-2010/10). West Lafayette, IN: Purdue University. <http://dx.doi.org/10.5703/1288284314262>
- Schlitter, J. L., Bentz, D. P., & Weiss, W. J. (2013). Quantifying stress development and remaining stress capacity in restrained, internally cured mortars. *ACI Materials Journal*, 110(1), 3–12. <http://dx.doi.org/10.14359/51684361>
- Schlitter, J. L., Senter, A. H., Bentz, D. P., Nantung, T., & Weiss, W. J. (2010). A dual concentric ring test for evaluating residual stress development due to restrained volume change. *Journal of ASTM International*, 7(9). <http://dx.doi.org/10.1520/JAI103118>
- Shah, S., Wang, K., & Weiss, W. (2000). Is high strength concrete durable. In O. E. Gjorv & K. Sakai (Eds.), *Concrete technology for a sustainable development in the 21st century* (pp. 102–114). Boca Raton, FL: CRC Press.
- Shah, S. P., Weiss, W. J., & Yang, W. (1998). Shrinkage cracking—Can it be prevented? *Concrete International*, 20, 51–55.
- SIMCO Technologies, Inc. (2010). *Technical guide, STADIUM V2.9*. Quebec City, Quebec, Canada: S. T., Inc.
- SIMCO Technologies, Inc. (2013). *STADIUM lab 3.0 user guide*. Quebec City, Quebec, Canada: S. T., Inc.
- Spragg, R. P. (2013). *The rapid assessment of transport properties of cementitious materials using electrical methods* (Master’s thesis). West Lafayette, IN: Purdue University. Retrieved from <http://docs.lib.purdue.edu/dissertations/AAI1549494/>
- Spragg, R. P., Castro, J., Nantung, T., Paredes, M., & Weiss, J. (2012). Variability analysis of the bulk resistivity measured using concrete cylinders. *Advances in Civil Engineering Materials*, 1(1). <http://dx.doi.org/10.1520/ACEM104596>
- Spragg, R. P., Jones, S. Z., Bu, Y., Lu, Y., Bentz, D. P., & Weiss, J. (2015). Alkali-leaching in cementitious systems: Implications to measurements of electrical resistivity. Submitted for publication to *Construction and Building Materials*.
- Spragg, R., Villani, C., Snyder, K., Bentz, D., Bullard, J., & Weiss, J. (2013). Electrical resistivity measurements in cementitious systems: observations of factors that influence

- the measurements. *Transportation Research Record*, 2342, 90–98. <http://dx.doi.org/10.3141/2342-11>
- Tazawa, E.-I., Miyazawa, S., & Kasai, T. (1995). Chemical shrinkage and autogenous shrinkage of hydrating cement paste. *Cement and Concrete Research*, 25, 288–292.
- Test Mark Industries. (2015). Pycnometer [Image]. Retrieved from <http://www.testmark.net/showitem-333.html>
- Trtik, P., Münch, B., Weiss, W., Kaestner, A., Jerjen, I., Josic, L., Lura, P. (2011). Release of internal curing water from lightweight aggregates in cement paste investigated by neutron and X-ray tomography. *Nuclear Instruments and Methods in Physics Research Section A: Accelerators, Spectrometers, Detectors and Associated Equipment*, 651(1), 244–249. <http://dx.doi.org/10.1016/j.nima.2011.02.012>
- Vlahinić, I., Jennings, H. M., & Thomas, J. J. (2009). A constitutive model for drying of a partially saturated porous material. *Mechanics of Materials*, 41, 319–328.
- Weiss, W. J. (1999). *Prediction of early-age shrinkage cracking in concrete* (Doctoral dissertation). Retrieved from ProQuest. (Accession No. 304536501.)
- Weiss, J., Bu, Y., Di Bella, C., & Villani, C. (2013). Estimated performance of as-built internally cured concrete bridge decks. In D. Bjegović, H. Beushausen, & M. Serdar (Eds.), *RILEM international workshop on performance-based specification and control of concrete durability* (pp. 369–376). Bagnaux, France: RILEM Publications.
- Weiss, W., Yang, W., & Shah, S. (2000). Factors influencing durability and early-age cracking in high-strength concrete structures. *ACI Special Publication*, 189, 387–410.
- Weiss, W. J., Yang, W., & Shah, S. P. (1998). Shrinkage cracking of restrained concrete slabs. *Journal of Engineering Mechanics*, 124(7), 765–774.
- Wiegink, K., Marikunte, S., & Shah, S. P. (1996). Shrinkage cracking of high-strength concrete. *ACI Materials Journal*, 93(5), 409–415. <http://dx.doi.org/10.14359/9844>
- Wyrzykowski, M., & Lura, P. (2013). Controlling the coefficient of thermal expansion of cementitious materials—A new application for superabsorbent polymers. *Cement and Concrete Composites*, 35(1), 49–58. <http://dx.doi.org/10.1016/j.cemconcomp.2012.08.010>

APPENDICES
APPENDIX A

LAPORTE DISTRICT

ADDED 10/5/2012
Contract No. B-30498

INTERNALLY CURED, HIGH PERFORMANCE, STRUCTURAL CONCRETE
FOR BRIDGE DECK

Description

This work shall consist of furnishing and placing internally cured high performance concrete (IC-HPC), for bridge deck in accordance with 105.03. IC-HPC contains portland cement and two pozzolanic materials, as well as a pre-soaked lightweight fine aggregate, to produce a concrete of high durability, low permeability, and low cracking potential. The absorbed water within the pre-soaked lightweight fine aggregate provides internal moisture that is released to the hydrating cement within the paste matrix of the placed concrete. The pre-soaked lightweight fine aggregate is intended to inhibit autogenous shrinkage by hydrating more of the cementitious materials and thereby reduce early age cracking of the bridge deck.

MATERIALS

Materials

Materials shall be in accordance with the following:

Admixtures.....	912.03
Castings 910.05	
Cast Iron Soil Pipe.....	908.10
Coarse Aggregate, Class A*, Size No. 8.....	904
Curing Materials.....	912.01
Fabric For Waterproofing.....	913.16
Fine Aggregate, Natural Sand Size No. 23.....	904
Fly Ash.....	901.02
Ground Granulated Blast Furnace Slag.....	901.03
Lightweight Fine Aggregate.....	**
Permanent Metal Forms.....	910.03
Portland Cement.....	901.01
Reinforcing Steel, Epoxy Coated.....	910.01
Steel Drain Pipe.....	910.07
Silica Fume.....	901.04
Utility Asphalt, UA-1.....	902.01 (d)
Water.....	913.01

* If the Contract requires stay-in-place metal forms for the bridge deck or if the Contractor elects to use such forms, the bridge deck concrete shall incorporate class AP coarse aggregate instead of Class A.

** Described Herein

Shipping and storage of cement shall be in accordance with 702.04.

Lightweight fine aggregate shall be an expanded shale meeting the requirements of ASTM C 330 except that compressive strength and splitting tensile strength testing are not required. Density Factor (Specific Gravity Factor) shall be determined by the method defined in this specification. Approval of the lightweight aggregate source will be based on a Type B Certification and the acceptance criteria stated in Job Control Testing.

Concrete Mix Design

The concrete shall be designed utilizing three cementitious materials as part of the binder systems. Portland cement, silica fume, fly ash and lightweight fine aggregate shall be proportioned in accordance with Concrete Mix Criteria. A concrete mix design, CMD, and trial batch shall be in accordance with requirements detailed elsewhere in this special provision. The CMD shall be submitted in a format acceptable to the Engineer and include the following:

- (a) list of all ingredients
- (b) source of all materials
- (c) gradation of the aggregates
- (d) absorption of the aggregates
- (e) SSD bulk specific gravity of the aggregates
- (f) Specific Gravity Factor of Lightweight Fine Aggregate
- (g) Specific gravity of each pozzolan
- (h) batch weights (mass)
- (i) names of all admixtures
- (j) range of admixture dosage rates as recommended by the manufacturer

A change in material source, class or type requires a new CMD.

A CMD in accordance with this special provision may be substituted only for concrete used in the RC Bridge Approach. IC-HPC may be substituted for other Class C concrete if approved in writing by the Engineer.

Concrete Mix Criteria

The CMD shall produce workable high performance concrete mixtures having the following properties:

1. The design paste volume of total cementitious material and water shall not exceed 25.0 % of the concrete volume design value (e.g. 6.75 ft³ maximum paste volume per cubic yard concrete). Each cementitious material shall be batched within a tolerance not to exceed 1.0% in accordance with 702.06.
2. The cement content in the ternary binder system shall be at least 390 lbs (231 kg) per cubic yard (cubic meter) of concrete. Air-entraining cements will not be permitted.
3. Class F or C fly ash shall be used as part of the total cementitious content in the ternary binder system. Fly ash shall constitute 20.0 to 25.0 percent by weight (mass) of the total cementitious content in the mix design. Fly ash shall not be used in conjunction with Type IP cement. In lieu of fly ash, ground granulated blast furnace slag (ggbfs) may be used in an amount of 15.0 to 20.0 percent by weight (mass) of the total cementitious content in the mix design. Ggbfs shall not be used in conjunction with Type IS cement.
4. Silica fume shall constitute 3.0%-7.0% of the total cementitious content in the mix design.

5. The water-cementitious ratio of the delivered IC-HPC shall be within a range of ± 0.025 of the target stated in the approved mix design, and shall not exceed 0.430 nor be less than 0.360. The Contractor shall achieve this by controlling water added to the batch and water occurring as surface moisture on the aggregates.

6. The CMD target air content shall be set at 6.5 %.

7. Total fine aggregate volume shall be no less than 35% nor more than 45% of the total aggregate volume for the IC-HPC. Coarse aggregate and natural sand volumes are to be based on Bulk Specific Gravities in the saturated surface dry (ssd) condition. Lightweight fine aggregate volume is to be determined based on Specific Gravity Factor (SGF), as determined by the methodology defined in this special provision. The Contractor and Department are to have concurrence on aggregate Bulk Specific Gravities (ssd), Specific Gravity Factor (SGF) and corresponding absorptions prior to submitting the design of IC-HPC concrete for DTE review.

8. The amount of lightweight fine aggregate needed for internal curing of the concrete shall be determined as follows:

a) Proportion the mix according the preceding requirements and establish the volume of fine aggregate based on the properties of the natural sand only.

b) Determine the weight (mass) of dry lightweight fine aggregate by the following equation

$$M_{DLWA} = 1.025(C_f \times 0.070) / \Phi_{LWA}$$

Where: M_{DLWA} = weight of dry lightweight fine aggregate in lbs/yd³ of IC-HPC.

C_f = Cementitious content (includes cement, fly ash and silica fume)

Φ_{LWA} = Absorption, as decimal, determined by AASHTO T 84, except soaking period is 24 hours and surface dry condition is established per criteria 4 of note 2. Testing absorption will also be accomplished per ACI 211.2 Appendix B, except that the minimum weight of sample is 500 grams. This test is to be used for purposes of comparison and finalizing a value

c) Determine the Specific Gravity Factor (SGF) of the lightweight fine aggregate per Section 10 of AASHTO T 84, except that S and S_i will be determine for the material in the condition as previously described for Φ_{LWA} in part 8.b).

d) Determine the design batch weight of soaked surface dry lightweight fine aggregate, which has absorbed water for 24 hours soak, using the following equation:

$$M_{\Phi LWA} = M_{DLWA} (1 + \Phi_{LWA})$$

- e) Determine the mix design volume of lightweight fine aggregate at Φ_{LMA} moisture content using the following equation:

$$V_{\Phi_{LMA}} = M_{\Phi_{LMA}} / (SGF \times 62.4)$$

Where: $M_{\Phi_{LMA}}$ = See 8.d) above

SGF = Bulk Specific Gravity as described previously in 8.c).

In no case shall $V_{\Phi_{LMA}}$ be less than 20% of the total fine aggregate volume determined previously in 8.a).

- f) Determine the volume of ssd natural sand for IC-HPC by subtracting $V_{\Phi_{LMA}}$ from the total fine aggregate volume determined previously in part 8.a).

9. The slump shall be within a range of 2.5" to 5.5" at point of placement.

10. The CMD target compressive strength at 28-days shall be a minimum of 5000 psi.

11. The CMD Target resistance to chloride ion permeability at 56 days shall be set such that the delivered concrete will be no greater than 1500 coulombs.

Absorption and SSD bulk specific gravity for the natural sand are to be determined in accordance with AASHTO T 84. Absorption and SSD bulk specific gravity of the coarse aggregate are to be determined in accordance with AASHTO T 85, by procedures 8.2. Values agreed upon by the Contractor and Engineer shall apply when calculating target batch mass (weights) and determining water/cementitious ratio.

The IC-HPC shall contain an air entraining agent and either a water reducing, high range, admixture (type F) or a water-reducing, high range, and retarding admixture (type G) as identified in the Department's list of approved PCC Admixture and Admixture Systems. The type admixture used shall not be changed during any individual contiguous pour. The type admixture to be used shall be selected based on the expected concrete temperature, ambient temperature, initial set time, lineal rate of deck placement in ft/h (m/h), and dead load deflection of any structural members containing the concrete. When either temperature is expected to be 65°F (18°C) or above and dead load deflection is of concern; type G admixture, or a system of Type B or D combined with a Type F, shall be used. A type F admixture shall be used when both temperatures are expected to be below 65°F (18°C) or dead load deflection is not of concern. Retardation may be required due to the structure design or the proposed pour sequence in accordance with 704.04. A higher temperature restriction regulating the need to retard the concrete initial set time may be requested in writing and shall substantiate the effects of IC-HPC initial set time, lineal rate of deck placement, and dead load deflection.

The admixture addition rate shall not be reduced below the minimum, or exceed the maximum rate recommended by the manufacturer, regardless of the temperature of the concrete or ambient temperature.

There will be no calendar date restrictions as to the use of high performance concrete with a ternary binder system.

The CMD by absolute volume method shall be submitted to the Engineer for verification at least seven days prior to the trial batch demonstration. An explanation of intended use for each mix design shall be provided.

Trial Batch

A trial batch demonstration shall be conducted by the Contractor. The Engineer will be in attendance. Both parties are to verify that the IC-HPC mix design meets the requirements of this specification. A representative from the lightweight aggregate supplier shall be present for the trial batch. This representative shall have the necessary test equipment and technical expertise to measure the properties of lightweight fine aggregate for use in structural concrete. The representative shall provide testing, guidance and direction in proportioning the IC concrete per ACI 211.2.

The Contractor shall construct lightweight fine aggregate stockpile(s) at the concrete production facility so as to maintain uniform moisture throughout the pile. Prior to the IC-HPC production the lightweight fine aggregate shall undergo a period of wetting and draining. The Contractor shall wet the lightweight fine aggregate stockpile(s) utilizing a sprinkler system, approved by the DTE, to continuously and uniformly apply water to soak the stockpile(s) for a minimum of 48 hours or until the moisture content can consistently be maintained above the absorption Φ_{LWA} . If steady rain of comparable intensity occurs, the sprinkler system may be turned off, with concurrence by the DTE. At the end of the wetting period the lightweight fine aggregate stockpile(s) shall be allowed to drain for 12 to 15 hours immediately prior to being used in IC-HPC production, unless otherwise directed by the DTE. Manipulation of the lightweight fine aggregate stockpile(s) may be necessary to assure uniform wetting and drainage. The soaked and drained lightweight fine aggregate shall achieve, and maintain, an absorbed moisture content equal to or greater than Φ_{LWA} prior to use. Transfer of the lightweight fine aggregate to the storage bin in the plant shall be monitored and controlled to assure that free water does not have time to drain down into the lower lightweight fine aggregate and significantly increase the water/cementitious ratio for a batched load of IC-HPC.

The target batch weight from the soaked and drained stockpiled lightweight fine aggregate, which has been soaked and drained, will be determined as follows:

1. Obtain a representative sample in accordance with AASHTO T 84. Weigh the soaked and drained sample of lightweight fine aggregate and record the value as W_{WET} .
2. Prepare the sample, to surface dry condition, by following criteria 4 of Note 2 of AASHTO T 84 or by ACI 211.2 Appendix B, except the minimum weight of sample is 500 grams. Weigh the wet sample in the surface dry condition. Record the value as W_{WSD} . Dry the sample to a constant weight and record the value as W_{DRY} .
3. Calculate the target batch weight for the stockpiled, soaked and drained lightweight fine aggregate (TBW_{LWA}) needed to produce each cubic yard of IC-HPC as follows:

$$TBW_{LMA} = M_{DLMA} \times [1.00 + (W_{NET} - W_{DRY}) / W_{DRY}]$$

The wet loose unit weight of the soaked and drained lightweight aggregate shall also be determined in accordance with ACI 211.2 in order to substantiate the target batch weight. The concrete shall be batched and mixed in accordance with 702.06 and 702.07. Sufficient IC-HPC shall be produced to accurately represent the mix design and provide an amount of concrete to provide samples for all parties to perform the required testing. The Engineer will test the trial batch IC-HPC and provide the Contractor with the results. The sample of IC-HPC shall not be used for more than one test, except the unit weight specimen may be used to conduct the air content test. The IC-HPC shall be agitated for a period of time that simulates delivery to the job site.

Test results from the Contractor and Department must both validate compliance with the required plastic properties. The Department's water to cementitious ratio measurement shall not exceed ± 0.015 from the value measured by the Contractor. The Contractor's air content shall measure at least 6.5% and the Department's corresponding measure is to be within ± 0.5 % points. The air content is to be measured by both AASHTO T 152 and T 196, in an effort to establish any difference between the two test methods for IC-HPC. The Departments measurement for slump is to be within a tolerance of ± 1 " of the Contractor's measurement. If comparison between Contractor and Department results is out of tolerance, an investigation will be conducted to ascertain the cause and determine corrective action(s) needed to resolve the discrepancy.

The measured relative yield, R_y , is to be determined and compared to the theoretical R_y value tabulated below. The theoretical R_y is selected based on measured air content.

Air Content %	Theor. Ry						
3.0	0.965	5.0	0.985	7.0	1.005	9.0	1.025
3.1	0.966	5.1	0.986	7.1	1.006	9.1	1.026
3.2	0.967	5.2	0.987	7.2	1.007	9.2	1.027
3.3	0.968	5.3	0.988	7.3	1.008	9.3	1.028
3.4	0.969	5.4	0.989	7.4	1.009	9.4	1.029
3.5	0.970	5.5	0.990	7.5	1.010	9.5	1.030
3.6	0.971	5.6	0.991	7.6	1.011	9.6	1.031
3.7	0.972	5.7	0.992	7.7	1.012	9.7	1.032
3.8	0.973	5.8	0.993	7.8	1.013	9.8	1.033
3.9	0.974	5.9	0.994	7.9	1.014	9.9	1.034
4.0	0.975	6.0	0.995	8.0	1.015	10.0	1.035
4.1	0.976	6.1	0.996	8.1	1.016	10.1	1.036
4.2	0.977	6.2	0.997	8.2	1.017	10.2	1.037
4.3	0.978	6.3	0.998	8.3	1.018	10.3	1.038
4.4	0.979	6.4	0.999	8.4	1.019	10.4	1.039
4.5	0.980	6.5	1.000	8.5	1.020	10.5	1.040
4.6	0.981	6.6	1.001	8.6	1.021	10.6	1.041
4.7	0.982	6.7	1.002	8.7	1.022	10.7	1.042
4.8	0.983	6.8	1.003	8.8	1.023	10.8	1.043
4.9	0.984	6.9	1.004	8.9	1.024	10.9	1.044

If a measured R_y is excessively low or high, an investigation will be conducted by the Contractor and Engineer to ascertain the cause and determine corrective action needed to resolve the discrepancy. The aggregates may need to be re-tested for bulk specific gravity (ssd), Specific Gravity Factor, absorption, or moisture content, as appropriate.

Once the IC-HPC has passed the requirements for batching, and testing the plastic concrete properties of slump and air content, specimens will be cast for testing compressive strength and permeability. Four 6"x12" cylinders will be cast for the purpose of compressive strength determination. Two cylinders will be tested at an age of 7-days and two cylinders will be tested at an age of 28-days. The compressive strength will be reported as the average of the two cylinders tested at the designated age. The compressive strength shall exceed 4400 psi at 28 days.

Two additional 6"x12" specimens will be cast for the purpose of testing the IC-HPC for resistance to chloride ion penetration at 56 days. The result will be the averaged of the two specimens cored from the cylinders. Two 4"x8" cylinders may also be cast and tested for resistance to chloride penetration at 28 days, after accelerated curing. The specimens for accelerated testing shall be cured in the same manner as the cylinders for compressive strength, for a period of 7 days, after which they will be cured at $100\text{ }^{\circ}\text{F} \pm 10\text{ }^{\circ}\text{F}$ for a period of 20 days.

All molds, facilities and materials necessary to prepare and initially cure these cylinders, shall be provided.

Samples representing the natural sand, lightweight fine aggregate and coarse aggregate used in the IC-HPC production will be tested for gradation. The gradation of each aggregate shall comply with the specification. Gradation, fineness modulus and dry loose density of the lightweight fine aggregate will be determined in accordance with ASTM C 330 for material used in the IC-HPC produced at the trial batch. Specific Gravity Factor will be determined as described in this special provision.

Except for adjustments to compensate for routine aggregate moisture fluctuations, changes in target aggregate (SSD) batch weights (mass) shall be documented and submitted to the Engineer for approval, prior to implementing. Changes to the dosage rate of admixtures will be permitted. A new CMD shall be prepared and successfully demonstrated for changes in the source, type or class of a material, the amounts of cementitious materials, increase in target water/cementitious ratio, or the addition or deletion of admixtures.

Test Methods and Procedures

The following test methods and procedures apply with exceptions as listed below.

Air Test	AASHTO T 152 or T 196*	
Compressive Strength	AASHTO T 22	
Flexural Strength	AASHTO T 97	
High Pressure Air Content of Hardened PCC		ITM 401
Making and Curing Specimens		AASHTO T 23
Moisture Content, Aggregate		AASHTO T 255
Obtaining and Testing of Drilled Cores		AASHTO T 24
Sampling Fresh Concrete		AASHTO T 141
Sampling Stockpiled Aggregates		ITM 207
Sieve Analysis of Aggregates		AASHTO T 27
Slump		AASHTO T 119
Specific Gravity and Absorption, Coarse Aggregate		AASHTO T 85**
Specific Gravity and Absorption, Fine Aggregate		AASHTO T 84
Resistance to Chloride Ion Penetration		AASHTO T 277
Unit Weight (Mass)	AASHTO T 121	
Water-Cementitious Ratio		ITM 403

* If the use of lightweight fine aggregate is found to produce significantly different results for air content then the method and procedure for the test shall be in accordance with AASHTO T 196.

** Section 8.2

(a) Exceptions to AASHTO T 23

The exceptions to AASHTO T 23 for making and curing specimens in the field shall be as follows.

1. Initial curing of cylinders shall be no less than 16 h or more than 48 h.
2. Non-watertight beam forms (molds) will be permitted.
3. After 24 h, the molded beam specimens shall be taken to the storage location and removed from the molds.
4. Field stored beams will not require 24 ± 4 h immersion in water saturated with calcium hydroxide prior to the time of testing.

(b) Exceptions to AASHTO T 27

The exceptions to AASHTO T 27 for conducting a sieve analysis are in accordance with 904.06.

(c) Exception to AASHTO T 84

The exceptions to AASHTO T 84 for determining SSD specific gravity and absorption for the fine aggregate shall be as follows:

1. The SSD bulk specific gravity shall be reported to the nearest 0.001 and the absorption reported to the nearest 0.01%.

(d) Exception to AASHTO T 85

The exceptions to AASHTO T 85 for determining SSD specific gravity and absorption for the coarse aggregate shall be as follows:

1. The 15 h soak period shall not be eliminated.
2. The in-water weight (mass) shall be determined following the 15 h soaking period prior to determining the SSD weight (mass).
3. The SSD bulk specific gravity shall be reported to the nearest 0.001 and the absorption reported to the nearest 0.01%.

(e) Exceptions to AASHTO T 97

The exceptions to AASHTO T 97 for conducting a flexural test shall be as follows:

1. The beam size shall be measured to the nearest 1/16 in. (1.0 mm).
2. The test result shall be discarded when the break occurs outside the middle third of the beam.

(f) Exceptions to AASHTO T 121

The exceptions to AASHTO T 121 for determining the unit weight (mass) of concrete shall be as follows:

1. Weight (mass) shall be determined to the nearest 0.01 lb (0.005 kg).

(g) Exceptions to AASHTO T 141

The exceptions to AASHTO T 141 for sampling fresh concrete in the field shall be as follows:

1. The entire sample may be obtained from one portion of the load after at least 0.25 yd³ (0.25 m³) of concrete has been discharged.

(h) Exceptions to AASHTO T 152

The exceptions to AASHTO T 152 for determining the air content in PCC shall be as follows:

1. The aggregate correction factor shall be determined in accordance with 6.4.3 except that the volume of water shall not be removed from the assembled and filled apparatus.
2. The aggregate correction factor test shall be re-run for confirmation if the test results for gravel is greater than 0.4% or if the test results for crushed stone is greater than 0.6%.

CONSTRUCTION**General**

Construction operations as applicable shall be in accordance with 702, 703 and 704.

Ready-Mixed Concrete

Ready mixed IC-HPC shall be in accordance with 702.09. Mixing at the work site, as described in 702.08 is prohibited.

The Contractor shall construct lightweight fine aggregate stockpile(s) at the concrete production facility so as to maintain uniform moisture throughout the pile. Prior to the IC-HPC production the lightweight fine aggregate shall undergo a period of wetting and draining.

The Contractor shall wet the lightweight fine aggregate stockpile(s) utilizing a sprinkler system, approved by the DTE, to continuously and uniformly apply water to soak the stockpile(s) for a minimum of 48 hours or until the moisture content can consistently be maintained above the absorption, Φ_{LWA} . If steady rain of comparable intensity occurs, the sprinkler system may be turned off, with concurrence by the DTE. At the end of the wetting period the lightweight fine aggregate stockpile(s) shall be allowed to drain for 12 to 15 hours immediately prior to being used in IC-HPC production, unless otherwise directed by the DTE. The soaked and drained lightweight fine aggregate shall achieve, and maintain, an absorbed moisture content equal to or greater than Φ_{LWA} prior to use. Manipulation of the lightweight fine aggregate stockpile(s) may be necessary to assure uniform wetting and drainage. Transfer of the lightweight fine aggregate to the storage bin in the plant shall be monitored and controlled to assure that free water does not have time to drain down into the lower lightweight fine aggregate and significantly increase the water/cementitious ratio for a batched load of IC-HPC.

A representative from the lightweight aggregate supplier shall be present for any IC-HPC production. This representative shall have the necessary test equipment and technical expertise to measuring the properties of lightweight fine aggregate for IC-HPC. The representative shall provide guidance and direction in proportioning the IC concrete per ACI 211.2 and the experienced gained from the trial batch demonstration. The Department will determine the amount of soaked and drained lightweight aggregate by the method established at the trial batch, which shall be used to establish the target batch weight of lightweight fine aggregate.

Testing Facilities and Equipment

An easily accessible means of obtaining concrete samples at the point of placement and transporting the samples from the bridge deck for testing shall be provided. All molds, facilities, and materials necessary to prepare and initially cure quality control and acceptance cylinders shall be provided at the work site.

Job Control Testing

Prior to any IC-HPC production, newly delivered or existing stockpiles of lightweight fine aggregate will be tested for fineness modulus and dry loose bulk density to verify uniformity in accordance with ASTM C 330. The fineness and loose bulk density parameters established at the trial batch will be the basis for making the comparison.

Department acceptance of IC-HPC will be determined on the basis of tests performed by the Engineer. Any necessary labor for sampling the IC-HPC shall be furnished to the Engineer, as required. During placement, the IC-HPC will be tested for slump, relative yield and air content. Testing for plastic and hardened concrete properties will be performed on the first load of IC-HPC and every 50 cubic yards. The slump shall be in accordance with concrete mix criteria stated herein. IC-HPC that may initially exceed the maximum allowable slump can be held in reserve until the slump is determined be within specification and the load does not exceed the 90 minute time limit as stated in 702.09(c)5. Air content shall be $6.5\% \pm 1.5\%$ at point of placement.

Relative yield will be determined and shared with the Contractor, through the representative from the lightweight aggregate supplier. The Contractor shall make adjustments to the aggregate batch weights, as appropriate, to correct problems with relative yield. Should the relative yield exceed the Theoretical value, for the measured air content, by 0.010; the Engineer will immediately increase the frequency of sampling and testing until the relative yield is reduced. Any increased sampling and testing will include cylinders for compressive strength and rapid permeability.

Two 6"x12" cylinders will be cast every 50 cubic yards and tested for compressive strength at an age of 28-days. Cylinders will be cured in accordance with AASHTO T 23. Compressive strength shall exceed 4000 psi.

Two 6"x12" cylinders will be cast every 50 cubic yards and tested for the purpose of testing resistance to chloride ion penetration at 56 days.

Falsework and Centering

Falsework and arch centering for structural elements shall be in accordance with 702.14.

Finishing

The concrete shall be finished in accordance with 702.21 and 704.05.

Wet Curing

After finishing and texturing in accordance with 704.05, the IC-HPC shall be cured in accordance with 704.06 and 702.22, except as modified herein.

An evaporation retardant shall be applied, in accordance with the manufacturer's recommendation, to the exposed concrete surface immediately after finishing or texturing operations. Reapplication of the retardant shall be performed whenever the surface is disturbed, or when drying of the surface is observed. The evaporation retardant shall be one of the products listed below. A type D certification for the evaporative retardant shall be in accordance with 916 and submitted to the Engineer prior to use.

(a) Confilm, manufactured by Master Builders Technologies; 3715 Bargetown Road, Room 214; Louisville, KY 40218

(b) Sika-Film, manufactured by Sika Corporation; 2930 Switzer Road; Columbus, OH 43219

(c) Eucobar, Euclid Chemical Company; 19218 Redwood Road; Cleveland, OH 44110

Evaporative retardant shall be applied to the finished or textured surface of IC-HPC regardless of the evaporation rate. If the evaporation rate exceeds 0.10 lbs/ft²/h (0.50 kg/m²/h) during placement of concrete, fog misting, as recommended by the silica fume manufacturer, shall be initiated prior to the texturing operation. Fog misting shall not be excessive to cause water to wash the fresh concrete surface, or to stand on the surface during floating or troweling operations.

The rate of water evaporation shall be determined during concrete placement in accordance with ACI 308, Section 1.2.1. or the following English (metric) equation:

$$E = [T_c^{2.5} - (r \times T_a^{2.5})][1 + 0.4V] \times 10^{-6}$$

$$(E = 5[(T_c + 18)^{2.5} - r(T_a + 18)^{2.5}][V + 4] \times 10^{-6})$$

where:

E = Evaporation rate, lb/ft²/h (kg/m²/h)
 T_c = Concrete temperature, °F (°C)
 T_a = Ambient temperature, °F (°C)
 r = (RH %)/100
 V = Wind velocity, mi/h (k/h)

Measurements of T_a, r, & V shall be obtained on-site and compared for accuracy with readings from the nearest weather station monitored by the National Climatic Data Center. Measurement of T_c shall be determined from the concrete placed.

The IC-HPC shall be wet cured continuously for at least 168 h commencing immediately after the surface is able to support the protective covering without deformation. The wet cure period shall be 240 h for concrete placed in cold weather.

Membrane forming curing compound shall not be applied to IC-HPC in bridge decks or the top surface of reinforced concrete slab bridges.

Surfaces to be cured shall be protected by covering with cotton mats, burlap, or other satisfactory protective material that is kept continuously and thoroughly wet, through the use of soaker hoses, during the curing period. The protective covering shall be suitably anchored. Curbs, walls, handrails, copings, and other surfaces requiring a finish in accordance with 702.21 may have the covering temporarily removed for finishing, but the cover shall be restored as soon as possible. Water application through the soaker hoses shall be discontinued 24 hours before the cure period ends and the protective covering is removed.

Cold Weather Concrete

Cold weather concrete operations shall be in accordance with 702.11, except that immediately after a pour is completed, the freshly poured concrete and forms shall be covered so as to form a protective enclosure and the air in the enclosure kept at a temperature above 50 °F (10 °C) for at least 240 hours.

Removal and Re-use of Forms

The forms for any portion of the structure shall not be removed until IC-HPC is strong enough to withstand damage. Field operations concerning IC-HPC shall be controlled by the Department through test beams in accordance with the requirements of 702.13(h).

Application of Loads

The application of loads to IC-HPC shall be in accordance with the test beam requirements of 702.24(a). Construction activities shall not interfere with wet curing of the bridge deck throughout the period specified.

No contract time extension will be considered for delays due to additional time necessary to attain specified strengths.

Sealing

The IC-HPC deck surface shall not be sealed.

Method of Measurement

IC-HPC will be measured by the cubic yard (cubic meter) in accordance with the neat lines or as directed. However, no allowance will be made for variations in beam fillet depths, coping depths, or diaphragm depths. Reinforcing steel will be measured in accordance with 703.07. Castings and cast iron pipe will be measured in accordance with 702.27.

Basis of Payment

The accepted quantities of IC-HPC will be paid for at the contract unit price by the cubic yard (cubic meter) of concrete, complete in place. Reinforcing steel will be paid for in accordance with 703.08. Castings and cast iron pipe will be paid for in accordance with 702.28.

Payment will be made under:

Pay Item	Pay Unit Symbol
Concrete, C, Superstructure, Modified, IC-HPC	CYS (m3)

The cost of conducting trial batch demonstrations, performing quality control testing, and similar requirements included herein will not be paid for directly but shall be included in the cost of IC-HPC.

BRIDGE RAILING

This work shall be in accordance with 706, except that internally cured high performance concrete (IC-HPC) shall be used in lieu of Class C concrete. IC-HPC in the bridge railing shall meet the requirements of the special provision entitled Internally Cured, High Performance, Structural Concrete For Bridge Decks.

APPENDIX B: RECOMMENDED TESTING
PROCEDURE FOR USING A CENTRIFUGE TO
DETERMINE THE MOISTURE STATES OF FINE
LIGHTWEIGHT AGGREGATE FOR THE
PURPOSE OF INTERNAL CURING
(MILLER ET AL., 2014B)

The following is adapted from ASTM 1761-13b (ASTM, 2013b) and represents the suggested testing method for using a centrifuge to determine properties of LWA.

B.1 ABSORPTION, SURFACE MOISTURE, AND TOTAL MOISTURE

B.1.1. Oven dry LWA specimen at a temperature of 110 ± 5 °C (230 ± 9 °F) to a constant mass. After constant mass is obtained, allow to return to room temperature, submerge in water, and allow to soak for 24 ± 4 h.

Note: If 72 h absorptions are desired, aggregate shall be soaked for 72 ± 4 h and agitated every 24 h. For field applications, LWA may be taken in “as delivered” condition and soaked and tested without oven drying.

B.1.2. For lab samples, decant excess water with care to avoid loss of fines. Once excess water is removed, mix sample to reduce segregation that may have occurred while soaking and decanting.

Note: For field applications, allow pile to drain for a sufficient amount of time after soaking to attain more stable stockpile surface moistures. Turn pile and obtain sample in accordance with ASTM D75.

B.1.3. Measure 600 ± 10 g of pre-wetted LWA into a centrifuge bowl. Record this mass of pre-wetted LWA as MW. Distribute LWA evenly inside of centrifuge to insure proper balance. If sample is improperly balanced, excessive vibrations will be observed while performing test and results may be inaccurate.

B.1.4. Place centrifuge bowl in centrifuge. Place 4 µm filter paper on top of centrifuge bowl and secure centrifuge bowl cover with cover nut. Place upper housing on top of centrifuge and secure with clamps.

B.1.5. Set centrifuge speed control to 2000 rpm. Power centrifuge on. Begin test, monitoring speed readout as to not exceed 2000 rpm. Testing time of 3 minutes shall begin when centrifuge speed reaches 2000 ± 20 rpm. If centrifuge does not have a digital readout, time shall begin when centrifuge reaches a steady spinning rate.

B.1.6. After specimen has been spun for 3 minutes at 2000 ± 20 rpm, turn centrifuge power off.

B.1.7. Once the centrifuge has come to rest, open the outer housing. Remove bowl cover nut and bowl cover. Remove filter paper with caution as aggregate may be pressed to the surface of the filter. Transfer pre-wetted surface-dry (WSD) aggregate to a vessel appropriate for

oven-drying. It may be necessary to use a spatula to scrape the specimen that has been pressed to the walls of the centrifuge bowl into the vessel. If specimen has been pressed to the filter, use a brush to transfer the aggregate from the filter to the vessel. Record the mass of WSD aggregate as MWSD.

B.1.8. Dry the WSD specimen to constant mass in an oven at a temperature of 110 ± 5 °C (230 ± 9 °F). Remove specimen from oven, and allow to cool to room temperature. Record the mass of the oven dry sample as MOD.

B.1.9. Note: For field applications, an open flame or hot plate may be used to return aggregate to an oven-dry state. Allow sample to cool to room temperature before weighing for mass equilibrium. Repeat drying and cooling until mass change is less than 0.1% of the original pre-wetted surface-dry mass.

B.1.10. Calculations.

MW – Mass of pre-wetted LWA, g

MWSD – Mass of pre-wetted surface dry LWA, g

MOD – Mass of oven-dry LWA, g

Calculate the absorption to the nearest 0.1 % according to Equation B.1.

$$\text{Absorption} (\%) = \frac{M_{WSD} - M_{OD}}{M_{OD}} \times 100\% \quad (\text{B.1})$$

Calculate the surface moisture* to the nearest 0.1% according to Equation B.2.

$$\text{Surface Moisture} * (\%) = \frac{M_W - M_{WSD}}{M_{WSD}} \times 100\% \quad (\text{B.2})$$

Calculate the total moisture to the nearest 0.1% according to Equation B.3.

$$\text{Total Moisture} (\%) = \frac{M_W - M_{OD}}{M_{OD}} \times 100\% \quad (\text{B.3})$$

B.2 RELATIVE DENSITY

B.2.1. Follow methodology listed above in steps B.1.1–B.1.6 to obtain aggregate in pre-wetted surface-dry condition.

B.2.2. Stir aggregate in centrifuge bowl and scrape sides to minimize segregation that may have occurred during spinning.

B.2.3. Add approximately 300 g of WSD sample to a glass jar or pycnometer with nominal capacity of 1 L (1 qt). Record the mass added as MWSD.

B.2.4. Partially fill the glass container to about 90% of capacity with water at 23.0 ± 2 °C (37.5 ± 3.5 °F). Agitate container to remove visible air bubbles from the sample. Refer to ASTM C128 for acceptable methods

of agitation. It is typical for agitation periods of 15-20 minutes to remove all air bubbles.

B.2.5. After all visible air bubbles have been removed, fill container to top or to calibrated measuring point. Record this mass, including pycnometer, specimen, and water to the nearest 0.1 g as MPS.

B.2.6. Transfer material to a vessel appropriate for oven drying. Rinse glass container with water and add material to vessel until the glass container is clean. Decant excess water from vessel avoiding loss of fines. Place sample in an oven and allow it to reach constant mass. Constant mass is reached when the specimen does not change by more than 0.1 % of its original WSD mass. Record this mass as MOD.

B.2.7. Calculations.

MWSD – Mass of pre-wetted surface-dry LWA, g

MPS – Mass of pycnometer, WSD specimen, and water to measuring point, g

MOD – Mass of oven-dry LWA, g

MPW – Calibration mass of pycnometer and water to measuring point, g

Calculate the oven-dry (OD) relative density (specific gravity) according to Equation B.4.

$$G_{OD} = \frac{M_{OD}}{M_{WSD} + M_{PW} - M_{PS}} \quad (\text{B.4})$$

Calculate the pre-wetted surface-dry (WSD) relative density (specific gravity) according to Equation B.5.

$$G_{WSD} = \frac{M_{WSD}}{M_{WSD} + M_{PW} - M_{PS}} \quad (\text{B.5})$$

B.3 DESORPTION AT 94% RH

B.3.1. Follow methodology listed above in steps 1.1–1.6 to obtain aggregate in pre-wetted surface-dry condition.

B.3.2. Stir aggregate in centrifuge bowl and scrape sides to minimize segregation that may have occurred during spinning.

B.3.3. Measure and record weight of empty weighing dish. Add approximately 5 g of WSD LWA to the dish and record mass again. Make all measurements to 0.01 g. Record specimen mass as MWSD.

B.3.4. Introduce specimen and dish to controlled humidity environment. Measure the mass of the specimen every day until the specimen mass change is not more than 0.01 g in 24 hours. Record this mass as M94.

B.3.5. Once equilibrium is reached in the controlled humidity environment and M94 has been obtained, place the dish and specimen in a drying oven. Allow specimen to reach constant mass in oven. Constant mass is considered to be when the specimen mass change does not exceed 0.01 g in 24 hours. Record this mass as MOD.

B.3.6. Calculations.

MWSD – Mass of pre-wetted surface dry LWA, g

M94 – Mass of LWA at equilibrium in 94% relative humidity chamber, g

MOD – Mass of oven-dry LWA, g

To calculate the mass of water released at 94% relative humidity, expressed as a fraction of the OD mass, use Equation B.6. Express result to the nearest 0.01.

$$W_{LWA} = \frac{M_{WSD} - M_{94}}{M_{OD}} \quad (\text{B.6})$$

To calculate the desorption at 94% relative humidity using Equation B.7.

$$Desorption_{94\%} = \frac{M_{WSD} - M_{94}}{M_{WSD} - M_{OD}} \quad (\text{B.7})$$

Moisture Property Calculations

A	Mass of empty centrifuge bowl:	
B	Mass of pre-wetted lightweight aggregate added to centrifuge bowl (600 ± 5 g):	
C	Mass of centrifuge bowl and pre-wetted surface-dry aggregate after spinning:	
D	Subtract line A from line C, (D = C - A):	
E	Mass of empty pan used for oven drying aggregate:	
F	Mass of pan and oven-dry aggregate:	
G	Subtract line E from line F, (G = F - E)	

$$\text{Surface Moisture } * (\%) = \frac{B - D}{D}$$

$$\text{Absorption } (\%) = \frac{D - G}{G}$$

$$\text{Total Moisture } (\%) = \frac{B - G}{G}$$

Results

Surface Moisture*	
Absorption	
Total Moisture	

****Note: Total Moisture - Absorption ≠ Surface Moisture****

Specific Gravity Calculations

H	Mass of pycnometer filled with water to calibration mark:	
I	Mass of pre-wetted lightweight aggregate added to centrifuge bowl (600 ± 5 g):	
J	Mass of pre-wetted surface-dry aggregate added to pycnometer (about 300 g):	
K	Mass of pycnometer, aggregate, and water to calibration mark:	
L	Mass of oven-dried aggregate from pycnometer:	

$$SG_{\text{Oven Dry}} = \frac{L}{J + H - K}$$

$$SG_{\text{Wetted Surface Dry}} = \frac{J}{J + H - K}$$

Results

Specific Gravity, Oven-dry	
Specific Gravity, Pre-wetted Surface Dry	

notes:

APPENDIX C

TABLE C.1
Results of single operator single laboratory absorption testing using the centrifuge method.

LWA Source	Average Absorption (%)	Standard Deviation (%)	Coefficient of Variation
Buildex Marquette	20.13	0.43	0.021
Stalite	8.98	0.06	0.007
Trinity* Boulder	18.84	0.18	0.010
Utelite	18.38	0.19	0.010
Pooled Standard Deviation (%)		0.25	—
Average Coefficient of Variation		—	0.012

*Formerly TXI.

TABLE C.2
Results from multiple operator single laboratory variability testing for absorption using both the paper towel test (top) and the centrifuge method (bottom).

LWA Source	Average Absorption (%)	Standard Deviation (%)	Coefficient of Variation
Paper Towel Method			
Buildex Marquette	21.26	2.26	0.106
Stalite	10.51	4.91	0.467
Utelite	21.75	5.34	0.246
Pooled Standard Deviation (%)		4.51	—
Average Coefficient of Variation		—	0.273
Centrifuge Method			
Buildex Marquette	20.18	0.56	0.028
Stalite	8.47	0.27	0.032
Utelite	18.96	0.47	0.025
Pooled Standard Deviation (%)		0.45	—
Average Coefficient of Variation		—	0.028

APPENDIX D

TABLE D.1

As-batched concrete mixture proportions for each truck during construction of bridge deck #3 [lb/yd³]. Admixtures are provided in [oz/cwt].

	Approved Design	1	2	3	4	5	6	7
W/CM	0.400	0.416	0.418	0.419	0.419	0.418	—	0.419
Cement	443	437	435	434	434	436	—	434
Fly Ash	115	116	115	116	116	114	—	115
GGBFS	—	—	—	—	—	—	—	—
Silica Fume	17	17	17	17	17	17	—	17
Coarse Aggregate	1740	1725	1725	1729	1727	1723	—	1729
Fine Aggregate	820	821	818	818	821	818	—	818
Lightweight Aggregate	340	334	334	334	334	334	—	334
Air Entrainer	0.1–6.0	0.99	0.99	0.99	0.99	0.99	—	1.08
HRWRA	10–40	9.54	9.63	9.81	9.63	9.63	—	9.81
MRWRA	1.5–5.0	2.88	2.88	2.88	2.88	2.88	—	2.88
Retarder	—	—	—	—	—	—	—	—
Air Content [%]	6.5	—	6.7	6.7	5.1	—	—	6.2
Slump [in]	2–5	—	—	6	3.5	—	—	7
Unit Weight [lb/ft³]	137.2	—	137.3	140.48	141.3	—	—	139.2
Paste Content [%]	25.00	25.32	25.26	25.26	25.26	25.27	—	25.26
Concrete Temp [°F]	N/A	—	—	80	—	—	—	—
Batch Time	N/A	8:46	9:35	10:14	10:44	11:19	—	11:49
Water Added?	N	—	Y	Y	—	—	—	Y

*Indicates measures not conforming to limits set within INDOT specifications for IC HPC (INDOT, 2014a).

APPENDIX E

TABLE E.1

As-batched concrete mixture proportions for each truck during construction of bridge deck #4 [lb/yd³]. Admixtures are provided in [oz/cwt].

	Approved Design	1	2	3	4	5	6	7	8
W/CM	0.403	0.430	0.436	0.436	0.437	0.438	0.438	0.435	0.436
Cement	435	437	436	436	436	437	436	439	436
Fly Ash	—	—	—	—	—	—	—	—	—
GGBFS	115	118	119	119	116	118	118	116	116
Silica Fume	25	25	25	25	25	25	25	25	25
Coarse Aggregate	1790	1783	1786	1807	1780	1786	1786	1783	1783
Fine Aggregate	782	781	790	778	787	801	787	793	781
Lightweight Aggregate	365	365	362	354	356	354	359	354	348
Air Entrainer	0.2–0.75	1.09	1.09	1.09	1.10	1.10	1.10	1.09	1.09
HRWRA	10–15	14.93	14.93	14.88	14.88	14.88	14.93	14.93	14.93
MRWRA	3	3.72	3.72	3.77	3.77	3.72	3.72	3.77	3.72
Retarder	—	—	—	—	—	—	—	—	—
Air Content [%]	6.5	—	7.3	—	—	—	6.9	—	—
Slump [in]	2–5	—	8.5	—	—	—	7.5	—	—
Unit Weight [lb/ft ³]	137.3	—	139.4	—	—	—	139.9	—	—
Paste Content [%]	24.92	25.33	25.75	25.74	25.80	25.77	25.91	25.91	25.96
Concrete Temp [°F]	N/A	—	80.4	—	—	—	82.3	—	—

TABLE E.2

As-batched concrete mixture proportions for each truck during construction of bridge deck #4 [lb/yd³]. Admixtures are provided in [oz/cwt].

	Approved Design	9	10	11	12	13	14	15	16
W/CM	0.403	0.437	0.438	0.436	0.436	0.434	0.435	0.435	0.435
Cement	435	437	437	437	439	442	438	438	439
Fly Ash	—	—	—	—	—	—	—	—	—
GGBFS	115	116	116	118	115	116	118	117	115
Silica Fume	25	25	25	25	25	25	25	25	25
Coarse Aggregate	1790	1786	1804	1783	1783	1786	1792	1783	1783
Fine Aggregate	782	787	787	781	781	793	784	787	778
Lightweight Aggregate	365	359	351	362	356	356	354	354	354
Air Entrainer	0.2–0.75	1.29	1.14	1.14	1.14	1.15	1.14	1.14	1.15
HRWRA	10–15	14.88	14.93	14.93	14.93	14.88	14.93	14.88	14.88
MRWRA	3	3.77	3.77	3.72	3.72	3.72	3.72	3.77	3.72
Retarder	—	—	—	—	—	—	—	—	—
Air Content [%]	6.5	6.6	—	—	6.8	—	—	6.1	—
Slump [in]	2–5	7.5	—	—	7.0	—	—	7.5	—
Unit Weight [lb/ft ³]	137.3	141.5	—	—	140.8	—	—	140.9	—
Paste Content [%]	24.92	25.95	25.94	26.00	25.96	25.94	25.94	26.16	26.20
Concrete Temp [°F]	N/A	82.5	—	—	82.1	—	—	82.9	—

TABLE E.3

As-batched concrete mixture proportions for each truck during construction of bridge deck #4 [lb/yd³]. Admixtures are provided in [oz/cwt].

	Approved Design	17	18	19	20	21	22	23
W/CM	0.403	0.437	0.439	0.434	0.437	0.434	0.441	0.440
Cement	435	436	435	443	436	437	436	437
Fly Ash	—	—	—	—	—	—	—	—
GGBFS	115	116	116	116	116	119	116	115
Silica Fume	25	25	25	25	25	25	25	25
Coarse Aggregate	1790	1786	1783	1795	1795	1792	1780	1802
Fine Aggregate	782	781	793	778	784	784	790	784
Lightweight Aggregate	365	354	359	354	351	351	367	363
Air Entrainment	0.2–0.75	1.14	1.14	1.15	1.14	1.15	1.14	1.14
HRWRA	10–15	14.93	14.93	14.88	14.93	14.93	14.88	14.92
MRWRA	3	3.77	3.72	3.72	3.77	3.77	3.77	3.75
Retarder	—	—	—	—	—	—	—	—
Air Content [%]	6.5	—	—	6.1	—	—	5.5	—
Slump [in]	2–5	—	—	4.5	—	—	2.5	—
Unit Weight [lb/ft³]	137.3	—	—	142.2	—	—	142.9	—
Paste Content [%]	24.92	26.13	26.05	26.23	26.08	26.16	26.25	26.17
Concrete Temp [°F]	N/A	—	—	83.9	—	—	84.3	—



SPR 3752

© SIMCO Technologies Inc. 2014
All rights reserved

STADIUM® VERSION 2.997

STADIUM® SIMULATION REPORT

Location: Indianapolis

Structure Type: Bridge

Project Ref.:



Apr. 02, 2014



www.simcotechnologies.com



SIMCO
Technologies inc.

Design Calculation

Approved by : _____ page 2/18

This Product is licensed to: Tim Barrett - Academic Account

Date : 04-02-2014 / 13:15:21
Engineer :
Client :
Project :
Project Ref.:

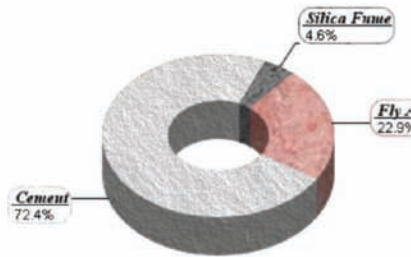
Project Database: [SPR 3752.sdb]

Erie Haven IC HPC

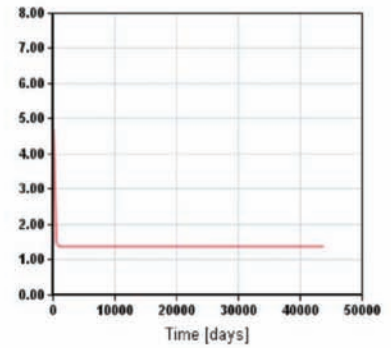
Structure Type: Bridge
Structural Element Type: [Deck]
Material Name:
[Modified Material - for Erie Haven IC HPC]

Cement Type	TYPE I
Water/Binder Ratio	0.405
Cement Content: (kg/m ³)	234
SCM #1: Fly Ash C (kg/m ³)	74
SCM #2: Silica Fume (kg/m ³)	15
SCM #3: None (kg/m ³)	0
Fine Aggregates: (kg/m ³)	939
Coarse Aggregates: (kg/m ³)	1083
Water: (kg/m ³)	131
Air: [%]	7.3
Material Density: (kg/m ³)	2476
Mixture Volume: (m ³)	1.077
Paste Volume: [%]	23.92

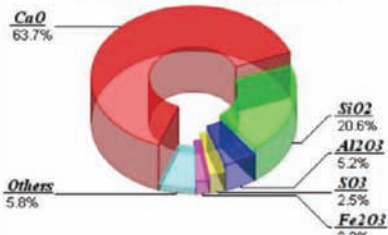
Binder Composition



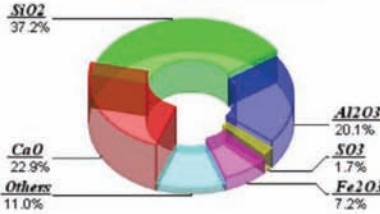
Diffusion Coefficient (e-11 m²/s)- a=.55 - alpha=5.00E-3



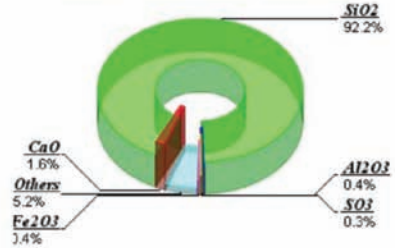
Cement Composition



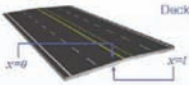
Fly Ash C Composition



Silica Fume Composition



Data for project: SPR 3752 - Structural element [Erie Haven IC HPC]



Deck
Dimension (mm) = 393.7
Scenario Duration (years) = 120
Temperature (°C) = 23.0
Water/Binder Ratio = 0.405
Binder Content (kg/m³) = 323
Total Aggregates (kg/m³) = 2022
Binder Density (kg/m³) = 2980
Porosity = 0.13
Cement Type = TYPE I

OH- Diffusion Coeff. (e-11 m²/s) = 2.48
Saturation at 50% R.H = 0.43
Age of First Exposure (days) = 28
Age at Lab Testing (days) = 91
Hydration Param. - a = 0.55
Hydration Param. - alpha (1/s) = 5.000E-03
Thermal Conductivity (W/m.K) = 2.000E+00
Specific Heat (J/kg.K) = 1.000E+03



page 2/18

© SIMCO Technologies Inc. 2014
All rights reserved

STADIUM® VERSION 2.997



SIMCO
Technologies inc.

Design Calculation

Approved by: _____ page 4/18

This Product is licensed to: Tim Barrett - Academic Account

Date : 04-02-2014 / 13:15:22

Engineer :

Client :

Project :

Project Ref.:

Project Database: [SPR 3752.sdb]

Erie Haven HPC

Structure Type: Bridge

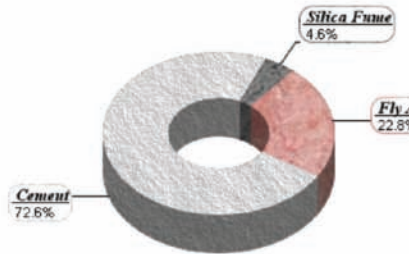
Structural Element Type: [Deck]

Material Name:

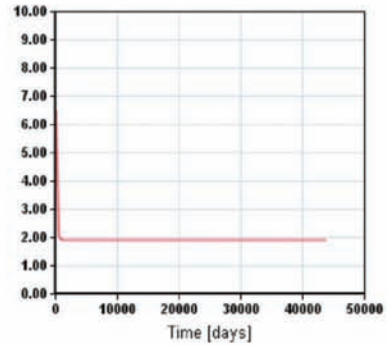
[Modified Material - for Erie Haven HPC]

Cement Type	TYPE I
Water/Binder Ratio	0.428
Cement Content: (kg/m ³)	236
SCM #1: Fly Ash C (kg/m ³)	74
SCM #2: Silica Fume (kg/m ³)	15
SCM #3: None (kg/m ³)	0
Fine Aggregates: (kg/m ³)	725
Coarse Aggregates: (kg/m ³)	1088
Water: (kg/m ³)	139
Air: [%]	7.1
Material Density: (kg/m ³)	2277
Mixture Volume: (m ³)	1.005
Paste Volume: [%]	24.81

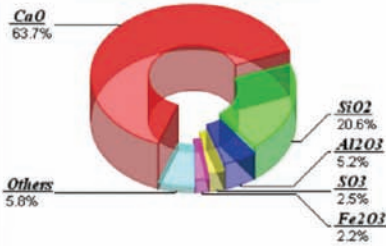
Binder Composition



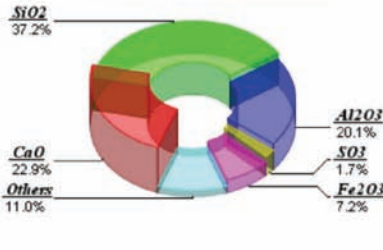
Diffusion Coefficient (e-11 m²/s) - a=.55 - alpha=5.00E-3



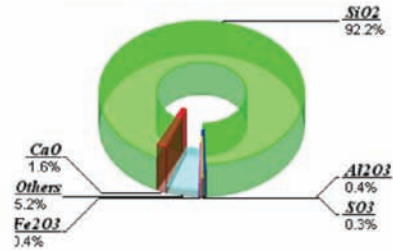
Cement Composition



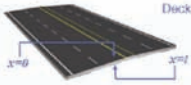
Fly Ash C Composition



Silica Fume Composition



Data for project: SPR 3752 - Structural element [Erie Haven HPC]



Dimension (mm) = 393.7
 Scenario Duration (years) = 120
 Temperature (°C) = 23.0
 Water/Binder Ratio = 0.428
 Binder Content (kg/m³) = 325
 Total Aggregates (kg/m³) = 1813
 Binder Density (kg/m³) = 2981
 Porosity = 0.117
 Cement Type = TYPE I

OH- Diffusion Coeff. (e-11 m²/s) = 3.43
 Saturation at 50% R.H. = 0.58
 Age of First Exposure (days) = 28
 Age at Lab. Testing (days) = 91
 Hydration Param. - a = 0.55
 Hydration Param. - alpha (1/a) = 5.000E-03
 Thermal Conductivity (W/m.K) = 2.000E+00
 Specific Heat (J/kg.K) = 1.000E+03



page 4/18

© SIMCO Technologies Inc. 2014
 All rights reserved

STADIUM® VERSION 2.997



Design Calculation

Approved by: _____ page 6/18

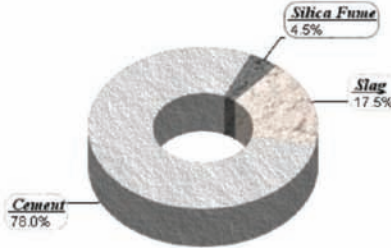
This Product is licensed to: Tim Barrett - Academic Account
 Date : 04-02-2014 / 13:15:23
 Engineer :
 Client :
 Project :
 Project Ref.:
Project Database: [SPR 3752.sdb]

IMI IC HPC

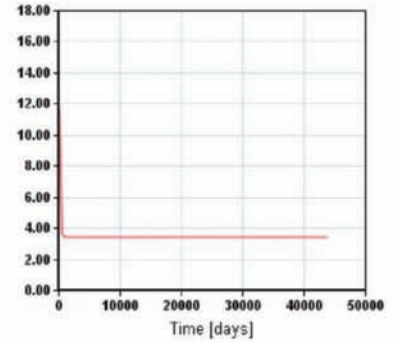
Structure Type: Bridge
 Structural Element Type: [Deck]
 Material Name:
 [Modified Material - for IMI IC HPC]

Cement Type	TYPE I
Water/Binder Ratio	0.396
Cement Content: (kg/m ³)	263
SCM #1: Slag (kg/m ³)	59
SCM #2: Silica Fume (kg/m ³)	15
SCM #3: None (kg/m ³)	0
Fine Aggregates: (kg/m ³)	977
Coarse Aggregates: (kg/m ³)	1069
Water: (kg/m ³)	133
Air: [%]	5.1
Material Density: (kg/m ³)	2516
Mixture Volume: (m ³)	1.072
Paste Volume: [%]	24.35

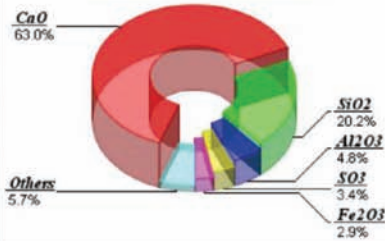
Binder Composition



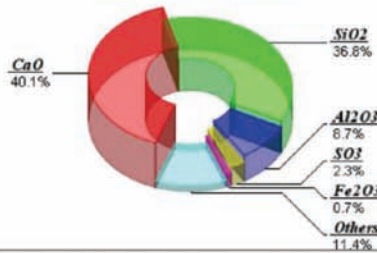
Diffusion Coefficient (e-11 m²/s)- a=55 - alpha=5.00E-3



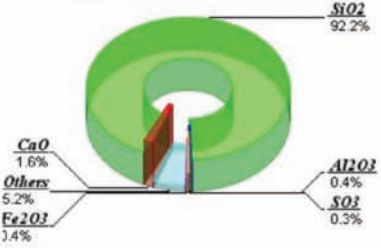
Cement Composition



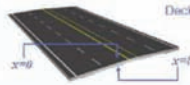
Slag Composition



Silica Fume Composition



Data for project: SPR 3752 - Structural element [IMI IC HPC]



Dimension (mm) = 203.2
 Scenario Duration (years) = 120
 Temperature (°C) = 23.0
 Water/Binder Ratio = 0.396
 Binder Content (kg/m³) = 337
 Total Aggregates (kg/m³) = 2048
 Binder Density (kg/m³) = 3062
 Porosity = 0.128
 Cement Type = TYPE I

OH- Diffusion Coeff. (e-11 m²/s) = 6.18
 Saturation at 50% R.H. = 0.41
 Age of First Exposure (days) = 28
 Age at Lab Testing (days) = 91
 Hydration Param. - a = 0.55
 Hydration Param. - alpha (1/a) = 5.000E-03
 Thermal Conductivity (W/m.K) = 2.000E+00
 Specific Heat (J/kg.K) = 1.000E+03



page 6/18

© SIMCO Technologies Inc. 2014
 All rights reserved
 STADIUM® VERSION 2.997



Design Calculation

Approved by: _____ page 8/18

This Product is licensed to: Tim Barrett - Academic Account

Date : 04-02-2014 / 13:15:24

Engineer :

Client :

Project :

Project Ref.:

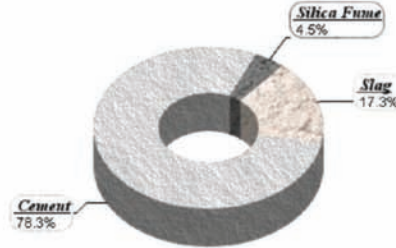
Project Database: [SPR 3752.sdb]

IMI HPC

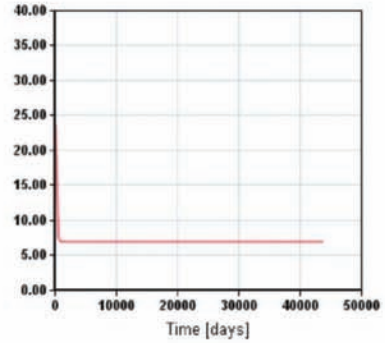
Structure Type: Bridge
 Structural Element Type: [Deck]
 Material Name:
 [Modified Material - for IMI HPC]

Cement Type	TYPE I
Water/Binder Ratio	0.403
Cement Content: (kg/m ³)	263
SCM #1: Slag (kg/m ³)	58
SCM #2: Silica Fume (kg/m ³)	15
SCM #3: None (kg/m ³)	0
Fine Aggregates: (kg/m ³)	792
Coarse Aggregates: (kg/m ³)	1069
Water: (kg/m ³)	135
Air: [%]	5.2
Material Density: (kg/m ³)	2332
Mixture Volume: (m ³)	1.004
Paste Volume: [%]	24.51

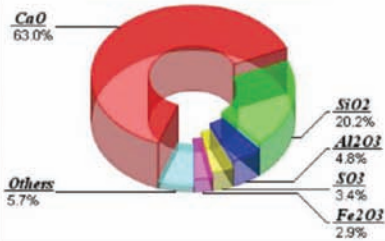
Binder Composition



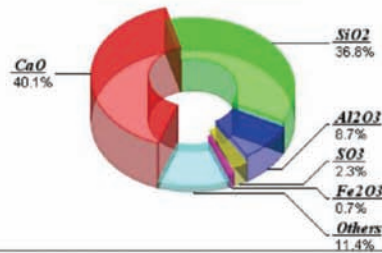
Diffusion Coefficient (e-11 m²/s). a=.55 - alpha=5.00E-3



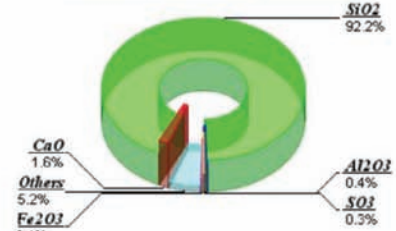
Cement Composition



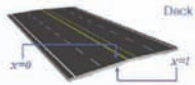
Slag Composition



Silica Fume Composition



Data for project: SPR 3752 - Structural element [IMI HPC]



Dimension (mm) = 203.2
 Scenario Duration (years) = 120
 Temperature (°C) = 23.0
 Water/Binder Ratio = 0.403
 Binder Content (kg/m³) = 336
 Total Aggregates (kg/m³) = 1861
 Binder Density (kg/m³) = 3063
 Porosity = 0.119
 Cement Type = TYPE I

OH- Diffusion Coeff. (e-11 m²/s) = 12.50
 Saturation at 50% R.H. = 0.40
 Age of First Exposure (days) = 28
 Age at Lab Testing (days) = 91
 Hydration Param. - a = 0.55
 Hydration Param. - alpha (1/s) = 5.000E-03
 Thermal Conductivity (W/m.K) = 2.000E+00
 Specific Heat (J/kg.K) = 1.000E+03



page 8/18

© SIMCO Technologies Inc. 2014
 All rights reserved

STADIUM® VERSION 2.997



SIMCO
Technologies inc.

Design Calculation

Approved by : _____ page 10/18

This Product is licensed to: Tim Barrett - Academic Account

Date : 04-02-2014 / 13:15:25

Engineer : _____

Client : _____

Project : _____

Project Ref.: _____

Project Database: [SPR 3752.sdb]

Shelby IC HPC

Structure Type: Bridge

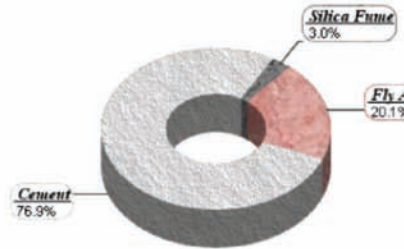
Structural Element Type: [Deck]

Material Name:

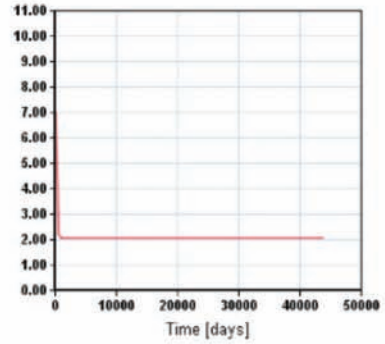
[Modified Material - for Shelby IC HPC]

Cement Type	TYPE I
Water/Binder Ratio	0.447
Cement Content: (kg/m ³)	256
SCM #1: Fly Ash C (kg/m ³)	67
SCM #2: Silica Fume (kg/m ³)	10
SCM #3: None (kg/m ³)	0
Fine Aggregates: (kg/m ³)	1111
Coarse Aggregates: (kg/m ³)	1027
Water: (kg/m ³)	149
Air: [%]	1.8
Material Density: (kg/m ³)	2620
Mixture Volume: (m ³)	1,082
Paste Volume: [%]	25.89

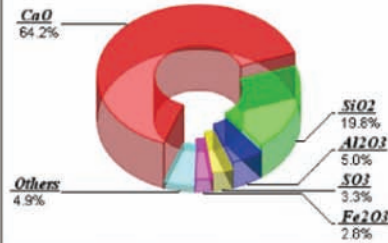
Binder Composition



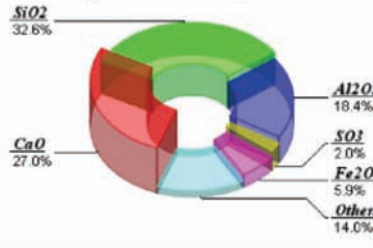
Diffusion Coefficient (e-11 m²/s): a=.55 - alpha=5.00E3



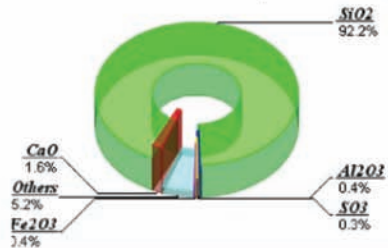
Cement Composition



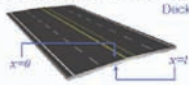
Fly Ash C Composition



Silica Fume Composition



Data for project: SPR 3752 - Structural element [Shelby IC HPC]



Dimension (mm) = 203.2
 Scenario Duration (years) = 120
 Temperature (°C) = 23.0
 Water/Binder Ratio = 0.447
 Binder Content (kg/m³) = 333
 Total Aggregates (kg/m³) = 2138
 Binder Density (kg/m³) = 3020
 Porosity = 0.15
 Cement Type = TYPE I

OH- Diffusion Coeff. (e-11 m²/s) = 3.72
 Saturation at 50% RH = 0.51
 Age of First Exposure (days) = 28
 Age at Lab Testing (days) = 91
 Hydration Param. - a = 0.55
 Hydration Param. - alpha (1/s) = 5.000E-03
 Thermal Conductivity (W/m.K) = 2.000E+00
 Specific Heat (kJ/kgK) = 1.000E+03



page 10/18

© SIMCO Technologies Inc. 2014
 All rights reserved

STADIUM® VERSION 2.997



SIMCO
Technologies inc.

Design Calculation

Approved by : _____ page 12/18

This Product is licensed to: Tim Barrett - Academic Account

Date : 04-02-2014 / 13:15:26

Engineer : _____

Client : _____

Project : _____

Project Ref. : _____

Project Database: [SPR 3752.sdb]

Shelby HPC

Structure Type: Bridge

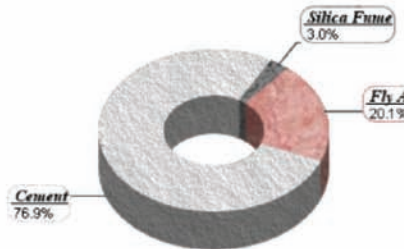
Structural Element Type: [Deck]

Material Name:

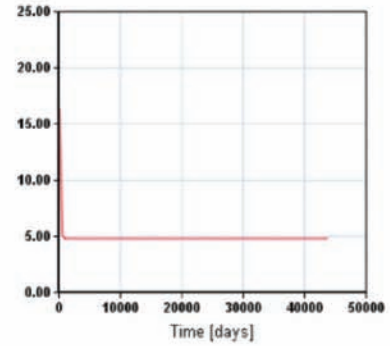
[Modified Material - for Shelby HPC]

Cement Type	TYPE I
Water/Binder Ratio	0.422
Cement Content: (kg/m ³)	256
SCM #1: Fly Ash C (kg/m ³)	67
SCM #2: Silica Fume (kg/m ³)	10
SCM #3: None (kg/m ³)	0
Fine Aggregates: (kg/m ³)	794
Coarse Aggregates: (kg/m ³)	1023
Water: (kg/m ³)	141
Air: [%]	5.9
Material Density: (kg/m ³)	2291
Mixture Volume: (m ³)	0.991
Paste Volume: [%]	25.06

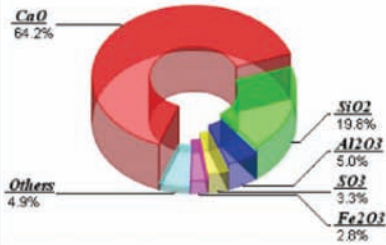
Binder Composition



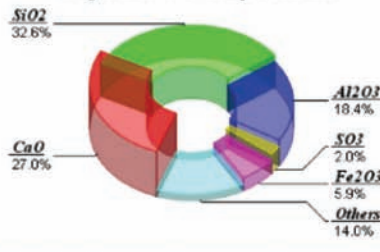
Diffusion Coefficient (e-11 m²/s) - a=.55 - alpha=5.00E-3



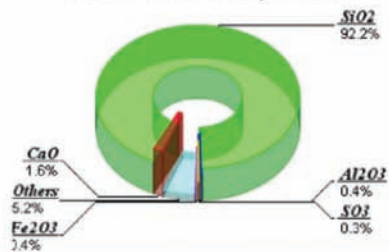
Cement Composition



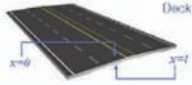
Fly Ash C Composition



Silica Fume Composition



Data for project: SPR 3752 - Structural element [Shelby HPC]



Dimension (mm) = 203.2
Scenario Duration (years) = 120
Temperature (°C) = 23.0
Water/Binder Ratio = 0.422
Binder Content (kg/m³) = 333
Total Aggregates (kg/m³) = 1817
Binder Density (kg/m³) = 3026
Porosity = 0.125
Cement Type = TYPE I

OH- Diffusion Coeff. (e-11 m²/s) = 8.62
Saturation at 50% RH = 0.50
Age of First Exposure (days) = 28
Age at Lab Testing (days) = 91
Hydration Param. - a = 0.55
Hydration Param. - alpha (1/a) = 5.000E+03
Thermal Conductivity (W/m.K) = 2.000E+00
Specific Heat (kJ/kg.K) = 1.000E+03



page 12/18

© SIMCO Technologies Inc. 2014
All rights reserved

STADIUM® VERSION 2.997



SIMCO
Technologies Inc.

Design Calculation

Approved by : _____ page 14/18

This Product is licensed to: Tim Barrett - Academic Account

Date : 04-02-2014 / 13:15:27

Engineer : _____

Client : _____

Project : _____

Project Ref.: _____

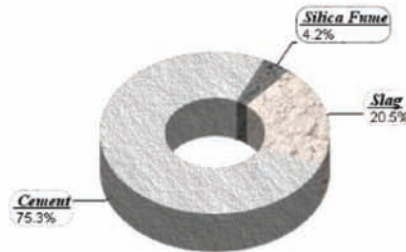
Project Database: [SPR 3752.sdb]

Transit IC HPC

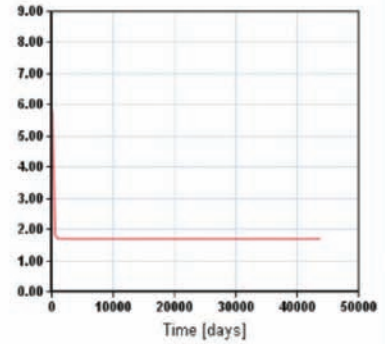
Structure Type: Bridge
Structural Element Type: [Deck]
Material Name:
[Modified Material - for Transit IC HPC]

Cement Type	TYPE I
Water/Binder Ratio	0.465
Cement Content: (kg/m ³)	213
SCM #1: Slag (kg/m ³)	58
SCM #2: Silica Fume (kg/m ³)	12
SCM #3: None (kg/m ³)	0
Fine Aggregates: (kg/m ³)	1025
Coarse Aggregates: (kg/m ³)	889
Water: (kg/m ³)	132
Air: [%]	8.1
Material Density: (kg/m ³)	2329
Mixture Volume: (m ³)	1.017
Paste Volume: [%]	22.36

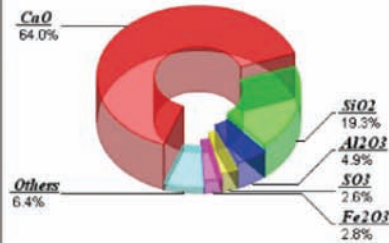
Binder Composition



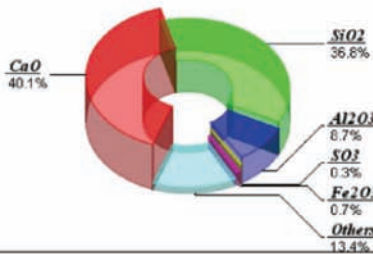
Diffusion Coefficient (e-11 m²/s) - a=.55 - alpha=5.00E3



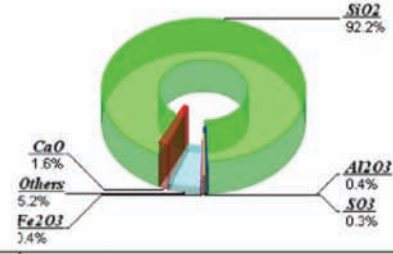
Cement Composition



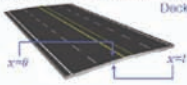
Slag Composition



Silica Fume Composition



Data for project: SPR 3752 - Structural element [Transit IC HPC]



Dimension (mm) = 203.2
Scenario Duration (years) = 120
Temperature (°C) = 23.0
Water/Binder Ratio = 0.465
Binder Content (kg/m³) = 283
Total Aggregates (kg/m³) = 1914
Binder Density (kg/m³) = 3077
Porosity = 0.138
Cement Type = TYPE I

OH- Diffusion Coeff. (m²/s) = 3.06
Saturation at 50% R.H. = 0.50
Age of First Exposure (days) = 28
Age at Lab Testing (days) = 91
Hydration Param. - a = 0.55
Hydration Param. - alpha (1/s) = 5.000E-03
Thermal Conductivity (W/m.K) = 2.000E+00
Specific Heat (J/kg.K) = 1.000E+03



page 14/18

© SIMCO Technologies Inc. 2014
All rights reserved

STADIUM® VERSION 2.997



SIMCO
Technologies Inc.

Design Calculation

Approved by : _____ page 16/18

This Product is licensed to: Tim Barrett - Academic Account

Date : 04-02-2014 / 13:15:28

Engineer : _____

Client : _____

Project : _____

Project Ref.: _____

Project Database: [SPR 3752.sdb]

Transit HPC

Structure Type: Bridge

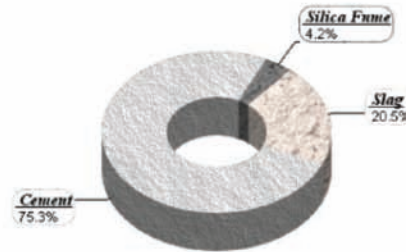
Structural Element Type: [Deck]

Material Name:

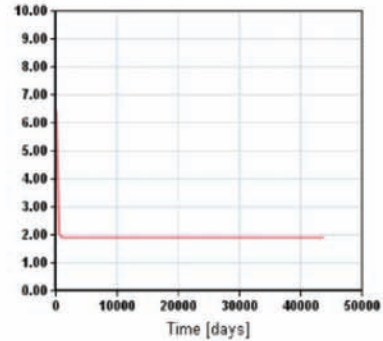
[Modified Material - for Transit HPC]

Cement Type	TYPE I
Water/Binder Ratio	0.398
Cement Content: (kg/m ³)	272
SCM #1: Slag (kg/m ³)	74
SCM #2: Silica Fume (kg/m ³)	15
SCM #3: None (kg/m ³)	0
Fine Aggregates: (kg/m ³)	821
Coarse Aggregates: (kg/m ³)	1067
Water: (kg/m ³)	144
Air: [%]	7.1
Material Density: (kg/m ³)	2393
Mixture Volume: (m ³)	1.031
Paste Volume: [%]	26.1

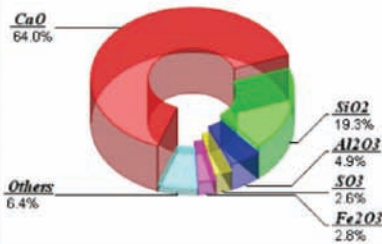
Binder Composition



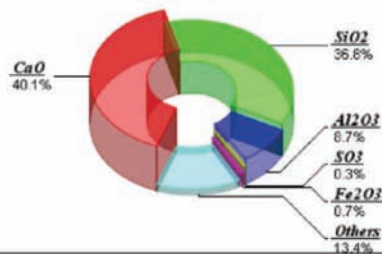
Diffusion Coefficient (e-11 m²/s)- a=.55 - alpha=5.00E3



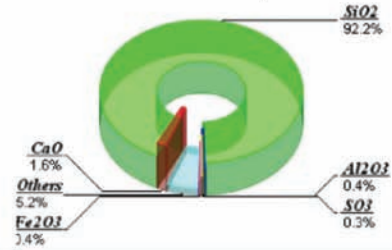
Cement Composition



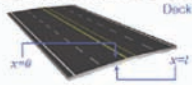
Slag Composition



Silica Fume Composition



Data for project: SPR 3752 - Structural element [Transit HPC]



Dimension (mm) = 203.2
Scenario Duration (years) = 120
Temperature (°C) = 23.0
Water/Binder Ratio = 0.398
Binder Content: (kg/m³) = 361
Total Aggregates (kg/m³) = 1888
Binder Density (kg/m³) = 3078
Porosity = 0.117
Cement Type = TYPE I

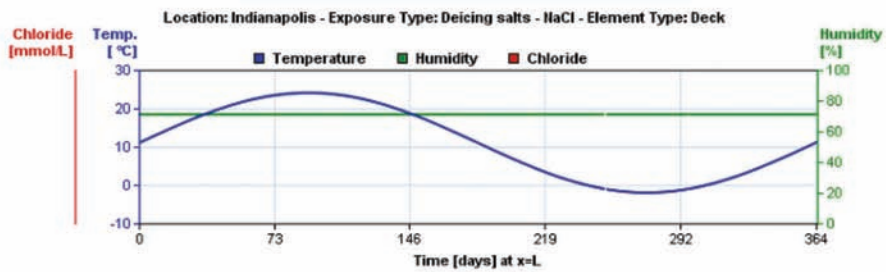
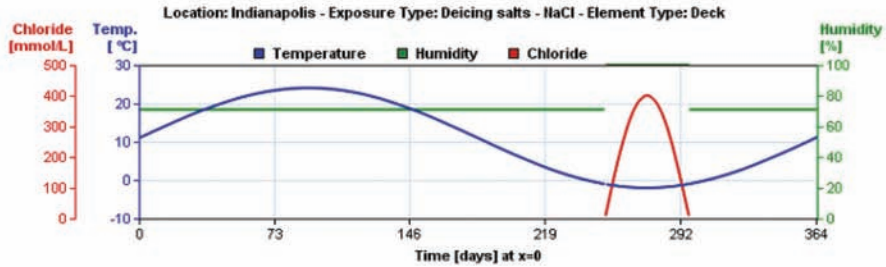
OH- Diffusion Coeff. (e-11 m²/s) = 3.42
Saturation at 50% R.H. = 0.58
Age of First Exposure (days) = 28
Age at Lab Testing (days) = 91
Hydration Param. - a = 0.55
Hydration Param. - alpha (1/s) = 5.000E-03
Thermal Conductivity (W/m.K) = 2.000E+00
Specific Heat (J/kg.K) = 1.000E+03



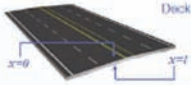
page 16/18

© SIMCO Technologies Inc. 2014
All rights reserved

STADIUM® VERSION 2.997



Data for project: SPR 3752 - Structural element [Transit HPC] - Scenario: INITIAL



Dimension (mm) = 203.2
 Scenario Duration (years) = 120
 Temperature (°C) = 23.0
 Water/Binder Ratio = 0.398
 Binder Content (kg/m³) = 361
 Total Aggregates (kg/m³) = 1888
 Binder Density (kg/m³) = 3078
 Porosity = 0.117
 Cement Type = TYPE I

OH- Diffusion Coeff. (e-11 m²/s) = 3.42
 Saturation at 50% R.H. = 0.58
 Age of First Exposure (days) = 28
 Age at Lab Testing (days) = 91
 Hydration Param. - a = 0.55
 Hydration Param. - alpha (1/s) = 5.000E-03
 Thermal Conductivity (W/m.K) = 2.000E+00
 Specific Heat (J/kg.K) = 1.000E+03



APPENDIX G

The Aggregate Moistures Worksheet is available for download at <http://dx.doi.org/10.5703/1288284315532>.

APPENDIX H

The Mixture Design Worksheet is available for download at <http://dx.doi.org/10.5703/1288284315532>.

About the Joint Transportation Research Program (JTRP)

On March 11, 1937, the Indiana Legislature passed an act which authorized the Indiana State Highway Commission to cooperate with and assist Purdue University in developing the best methods of improving and maintaining the highways of the state and the respective counties thereof. That collaborative effort was called the Joint Highway Research Project (JHRP). In 1997 the collaborative venture was renamed as the Joint Transportation Research Program (JTRP) to reflect the state and national efforts to integrate the management and operation of various transportation modes.

The first studies of JHRP were concerned with Test Road No. 1—evaluation of the weathering characteristics of stabilized materials. After World War II, the JHRP program grew substantially and was regularly producing technical reports. Over 1,500 technical reports are now available, published as part of the JHRP and subsequently JTRP collaborative venture between Purdue University and what is now the Indiana Department of Transportation.

Free online access to all reports is provided through a unique collaboration between JTRP and Purdue Libraries. These are available at: <http://docs.lib.purdue.edu/jtrp>

Further information about JTRP and its current research program is available at: <http://www.purdue.edu/jtrp>

About This Report

An open access version of this publication is available online. This can be most easily located using the Digital Object Identifier (doi) listed below. Pre-2011 publications that include color illustrations are available online in color but are printed only in grayscale.

The recommended citation for this publication is:

Barrett, T. J., Miller, A. E., & Weiss, W. J. (2015). *Documentation of the INDOT experience and construction of the bridge decks containing internal curing in 2013* (Joint Transportation Research Program Publication No. FHWA/IN/JTRP-2015/10). West Lafayette, IN: Purdue University. <http://dx.doi.org/10.5703/1288284315532>